

**Fault Displacement Effects on Transport in the Unsaturated Zone**

**OFFICE OF CIVILIAN RADIOACTIVE WASTE MANAGEMENT  
ANALYSIS/MODEL COVER SHEET**

1. QA: QA

Page: 1 of 54

**Complete Only Applicable Items**

2.  Analysis Check all that apply

Type of Analysis	<input type="checkbox"/> Engineering <input checked="" type="checkbox"/> Performance Assessment <input type="checkbox"/> Scientific
Intended Use of Analysis	<input type="checkbox"/> Input to Calculation <input type="checkbox"/> Input to another Analysis or Model <input checked="" type="checkbox"/> Input to Technical Document <input type="checkbox"/> Input to other Technical Products

Describe use:  
To investigate the potential effects of fault displacements on transport characteristics between the potential repository and the water table.

3.  Model Check all that apply

Type of Model	<input type="checkbox"/> Conceptual Model <input type="checkbox"/> Mathematical Model <input type="checkbox"/> Process Model	<input type="checkbox"/> Abstraction Model <input type="checkbox"/> System Model
Intended Use of Model	<input type="checkbox"/> Input to Calculation <input type="checkbox"/> Input to another Model or Analysis <input type="checkbox"/> Input to Technical Document <input type="checkbox"/> Input to other Technical Products	

Describe use:

4. Title:  
Fault Displacement Effects on Transport in the Unsaturated Zone

5. Document Identifier (including Rev. No. and Change No., if applicable):  
ANL-NBS-HS-000020 REV 01

6. Total Attachments:  
7

7. Attachment Numbers - No. of Pages in Each:  
I - 6; II - 5; III - 11; IV - 8; V - 29; VI - 3; VII - 7.

	Printed Name	Signature	Date
8. Originator	Yanyong Xiang	<i>Y. Xiang</i>	8/15/2000
9. Checker	Banda Ramarao	<i>B S Ramarao</i>	08-15-2000
10. Lead/Supervisor	Jerry McNeish	<i>Jerry A McNeish</i>	8.15.00
11. Responsible Manager	Jerry McNeish	<i>Jerry A McNeish</i>	8.15.00

12. Remarks:  
Initial Issue of Rev 01.

**OFFICE OF CIVILIAN RADIOACTIVE WASTE MANAGEMENT  
ANALYSIS/MODEL REVISION RECORD**

***Complete Only Applicable Items***

1. Page: 2 of 54

2. Analysis or Model Title:

Fault Displacement Effects on Transport in the Unsaturated Zone

3. Document Identifier (including Rev. No. and Change No., if applicable):

ANL-NBS-HS-000020 REV 01

4. Revision/Change No.

5. Description of Revision/Change

Rev 00

Initial issue.

Rev 01

Revision for documenting upgrades in UZ flow and transport models.

**CONTENTS**

	<b>Page</b>
1. PURPOSE.....	7
2. QUALITY ASSURANCE.....	8
3. COMPUTER SOFTWARE AND MODEL USAGE.....	9
3.1 QUALIFIED SOFTWARE.....	9
3.2 SOFTWARE UNDER CONFIGURATION MANAGEMENT CONTROL.....	9
3.3 SOFTWARE ROUTINES.....	10
4. INPUTS.....	11
4.1 DATA AND PARAMETERS.....	11
4.2 CRITERIA.....	11
4.3 CODES AND STANDARDS.....	11
5. ASSUMPTIONS.....	12
5.1 ASSUMPTION 1.....	12
5.2 ASSUMPTION 2.....	12
5.3 ASSUMPTION 3.....	12
5.4 ASSUMPTION 4.....	13
5.5 ASSUMPTION 5.....	13
5.6 ASSUMPTION 6.....	13
5.7 ASSUMPTION 7.....	13
5.8 ASSUMPTION 8.....	14
5.9 ASSUMPTION 9.....	14
5.10 ASSUMPTION 10.....	14
6. ANALYSIS/MODEL.....	15
6.1 SITE DESCRIPTION INFORMATION.....	15
6.1.1 Geologic Setting.....	15
6.1.2 Fault Displacement Hazards.....	23
6.1.3 Climate Data.....	24
6.2 EFFECTS OF FAULT DISPLACEMENTS ON UZ FLOW AND TRANSPORT.....	24
6.2.1 Analysis Approach.....	25
6.2.2 Results.....	36
6.2.3 Discussion.....	45
7. CONCLUSIONS.....	46
8. INPUT AND REFERENCES.....	48

**ATTACHMENTS**

	<b>Page</b>
I SOFTWARE ROUTINE ‘extract_xd.f v.1’ .....	I-1
II SOFTWARE ROUTINE ‘sr_ini_ext.f v.1’ .....	II-1
III SOFTWARE ROUTINE ‘alt_tough2sr.f v.1’ .....	III-1
IV SOFTWARE ROUTINE ‘fehm_post.f v.1’ .....	IV-1
V SOFTWARE ROUTINE ‘t2fehm2_v3x.f v.1’ .....	V-1
VI SOFTWARE ROUTINE ‘mb_tough2_v1.4.f v.1’ .....	VI-1
VII SOFTWARE ROUTINE ‘post_tough2sr.f v.1’ .....	VII-1

**FIGURES**

	<b>Page</b>
Figure 1. Conceptual Connection Diagram for a One-Dimensional Dual-Permeability Model.....	28
Figure 2. Conceptual Connection Diagram for a Two-Dimensional Dual-Permeability Model.....	29
Figure 3. Schematic Diagram of a Breakthrough Curve.....	30
Figure 4. Plan View of the Locations of the Two-Dimensional Cross Section and the Nearby Faults within the TSPA-SR UZ Grid. The Location of the One-Dimensional Column Is Shown with a ‘•’ Symbol.....	31
Figure 5. Breakthrough Curves for the One-Dimensional Column Model under Present-Day Infiltration. DTN: MO0006SPAUZT20.002.....	37
Figure 6. Water Saturation Distributions in the Fractures for the One-Dimensional Column Model under Present-Day Infiltration. DTN: MO0006SPAUZT20.002. ....	38
Figure 7. Water Saturation Distributions in the Matrix for the One-Dimensional Column Model under Present-Day Infiltration. DTN: MO0006SPAUZT20.002. ....	38
Figure 8. Normalized Water Flux Distributions in the Fractures for the One-Dimensional Column Model under Present-Day Infiltration. DTN: MO0006SPAUZT20.002. ....	39

Figure 9. Normalized Water Flux Distributions in the Matrix for the One-Dimensional Column Model under Present-Day Infiltration. DTN: MO0006SPAUZT20.002. .... 39

Figure 10. Capillary Pressure Distributions in the Fractures for the One-Dimensional Column Model under Present-Day Infiltration. DTN: MO0006SPAUZT20.002. .... 40

Figure 11. Capillary Pressure Distributions in the Matrix for the One-Dimensional Column Model under Present-Day Infiltration. DTN: MO0006SPAUZT20.002. .... 41

Figure 12. Capillary Pressure-Difference Distributions for the One-Dimensional Column Model under Present-Day Infiltration. DTN: MO0006SPAUZT20.002. .... 41

Figure 13. Breakthrough Curves for the Two-Dimensional Model under Present-Day Infiltration. DTN: MO0006SPAUZT20.002. .... 42

Figure 14. Breakthrough Curves for the Two-Dimensional Model under Glacial-Transition Infiltration. DTN: MO0006SPAUZT20.002. .... 43

Figure 15. Breakthrough Curves for the Three-Dimensional Model under Present-Day Infiltration. DTN: MO0006SPAUZT20.002. .... 44

Figure 16. Breakthrough Curves for the Three-Dimensional Model under Glacial-Transition Infiltration. DTN: MO0006SPAUZT20.002. .... 45

Figure 17. Breakthrough Curves for the Three-Dimensional Model under Present-day Infiltration when Fault Fractures Are Altered. DTN: MO0006SPAUZT20.002. .... 45

Figure 18. Breakthrough Curves for the Three-Dimensional Model under Glacial-Transition Infiltration when Fault Fractures Are Altered. DTN: MO0006SPAUZT20.002. .... 45

**TABLES**

	<b>Page</b>
Table 1. Computer Software and Software Routines Used in this Report.....	9

## ACRONYMS

AMR	Analysis and Model Report
AP	administrative procedure
ASTM	American Society for Testing and Materials
CRWMS M&O	Civilian Radioactive Waste Management System Management and Operating Contractor
DOE	United States Department of Energy
DTN	data tracking number
ECRB	enhanced characterization of the repository block
ESF	exploratory studies facility
FEP	features, events, and processes
NRC	Nuclear Regulatory Commission
QAP	Quality Administrative Procedure(s)
SZ	saturated zone
SCFZ	Solitario Canyon fault zone
TBV	to be verified
TSPA	total-system performance assessment
TSPA-SR	total-system performance assessment – site recommendation
TSPA-VA	total-system performance assessment – viability assessment
UZ	unsaturated zone
VA	viability assessment
YMP	Yucca Mountain Site Characterization Project

## 1. PURPOSE

The purpose of this analysis is to evaluate the potential for changes to the hydrogeologic system caused by fault displacement to affect radionuclide transport in the unsaturated zone at Yucca Mountain. The potential repository is bounded on the west by the Solitario Canyon fault and on the east by the Bow Ridge fault. The northern boundary of this structural block is bounded by the Drill Hole Wash fault. In addition, there are intrablock faults consisting of the Ghost Dance, Sundance, and Dune Wash faults. For the purposes of this analysis, the focus is on two possible effects of fault displacement along the bounding faults: (1) uniform change in fracture properties throughout the UZ flow model domain and (2) change in fracture properties within the faults only. These two hypothetical end-member cases relate to the mechanical strain that's either uniformly distributed throughout the strata bounded by the faults, or localized to the individual fault zones. In the physical system, the strain would be spatially distributed in some manner that lies between these end-member cases. This evaluation used the bounding case estimates to determine if fault displacement can be excluded from consideration with respect to unsaturated zone (UZ) transport in total system performance modeling.

These two end-member cases were evaluated by simulating the flow and transport in the unsaturated zone (UZ) for a pulse input tracer at the potential repository location. For a specific cross-section, computer simulations were performed assuming (1) a change in fracture properties throughout the UZ models (which assumes all fracture apertures are uniformly altered), and (2) a change in fracture properties in the fault zones only. Simulations were performed for the present-day climate and a wetter, glacial-transition climate case. Tracer breakthrough curves computed at the water table were used to examine the potential impact induced on transport in the UZ.

This evaluation supports the analysis of Features, Events, and Processes (FEPs) that may affect total system performance. The evaluation of FEPs are conducted to comply with the specifications in the DOE Interim Guidance (Dyer 1999) for justifying the inclusion or exclusion of FEPs from the total system performance assessment (TSPA). The specific issue of the effects of fault displacement on UZ transport encompasses four FEPS:

- Faulting (1.2.02.02.00)
- Seismic activity (1.2.03.01.00)
- Hydrologic response to seismic activity (1.2.10.01.00)
- Changes in stress produce change in permeability of faults (2.2.06.02.00)

The numbers in parentheses indicate the numerical identification used in the TSPA FEPs database (CRWMS M&O 1999a). The evaluation and screening of the other aspects of the FEPs listed above are documented in the UZ FEPs Analysis and Model Report (AMR) (CRWMS M&O 2000b) and saturated zone (SZ) FEPs AMR (CRWMS M&O 2000c).

Constraints and limitations of this work include the preliminary status of the input data and software used in the analysis (see Sections 3, 4, and 5). Once these source data and software are qualified, the results of this analysis can be considered qualified. Until then, the information developed from this analysis must be considered unqualified. This report has been prepared in accordance with the work plan, "Fault Displacement Effects on Transport in the Unsaturated Zone" (CRWMS M&O 2000d).

## 2. QUALITY ASSURANCE

The quality assurance program is applicable to this report. The Performance Assessment Operations responsible manager has evaluated this activity in accordance with QAP-2-0, *Conduct of Activities*. The QAP-2-0 activity evaluation (CRWMS M&O 1999b) determined that the development of this AMR is subject to the *Quality Assurance Requirements and Description* (DOE 2000) requirements. This report is prepared in accordance with AP-3.10Q, *Analyses and Models*.

The methods used to control the electronic management of data as required by AP-SV.1Q, *Control of the Electronic Management of Data*, were accomplished in accordance with the controls specified in the Supplement V evaluation, *AP-SV.1Q Control of the Electronic Management of Data Evaluation for Natural Systems Analysis/Model Reports* (Andrews 2000). The evaluation determined that current work processes and procedures (e.g., AP-SIII.3Q, Submittal and Incorporation of Data to the Technical Data Management System) are adequate for the control of electronic management of data for this activity.

The unsaturated and saturated zone natural barriers have not been classified per QAP-2-3, *Classification of Permanent Items*. However, the natural barriers have been classified by hydrogeologic units in the current project Q-List (YMP/90-55Q Rev. 5, 1998). In this document, the following hydrogeologic units in the UZ were identified as important to waste isolation: Tiva Canyon Welded, Paintbrush Nonwelded, Topopah Spring Welded, Calico Hills Nonwelded. In addition, the SZ was listed as a natural barrier important to waste isolation.

### 3. COMPUTER SOFTWARE AND MODEL USAGE

The computer software and models used in this report are listed below in Table 1:

Table 1. Computer Software and Software Routines Used in this Report

Software Name	Version	SCM Identifier	Computer Type	Documentation
TOUGH2	V1.4	10007-1.4-01	DEC/ UNIX OS	Wu et al. 1999
FEHM	V2.00	10031-2.00-00	SUN/ UNIX OS 5.7	Dash and Zyvoloski 1999
extract_xd.f	V1	software routine	HP Workstation J2240	Attachment I
sr_ini_ext.f	V1	software routine	HP Workstation J2240	Attachment II
alt_tough2sr.f	V1	software routine	HP Workstation J2240	Attachment III
feh_m_post.f	V1	software routine	HP Workstation J2240	Attachment IV
t2feh_m2_v3x.f	V1	software routine	HP Workstation J2240	Attachment V
mb_tough2_v1.4.f	V1	software routine	HP Workstation J2240	Attachment VI
post_tough2sr.f	V1	software routine	HP Workstation J2240	Attachment VII

In this report, TOUGH2 V1.4 (documented in Wu et al. 1999) and FEHM V2.00 (Dash and Zyvoloski 1999) are employed for modeling unsaturated zone flow and radionuclide transport in the unsaturated zone, respectively. TOUGH2 V1.4 is qualified for use on DEC with UNIX OS, located in the Lawrence Berkeley National Laboratory. FEHM V2.00 is qualified for use on the SUN UNIX OS, located in the Sandia National Laboratories. The software routine ‘t2feh\_m2\_v3x.f’ is a modified version of the routine ‘t2feh\_m2\_v3.f’ (CRWMS M&O 2000e). The modifications are explained in Sections 3.3 titled ‘Software Routines’ and 6.2.1.7 titled ‘Calculation Procedures’ of this report.

The selection of TOUGH2, ‘t2feh\_m2\_v3x.f’, and FEHM to evaluate UZ flow and transport is based on the fact that these software codes have been developed on the Yucca Mountain Project for just this purpose.

#### 3.1 QUALIFIED SOFTWARE

TOUGH2 V1.4 is qualified in accordance with AP-SI.1Q, *Software Management*, so are the software routines discussed in Section 3.3. FEHM V2.00 as used in this AMR should be treated as unqualified software.

#### 3.2 SOFTWARE UNDER CONFIGURATION MANAGEMENT CONTROL

In this AMR, TOUGH2 V1.4 and FEHM V2.00 are employed for modeling UZ flow and radionuclide transport, respectively. The code TOUGH2 V1.4 resides at LBNL’s DEC computer. FEHM V2.00 was obtained from configuration management in accordance with Section 5.11 of AP-SI.1Q, *Software Management*, and was determined to be appropriate for its applications in the context of this AMR. These software codes were installed and used in accordance with the available software documentation, indicated in Table 1.

### 3.3 SOFTWARE ROUTINES

The software routine 't2fehm2\_v3x.f' is a software routine modified from 't2fehm2\_v3.f' (CRWMS M&O 2000e). The modifications are to enable the accommodation of new names for the altered fracture types as identified by the character '&' in replacement of 'F'. This software routine is appropriate for the application used in this analysis and is used only within the range of validation established for the software routine.

Additional pre- and post-processing routines listed in Table 1 were specifically developed for use in this analysis (extract\_xd.f, sr\_ini\_ext.f, alt\_tough2sr.f, fehm\_post.f, post\_tough2sr.f, mb\_tough2\_v1.4.f). These software routines are qualified through the documentation given in attachments to this analysis, as shown in Table 1. The executables of these software routines have been obtained using the HP FORTRAN 90/S700 compiler (version: B.10.20.00).

All software routines are documented in accordance with AP-SI.1Q, *Software Management*, and have been verified through visual inspections and/or hand checks as shown in Attachments I through VII.

## 4. INPUTS

### 4.1 DATA AND PARAMETERS

The data and parameter inputs for UZ flow calculations using TOUGH2 presented in this analysis are contained in the AMR titled 'UZ Flow Models and Submodels' (CRWMS M&O 2000g). This data set (DTN: LB990701233129.001, LB990801233129.003, LB990801233129.009) is designated as TBV in the technical database. UZ flow properties affected by fracture aperture were varied for the sensitivity study reported in this analysis. For the UZ transport calculations, diffusion and sorption were neglected. Dispersion has been shown to have little effect on transport results in the UZ over a wide range of dispersivities investigated (CRWMS M&O 1998b; Section 7.6.1.2.6). A dispersivity of 25 m is the nominal value used for these calculations.

### 4.2 CRITERIA

A criterion established by the NRC that is relevant to this analysis concerns whether or not an event is sufficiently unlikely to be excluded from further consideration. According to the DOE's Interim Guidance Section 102(j) (Dyer 1999), if the probability of occurrence for an event is less than  $10^{-4}$  per  $10^4$  years, then the event may be excluded from further consideration in the total system performance assessment. In this analysis, events with probability of occurrence less than this magnitude are excluded from further consideration.

### 4.3 CODES AND STANDARDS

The applicable standard for this work is ASTM D 5718 – 95, Standard Guide for Documenting a Ground-Water Flow Model Application. Not all aspects of this standard are applicable to the present investigation. In particular, this AMR addresses the sensitivity of unsaturated-zone radionuclide transport to perturbations of fracture parameters due to possible fault movements, while the base case is taken from the calibrated TSPA-SR UZ flow model.

This AMR was prepared to comply with DOE's Interim Guidance (Dyer 1999) which specifies guidance to be used for evaluations in the absence of the NRC's final Yucca Mountain regulation. Subparts of this guidance that are particularly applicable to the data in this investigation include Subpart B, Section 15 (Site Characterization) and Subpart E, Section 114 (Requirements for Performance Assessment). Subparts applicable to models are outlined in Subpart E, Sections 114 (Requirements for Performance Assessment) and 115 (Required Characteristics of the Reference Biosphere and Critical Group).

## 5. ASSUMPTIONS

### 5.1 ASSUMPTION 1

The sensitivity studies reported in this AMR are based on the most up-to-date three-dimensional UZ model **C** the TSPA-SR UZ flow model, and one one-dimensional column model and one two-dimensional vertical cross-sectional model extracted from the three-dimensional model. The three-dimensional model and data is built as a dual-permeability model based on the active fracture concept (Liu et al. 1998; CRWMS M&O 2000f). The TSPA-SR UZ flow model and its 'active fracture' parameters are assumed to be adequate to represent UZ flow and transport processes, even when the fracture parameters are perturbed to reflect potential fault displacement effects. This assumption is used in Section 6.2.

Basis: The TSPA-SR UZ model, based on all the past years of data gathering-analyses and model development, supposedly represents the project's best understanding of the UZ system at Yucca Mountain. This assumption does not require further verification.

### 5.2 ASSUMPTION 2

Fault displacement effects on radionuclide transport behavior in the UZ are assumed to be entirely the result of changes to fracture properties in fault zones and/or in the surrounding rock. The effects of fault displacement on matrix properties are assumed to be negligible. This assumption is used in Sections 6.2 and 6.2.1.

Basis: Several fracture properties (permeability, capillary pressure, porosity) are a function of fracture aperture, which can be changed significantly by small strains if these strains are allocated entirely to the fracture apertures. The sensitivity of fracture aperture to mechanical strain is due to the small porosity of the fracture continuum. The matrix, on the other hand, has much greater porosity than the fractures in general, and its properties are not expected to be as sensitive to mechanical strain. This assumption is reasonable given the fact that fracture porosity is much less than matrix porosity at Yucca Mountain. Therefore, further verification of this assumption is not required.

### 5.3 ASSUMPTION 3

Changes in fracture properties are related to dilation or compression of existing fractures rather than the generation of new fractures. This assumption is used in Section 6.2.1.

Basis: This assumption relies on the fact that the rock at Yucca Mountain is highly fractured and that fractured rock is mechanically weaker along existing fractures than intact rock. This assumption is supported by the results of the Probabilistic Seismic Hazard Analysis, which show that the probability for fault displacement to occur along existing fractures is more likely than for intact rock (USGS 1998, Section 8.2.1). Therefore, strain due to fault displacement is likely to occur along existing fractures rather than initiate new fractures. This assumption is reasonable and does not require further verification.

#### **5.4 ASSUMPTION 4**

The effects of fault displacement on mountain-scale UZ transport can be evaluated from the response for a simulated non-diffusing, non-sorbing tracer. This assumption is used in Section 6.2.1.

Basis: Transport of a non-sorbing tracer is more sensitive to changes in fracture aperture, because the effects of fracture aperture dominate fracture/matrix interaction for such a tracer (given fixed matrix properties). For a non-sorbing tracer, the effects of diffusion are generally small (CRWMS M&O 1998b; Section 7.6.1.1.6). This assumption is reasonable and does not require further verification.

#### **5.5 ASSUMPTION 5**

Changes to fracture properties are assumed to be uniform, either throughout the UZ domain or localized to the fault zones. This assumption is used in Section 6.2.1.

Basis: A large change in fracture properties over the entire UZ domain (fault zones and fractured rock) is one bound for the possible effects of fault displacement. Isolating the effects of fault displacement to the fault zones provides another bound which emphasizes the effects of property contrasts between the fault zones and the fractured rock. Clearly, this assumption bounds the expected extremes for the spatial distribution of changes to fracture properties as a result of fault displacement. This assumption is conservative and does not require further verification.

#### **5.6 ASSUMPTION 6**

The transient effects of changes in fracture properties can be neglected (i.e. transport for steady flow equilibrated to the changed conditions bounds the effects of the change). This assumption is used in Section 6.2.1.

Basis: This assumption is analogous to the assumption that transient flow effects are negligible. Tests of transient flow processes related to climate change have shown that transport in a transient flow environment is accurately approximated using a quasi-steady flow approximation (CRWMS M&O 1998b; Section 7.4.4.1 and Figures 7-12 and 7-13). Therefore, the transient effects of changes in fracture aperture are likewise expected to be inconsequential compared with the resulting changes in steady flow and transport associated with the change. Verification of this assumption by analogy with the transient flow problem is reasonable and does not require further verification.

#### **5.7 ASSUMPTION 7**

Water table elevation is unchanged by any fault displacement. This assumption is used in Section 6.2.1.

Basis: This assumption provides a fixed reference point for comparisons of the effects of fault displacements on radionuclide transport. This assumption is reasonable as a basis for comparison of the effects of fault displacement. Therefore, further verification of this

assumption is not required. The effects of fault displacement on water table rise is analyzed in CRWMS M&O (2000b), and the effects are found to be negligible.

### **5.8 ASSUMPTION 8**

The flow model based a dual-permeability, active fracture conceptualization (CRWMS M&O 2000g) is adequate to represent UZ flow in this sensitivity study. This assumption is used in Section 6.2.1.

Basis: Because of reasons similar to Assumption 1, this assumption is derived from the confinement of the current stage of model development, and thus does not require further verification.

### **5.9 ASSUMPTION 9**

Fault displacements may result in changes to perched water. However, the effects of these changes in perched water on potential radionuclide transport are assumed to be negligible. This assumption is used in Section 6.2.1.

Basis: The sensitivity of radionuclide transport to different perched water models has been shown to be small (CRWMS M&O 2000a). Furthermore, the potential release of the perched water (and associated radionuclides) due to some disruptive event is expected to have a negligible effect on radionuclide releases at the water table (CRWMS M&O 2000b). This assumption is based on TBV information and, therefore, is also TBV.

### **5.10 ASSUMPTION 10**

Thermal-hydrologic processes due to waste heat from the potential repository will affect UZ flow and transport. However, the effects of thermal-hydrologic processes are expected to be negligible with respect to the sensitivity study conducted in for this report on the effects of fault displacements on mountain-scale UZ transport. This assumption is used in Section 6.2.1.

Basis: Waste heat from the potential repository will perturb the UZ flow fields and potentially alter hydrogeologic and transport properties in the UZ. However, these effects are assumed to be small in comparison with effects caused by the changes in fracture aperture and different climate conditions (infiltration rates) investigated here. If so, the conclusions based on an isothermal analysis should also be valid for a thermally-perturbed condition. This assumption requires further verification and, therefore, is TBV.

## 6. ANALYSIS/MODEL

As stated in Section 1, the purpose of this report is to describe the potential for fault displacement events during the potential repository post-closure period that affect performance through changes in radionuclide transport in the UZ at Yucca Mountain. In particular, the effects of fault displacement on potential repository performance will be addressed in terms of changes in the simulated breakthrough at the water table of a pulse input of tracer at the potential repository.

The approach for the analysis of fault displacement effects on transport in the UZ is divided into two distinct components: a review of site description information which provides a basis for defining bounding conditions and for understanding the physical significance of the results (Section 6.1); and a modeling component to provide quantitative analysis of the sensitivity of the UZ flow system to changes in hydrologic parameters (Section 6.2).

This Rev01 differs from Rev00 of the subject AMR in that Rev01 is based on the newly developed TSPA-SR UZ flow model (CRWMS M&O 2000g), whereas Rev00 builds its analyses on the TSPA-VA UZ flow model (CRWMS M&O 1998a). The TSPA-SR model is constructed as an active-fracture-dual-permeability model (see Section 6.2.1.2) as opposed to the conventional dual-permeability model (see Section 6.2.1.1) used for TSPA-VA.

### 6.1 SITE DESCRIPTION INFORMATION

The spatial and temporal patterns of faulting and fracturing of the volcanic bedrock are the fundamental elements of the structural geology of the potential repository for high-level radioactive wastes at Yucca Mountain. To document and discuss these patterns, a comprehensive program of geologic mapping and fractured rock mass studies has been conducted as an integral part of the site characterization. Of particular importance to this analysis are geologic observations related to displacement in fault zones and observations of the characteristics of the faults zones made during the excavation of the Exploratory Studies Facility (ESF) and in the enhanced characterization of the repository block (ECRB) Cross Drift. The observations are briefly described in Section 6.1.1. These observations provide a basis for determining the reasonableness and appropriateness of the range of inputs used in the modeling analysis in Section 6.2 and for interpreting the level of conservatism represented by the models.

However, the primary controlling factor for amount of flux through the UZ is the amount of precipitation available to infiltrate and percolate through the UZ. This variable is highly dependent on climate conditions. To address this variable, present day average and glacial-transition climate conditions (CRWMS M&O 1998a, Section 2.4.1.1) were used as bounding conditions. The differences in these climate states are briefly explained in Section 6.1.2.

#### 6.1.1 Geologic Setting

The Yucca Mountain area is cut by steeply dipping, north-south-striking normal faults which separate the Tertiary volcanics into blocks one to four kilometers wide (Scott 1990). The potential repository lies in the central block of the central Yucca Mountain structural domain. The central block is bounded on the west by the Solitario Canyon fault, on the east by the Bow

Ridge fault, and on the north by the northwest-striking Drill Hole Wash fault. The southern boundary is marked by a transition to structural styles that accompany greater magnitudes of extension and continue south. Intrablock faults include the Ghost Dance, Sundance, and the Dune Wash faults.

The potential repository area is bounded by the Solitario Canyon fault to the west and the Ghost Dance fault to the east. Both faults dip steeply toward the west, and displacement, amount of brecciation, and number of associated splays vary considerably along their trace. (Scott and Bonk 1984; Day et al. 1998a). The two-dimensional cross-section used for the basis of the modeling for this analysis (Section 6.2.1.4) intersects the Solitario Canyon, Ghost Dance, and Dune Wash faults.

Surface geologic mapping (Scott and Bonk 1984; Day et al. 1998a), underground mapping of the ESF, geophysical surveys, and borehole studies show that the Yucca Crest subblock is little deformed, and cut only by widely spaced intrablock faults (Ghost Dance and Dune Wash). Within structural blocks, small amounts of strain are accommodated along intrablock faults. In many cases, intrablock faults appear to represent local structural adjustments in response to displacements on the block-bounding faults. Many of the intrablock faults within this part of Yucca Mountain are short, discontinuous, have minor cumulative displacement (1 to 10 m), and represent the localization of slip along pervasive preexisting weaknesses in the rock mass (Potter et al. 1996a, 1996b). In some cases, intrablock faults are expressions of hanging wall or footwall deformation that affect the block within a few hundred meters of the block-bounding faults. The eastern and southern edges of the central block, however, are cut by numerous faults associated with block margin deformation (Solitario Canyon and Bow Ridge faults).

### **6.1.1.1 Fracture Attributes**

The fracture network acts as a significant preexisting weakness in the rock mass that can accommodate extensional strain through distributed slip along many reactivated joints. Evidence for reactivation of joints includes the presence of thin breccia zones along cooling joints and observable slip lineations along joint surfaces (Sweetkind, Potter, and Verbeek 1996). Cooling joints originally formed as tensional openings, having only face separation, not shear. However, thin selvages of tectonic breccia are often present along the trace of cooling joints, indicating later slip. Subsequent analyses performed here (see Sections 6.2.1 and 6.2.2.1) will consider the dilation or compression of any hydraulically connected fractures at Yucca Mountain, regardless of whether the fractures originated as tensional openings during cooling of the rock or from past seismic activity and regardless of distance from the fault.

There are a number of primary controls on fracture characteristics within the Paintbrush Group that are related to stratigraphy, upon which any later tectonic signature (such as fault displacement) is superimposed. Fracture characteristics in the pyroclastic flows at Yucca Mountain are primarily controlled by variations in the degree of welding (CRWMS M&O 1998c, Section 3.6). The intensity of fracturing increases with degree of welding within the welded pyroclastic flows because of the presence of cooling joints, and because increasing brittleness of the rock favors an increase in the number of tectonic joints. Lithophysal development, alteration, and pumice content are secondary controls important in specific stratigraphic intervals. These lithostratigraphic controls affect fracture spacing, type, number of sets, continuity of individual

fractures within each lithostratigraphic zone, and they also affect the fracture connectivity of the network as a whole (Sweetkind and Williams-Stroud 1996, pp. 60 to 66; Sweetkind, Barr et al. 1997, pp. 62 to 67).

Each lithostratigraphic zone at Yucca Mountain has characteristic fracture attributes, including predominant orientations, spacing, trace length, and joint type (Sweetkind, Barr et al. 1997, p. 76); each is unique in its ability to deform by distributed slip. The result is stratigraphic control of structural geometry—what may be a discrete break in one lithostratigraphic unit may be a broad zone of distributed deformation in another.

An analysis of fracture apertures is available from the ECRB Cross Drift Study (DTN GS990408314224.001 and GS990408314224.002). The largest aperture recorded was 520 mm. Approximately 64 percent of the observed fractures exhibited zero aperture. Of the over 1800 fractures measured, only 40 apertures were measured as greater than 20 mm, or about 2 to 3 percent. The remaining apertures were less than 20 mm.

The relationship of fractures smaller than 1 m in length to faults was evaluated by visual examination of every fault in the ESF (Sweetkind, Barr et al. 1997, p. 68) that could be correlated with a fault mapped at the surface (Day et al. 1998a). Four principal conclusions were reached, based on observations in the ESF (Sweetkind, Barr et al. 1997, pp. 68, 71).

The first conclusion is that the width of the zone of influence on fracture frequency in the immediate vicinity of a fault is, in general, quite narrow, ranging from less than 1 m to about 7 m from the fault.

The second conclusion regarding the relationship between faults and fracture attributes is that the width of the zone of influence in the immediate vicinity of a fault correlates, in a general way, with the amount of cumulative fault offset. Therefore, faults with the largest potential future displacement are the most likely to influence the potential repository block. Intrablock faults with very small amounts of cumulative offset (1 to 5 m) have zones of influence that are 1 to 2 m in width. Block-margin faults with tens of meters of cumulative offset (faults at ESF Stations 11+20 and 70+58) have zones of influence that range up to 6 to 7 m wide. The limited available data from block-bounding faults are not definitive regarding the nature of attendant fracturing.

The third conclusion is that the width of the zone of influence around a fault does not appear to be related to depth, at least within the ESF. The width of the zones of influence is similar for small faults observed along the North Ramp, where overburden is 50 to 60 m thick, as it is for small faults observed elsewhere in the ESF, where overburden thickness is two to three times greater. However, upward-splaying faults can result in apparent broad zones of influence at the surface because of the overlap of fractured zones surrounding individual fault splays.

The fourth conclusion is that the amount of deformation associated with faults appears, in part, to be dependent upon which lithologic unit is involved in the faulting. In the ESF, overall variability in the frequency of fractures 1 m long or longer is primarily a function of lithology, not proximity to faults (Sweetkind, Barr et al. 1997, p. 68). Fracture intensity correlates to lithologic differences, lowest in lithophysal units and nonwelded to partially-welded tuffs, and

highest in densely welded, nonlithophysal rock. Faults within nonwelded to partly welded portions of the crystal-poor vitric zone of the Tiva Canyon Tuff are generally sharp, discrete breaks with minimal fault gouge or secondary shear surfaces. Individual pumice clasts along some faults can be traced to the fault surface without visible sign of breakage, and wall rocks show little evidence of deformation. In comparison to brittle, welded rocks, nonwelded units apparently can accommodate a greater amount of extensional strain before failing by fracture.

### 6.1.1.2 Fault Attributes

Information on the significant faults present in the repository area follow. The three faults that are included in the two-dimensional cross-section used in this analysis (Solitario Canyon, Ghost Dance, Dune Wash) are specifically described. Neither the Bow Ridge nor the Sundance faults are included in the two-dimensional cross-section used for the modeling portion of the analysis. However, information for these faults is pertinent for discussion about the reasonableness of bounding conditions.

In the following descriptions fault length refers to the maximum length of a given fault or fault zone as reported or shown on maps in published references (e.g., Piety 1996). Unless otherwise indicated, the following descriptions for regional faults, including temporal and behavioral data, are from Piety (1996), and the field reconnaissance work is from Anderson, Bucknam et al. (1995) and Anderson, Crone et al. (1995). Piety's report (1996) is an excellent synthesis of most of the data available for characterizing regional faults, and contains an extensive list of published references.

**The Solitario Canyon Fault Zone (SCFZ)** The SCFZ is the most laterally continuous fault and displays the most total offset of any structure in the immediate vicinity of Yucca Mountain. Day et al. (1998a, p. 6) consider the SCFZ to be one in a series of major north-south trending, block-bounding faults. The fault has been extensively investigated by trenching at the surface in Solitario Canyon (Ramelli et al. 1996). The Solitario Canyon fault has normal down-to-the-west displacement of about 260 m near the potential repository block and is the most significant of the faults involved in this analysis.

The main trace of this fault extends southward from Yucca Wash for about 18 km. It is located about 1 km from the western boundary of the potential repository site (Simonds et al. 1995). Total bedrock displacement varies from 61 m down-to-the-east at the northern end, to more than 500 m down-to-the-west at the southern end (Scott and Bonk 1984). Average dip of the fault plane is 72°W. Slickensides indicate a component of left-lateral slip.

A continuous 14 km-long Quaternary tectonic and erosional scarp is present at the bedrock-surficial deposit contact. Trenching evidence suggests four to six mid- to late-Quaternary surface-rupture events. The evidence for these events provides an estimated cumulative dip slip of  $2.2 \pm 0.4$  m (Ramelli et al. 1996). Preliminary average slip rates range from 0.01 to 0.02 mm/yr (Ramelli et al. 1996). Minimum and maximum individual displacements range from 0 to 1.4 m, based on data for events more recent than 500 kilo-annum.

Map patterns demonstrate that tectonic mixing of various Paintbrush Group lithologies has occurred within the most intensely deformed parts of block-bounding fault systems. This is most

apparent in the Solitario Canyon fault system (Scott and Bonk 1984; Day et al. 1998a). In this system, which is up to 400 m wide, there are domains in which lenses from stratigraphically diverse parts of the Tiva Canyon Tuff are juxtaposed; similar zones in which slices of Topopah Spring Tuff are mixed; and several areas where lenses from more than one Paintbrush Group formation are tectonically mixed (Day et al. 1998a). Individual fault strands within these tectonically-mixed zones are highly brecciated, and in some cases, the fault-bounded lenses have a high degree of internal brecciation.

The SCFZ was not crossed during the ESF excavation. In the ECRB Cross Drift, the SCFZ was expected to be composed of two major normal fault strands; the first (eastern strand) was projected as the “main splay” with a predicted total offset of about 230 m. The second (western strand) was projected with a predicted cumulative offset of about 165 m (CRWMS M&O, 1998e). Between these two larger strands, several smaller faults were expected to be associated with the SCFZ faulting. The tunnel boring for the ECRB Cross Drift was stopped between the two strands based on programmatic considerations, and the western strand was not intersected.

The as-built geologic cross-section for the ECRB Cross Drift (DTN GS990408314224.006) shows that the eastern strand was encountered at Station 25+85 (Station 25 means 2500 m from the start of the survey line and +85 means 85 m from that Station point) and has approximately 260 m of cumulative normal offset. Shears and small faults increase in intensity prior to (east of) of Station 25+00. The SCFZ influences rock in the footwall of the fault to about Station 25+00 (or approximately 85 m from the fault proper) in the form of increased shear intensity. Spacing of faults and shears decreases, while continuity and amount of cumulative offset increases with proximity to the eastern strand of the SCFZ. At Station 25+30, a small fault oriented 200/83 is intercepted by the tunnel. Although the cumulative offset along the fault is approximately 1 m or less, the rock is intensely fractured after (west of) Station 25+40. The rock from Station 25+80 to 25+82 (between 3 and 5 m from the fault) is a clast-supported breccia. The rock is shattered to the point of not having recognizable structure. From Station 25+82 to 25+85, the rock is a clast-supported breccia. The main plane of displacement along the eastern strand of the SCFZ is at Station 25+85, (left wall, springline). The fault plane is defined by an 8 to 12 cm thick zone of fault gouge composed of about 85 percent clay and about 15 percent fine to medium sand. The gouge is firm and was slightly damp at the time of excavation in October 1998, but dry by February 1999. On the west (hanging wall) side of the fault plane described above, there is a zone of matrix-supported breccia that extends along the left wall from Station 25+85.5 to 25+89.90. The farthest western zone along the eastern strand of the SCFZ is composed of a clast-supported breccia extending along the left wall from Station 25+89.9 to 25+99.15 (or a distance of approximately 14 m west of the fault). This zone is bounded on the west side by a thin, discontinuous, matrix-supported breccia about 10 to 20 cm thick.

**Ghost Dance Fault Zone**—The Ghost Dance fault is in the central part of the potential repository block. It is mapped for approximately 3 km as a zone of numerous splays that not only parallel the main north-trending trace of the zone, but locally branch away from the main trace. In general, it is a north-striking normal fault zone, dipping steeply west (75° to 85°) with down-to-the-west displacement. The Ghost Dance fault bifurcates; one branch connects with the Abandoned Wash fault to the southwest (Scott and Bonk 1984; Day et al. 1996), and a second

branch trends southeast, but does not appear to connect with the Dune Wash fault (Day et al. 1996) subdivided the fault into three sections on the basis of cumulative offset and brecciation.

Along the northern segment, north of Split Wash, the fault is a relatively narrow zone (2 to 4 m wide) with as much as 6 m of down-to-the-west total displacement.

The central segment of the Ghost Dance fault zone has greater down-to-the-west displacement than the northern segment, and extends from Split Wash to Broken Limb Ridge. On Antler Ridge, there is 13 to 20 m of cumulative displacement across several splays of the Ghost Dance that are distributed over a map width of approximately 100 to 150 m (Day et al. 1998a, p. 9). Individual splays are characterized by 1 to 2 m-wide breccia zones.

To the south on Whale Back Ridge, the fault zone is about 55 m wide and has about 30 m cumulative down-to-the-west offset. There, the zone is bounded by two north-striking faults. The eastern fault is the main trace of the Ghost Dance. Locally, the immediate hanging wall of the principal splay of the Ghost Dance fault is highly fractured. On the south-facing slope of Broken Limb Ridge, the cumulative offset is less than 6 m, and intense fracturing in the hanging wall extends about 15 m to the west.

The amounts of displacement and brecciation along the southwestern projection of the Ghost Dance fault across Highway Ridge are considerably less than those preserved along the central segment. Cumulative offset on the fault increases to the southwest from Ghost Dance Wash, becoming about 17 m down-to-the-west in Abandoned Wash on the eastern splay of the Abandoned Wash fault (Day et al. 1998a, p. 10).

In the Ghost Dance Wash area (near the southern bend in the ESF), displacement on the fault is less than 3 m both on the surface and in the ESF, and deformation is also confined to a relatively narrow zone (2 m) of intense fracturing and brecciation.

The Geotechnical Baseline Report (CRWMS M&O 1998d, p. 4-15) stated that the Ghost Dance fault might be encountered in the ECRB Cross Drift, but the fault should have minimal cumulative offset. The geologic cross section from the Baseline Report accurately predicted the fault in the vicinity of Station 4+80. A shear (i.e., less than 0.1m displacement) was encountered at Station 4+99 (left wall, springline) which has been identified as the northern distal end of the Ghost Dance fault. This feature is the only north-trending, conspicuous discontinuity in this portion of the tunnel. The feature consists primarily of a 1 to 10-cm thick zone of silty/sandy gouge with clasts. The gouge thickens slightly in the crown to 10 cm, but is only 2 to 4-cm thick elsewhere. The gouge is surrounded by a zone of intensely fractured and crushed rock. On the right wall, this fractured zone is approximately 0.4 m thick on the east side of the feature, and 0.6 m thick on the west side of the feature (DTN GS990408314224.003) .

**Dune Wash Fault**—This south- and southeast-trending fault is mapped along the eastern side of the potential repository site for a distance of 3 km. It is mapped in exposures of bedrock as a west-dipping normal fault with down-to-the-west displacement. Toward the northern end of the fault, Tertiary volcanic rocks are displaced a total of 50 to 100 m (Day et al. 1996, 1998b; Scott and Bonk 1984). However, no evidence of Quaternary movement has been found in surficial deposits that bury the fault toward the south, and no per-event displacement data are available.

The Dune Wash fault is exposed in the ESF near Station 67+88, where the cumulative offset is 65 m (Sweetkind, Barr et al. 1997, Table 21), and the zone of increased fracture frequency in the vicinity of the fault is 6 to 7 m wide. This fault was not encountered in the Cross Drift.

**Sundance Fault**—The Sundance fault is located in the north-central portion of the potential repository block and lies northward of the line of the two-dimensional model cross section used in the model for this analysis.

A detailed investigation of the Sundance fault has been conducted by Potter et al. (1999). The maximum width of the Sundance fault zone is about 75 m, and the cumulative down-to-the-northeast vertical displacement across the fault zone does not exceed 11 m. The faults in this zone are almost exclusively characterized by down-to-the-northeast displacement (Potter et al. 1999, pp. 5 to 6). Even though some horizontal slickensides have been observed, significant strike-slip displacement along the Sundance fault zone is not evident. Potter et al. (1999, p. 9) concluded that the Sundance fault zone has a significantly smaller along-strike extent than had been suggested by previous workers.

Individual faults in the Sundance fault zone and elsewhere at Yucca Mountain are vertically and laterally discontinuous; one or more mechanisms of strain accommodation must operate in the Tiva Canyon Tuff to accommodate displacements in the rock volume between the discontinuous discrete fault segments. Two probable mechanisms are: distributed brittle deformation associated with diffuse breccia bodies, and minor cumulative offsets along numerous preexisting cooling joints (Potter et al. 1999, pp. 13 to 14).

The ESF passes beneath the southeastern end of the Sundance fault zone, as mapped by Potter et al. (1999), where displacement is minimal on the south flank of Live Yucca Ridge. In the ESF, the fault is identified within a broad zone of discontinuous minor northwest-striking faults and joints in the middle nonlithophysal zone of the Topopah Spring Tuff. The exposure in the ESF is similar in character to the fault zone mapped at the surface near its southeastern termination on the south-facing slope of Live Yucca Ridge (Potter et al. 1999, p. 8; Day et al. 1998a).

The Geotechnical Baseline Report (CRWMS M&O, 1998e, p. 4-15) predicted the Sundance fault to be near Station 10+70 to 11+00. The Sundance fault was encountered along the left wall at Station 11+35.40 to 11+36.70 (DTN GS990408314224.003). The fault intercepts the right wall at Station 11+35 to 11+36.2, approximately 35 m southwest of the location predicted. The amount of displacement is thought to be on the order of several meters, but is indeterminate. The margins of the fault zone were unaltered except in the immediate area of the fault, which exhibits some iron oxide stainings along the right wall. All portions of the Sundance fault were dry at the time of excavation.

The fault zone is composed of three distinct zones along the left wall. Zone 1 is adjacent to the footwall plane, and is a matrix-supported, uncemented breccia. Zone 1 is approximately 20 cm thick on the left wall, thinning to 4 cm on the right wall. Zone 2 along the exposure of the Sundance fault is approximately 0.7 m thick and is a matrix-supported breccia. Zone 3 varies in thickness from 0.3 m on the left wall, to zero on the right wall. Despite the very sharp and distinct plane of the fault at the footwall, distinct slickensides are not evident. Faint, low-angle slickensides can be interpreted on the left wall, and undulations in the fault plane with low-angle

plunges occur at the boundary between Zones 1 and 2. The footwall rock is intact, even within 10 cm of the fault plane. The hanging wall is slightly more fractured, with an intensely fractured zone about 1 m thick.

**Bow Ridge Fault**—This fault is a prominent north-striking, west-dipping, normal-oblique (sinistral) slip fault. It is about 10 km long and lies along the east side of the potential repository area. The fault is buried beneath alluvium and colluvium for most of its extent along the western margin of Midway Valley. The best topographic expression of the fault occurs where a 760-m-long section follows the base of the west side of Exile Hill (Simonds et al. 1995; Menges and Whitney 1996; Menges et al. 1997). Tertiary volcanics are displaced at least 125 m down-to-the-west at this locality. The fault dips 65°E to 75°E.

Trenches on the surface and the ESF expose a complex fault zone in highly-fractured Tertiary volcanic bedrock and colluvial deposits that have been subjected to multiple Quaternary faulting events. At least two and possibly three surface-rupture events are evident in late to middle Pleistocene colluvial deposits at trench 14D (Menges and Whitney 1996; Menges et al. 1997). A minimum age of  $48 \pm 20$  kilo-annum is established for the most recent surface-rupture event. Displacements range from 14 to 44 cm for individual faulting events, and cumulative displacement is from 30 to 70 cm for all events younger than 500 kilo-annum. Average recurrence intervals vary from 70 to 215 kilo-annum. Recurrence intervals for individual events vary more widely from 40 to 350 kilo-annum. Average slip rates are 0.002 to 0.007 mm/yr (Menges and Whitney 1996; Menges et al. 1997).

The Bow Ridge fault has very little attendant fracturing despite the 100 m cumulative offset and its exposure near the surface (approximately 35 m of overburden). Lack of deformation around the fault zone probably results from the presence of nonwelded pre-Rainier Mesa Tuff in the hanging wall of the fault.

### 6.1.1.3 Significance of Geologic Setting to the Analysis

The descriptions in Sections 6.1.1.1 and 6.1.1.2 suggest that an analysis of fault displacement effects needs to be considered from two perspectives: the impact on fractures throughout the potential repository as a whole, and the effect on fractures in the immediate vicinity of the faults only. Furthermore, the range of fault characteristics that was described supports the idea that movement on the Solitario Canyon fault may be considered the bounding scenario.

As stated in Section 6.1.1.1, the fracture network at Yucca Mountain acts as a significant preexisting weakness in the rock mass that can accommodate extensional strain through distributed slip along many reactivated joints. Evidence for reactivation of joints includes the presence of thin breccia zones along cooling joints and observable slip lineations along joint surfaces (Sweetkind, Potter, and Verbeek 1996). There are a number of primary controls on fracture characteristics within the Paintbrush Group that are related to stratigraphy, upon which any later tectonic signature (such as fault displacement) is superimposed. The existence of distributed slip suggests that changes in strain (such as would be associated with a significant fault displacement) are likely to be propagated throughout the repository area. Also, some fault zones (such as the Ghost Dance and Solitario Canyon) may be on the order of 100 to 400 m wide. Although strain is expected to diminish with distance from the fault, these observations

suggest that the effect of strain distributed in the fractures throughout the potential repository should be considered (Sections 6.2.2.1 and 6.2.2.2).

The presence of gouge and brecciated zones only in limited proximity to the fault planes, however, suggests that much of the strain will be mechanically dissipated within or near the fault plane itself. For instance, as described in Section 6.1.1.2, in the Solitario Canyon fault zone in the ECRB Cross Drift, the total displacement is approximately 260 m, but the gouge and brecciated zones are limited to less than 20 m. Similarly, the Dune Wash fault as exposed in the ESF exhibits a cumulative offset of 65 m (Sweetkind, Barr et al. 1997, Table 21), but the zone of increased fracture frequency in the vicinity of the fault is only 6 to 7 m wide. A third example is the observation of the Sundance fault in the ECRB Cross Drift; with an assumed, though indeterminate displacement of several meters, the footwall rock is intact, even within the 10 cm of the fault plane. The hanging wall is slightly more fractured, with an intensely fractured zone about 1 m thick. Consequently, an analysis of fault displacement should also consider a case where the effects of strain are limited to the immediate vicinity of the fault zone (Section 6.2.2.3).

### 6.1.2 Fault Displacement Hazards

Fault displacement hazards at Yucca Mountain have been investigated in detail in the report “Probabilistic Seismic Hazard Analyses for Fault Displacement and Vibratory Ground Motion at Yucca Mountain, Nevada” (CRWMS M&O 1998e). Several original approaches to characterizing the fault displacement potential were developed by the seismic source expert teams. The approaches were based primarily on empirical observations of the pattern of faulting at the site during past earthquakes (determined from data collected during fault studies at Yucca Mountain). Empirical data were fit by statistical models to allow use by the experts. The results of this analysis were curves representing probabilistic predictions of fault displacements.

Nine locations within the preclosure controlled area were identified to demonstrate the fault displacement methodology. The term “preclosure controlled area” is defined in DOE’s Interim Guidance (Dyer 1999). These locations were chosen to represent the range of potential faulting conditions. Two of the nine sites each had four identified faulting conditions. Some of these locations lie on faults that may experience both principal faulting and distributed faulting. The other points are sites only of potential distributed faulting.

With the exception of the block-bounding Bow Ridge and Solitario Canyon faults (sites 1 and 2, respectively), the mean displacements are 0.1 cm or less at a  $10^{-5}$  annual exceedance probability, and on the order of 1 m or less at  $10^{-8}$  annual exceedance probability (USGS 1998, Figures 8-4 through 8-14). For the Ghost Dance fault, the range of displacements per event is 0.6 m to about 1.5 m at  $10^{-8}$  mean annual exceedance probability (USGS 1998, Figure 8-5). Thus, sites not located on a block-bounding fault, such as sites on the intrablock faults, other small faults, shear fractures, and intact rock, are estimated to have displacements significantly less than 0.1 cm for mean annual exceedance probabilities of  $10^{-5}$ .

For Solitario Canyon fault and Bow Ridge fault (USGS 1998, Figures 8-2 and 8-3), the mean displacements are 7.8 and 32 cm, respectively, for these two faults at a  $10^{-5}$  annual exceedance

probability. At lower annual exceedance probabilities, the fault displacement hazard results are driven by the upper tails of uncertainty distributions and are close to 5 m.

For purposes of determining the appropriateness of the chosen bounding conditions based on the Probabilistic Seismic Hazard Assessment, per-event displacements can be used as a comparison. As described in Section 6.1.1 above, the largest estimate of per event displacement for the faults intersected by the 2-D cross section used for the analysis is 1.4 m along the Solitario Canyon fault. A displacement of 1.2 m corresponds to the 15<sup>th</sup> fractile curve at a 10<sup>-8</sup> annual exceedance probability. (USGS 1998, Figures 8-3). As described in Section 6.2.1.5, strains associated with a displacement of 10 m are used as bounding conditions. Given that the assumed bounding condition is about a factor of 10 greater than measured displacement and the probabilistic displacement event suggested by the 15<sup>th</sup> fractile curve, the values used in this analysis are judged to be extremely conservative.

### **6.1.3 Climate Data**

The primary controlling factor for flow through the UZ is the amount of infiltration through the system. This variable is highly dependent on precipitation and climate conditions. To address this constraint, present-day average and long-term average conditions were used as bounding conditions.

Present day climate conditions represent relatively dry, interglacial conditions, while the long term average conditions represent typical conditions at Yucca Mountain between the wet and dry extremes based on available paleoclimate data. (CRWMS M&O 1998a, Section 2.4.1.1). Because these two sets of conditions represent relatively stable (i.e., long-term conditions) rather than extreme conditions (i.e., short-duration climatic states such as superpluvial periods), they were chosen as representative conditions for this analysis.

The primary difference in these conditions is a doubling of the precipitation rate, with an approximately 6- to 8- fold increase in the average net base infiltration rates (CRWMS M&O 1998a, Table 2-5 and Table 2-16). The total water influx used for the two-dimensional model for the present-day climate is 0.11471 kg/s (3.2 mm/yr), while the total water influx to the model for the long-term average climate is 0.98413 kg/s (27.3 mm/yr).

## **6.2 EFFECTS OF FAULT DISPLACEMENTS ON UZ FLOW AND TRANSPORT**

As discussed in Section 6.1, fault displacements are expected to occur along existing faults in the vicinity of Yucca Mountain. The movement produced by a fault displacement will result in changes in the rock stress in the vicinity of the fault. Obviously, the change in rock stress will decrease with distance from any given fault that does move. However, the magnitude of the changes in rock stress as a function of distance from the fault depends on the specific details of the fault displacement (e.g., magnitude of fault motion, direction of fault movement, extent of the fault that participates in the movement) and the mechanical properties of the surrounding rock (e.g., fracture spacing, fracture stiffness, geomechanical properties of the rock matrix). Given some change in rock stress, the fractured rock mass will respond to the change in stress through deformation, or strain, in the rock. Of particular importance is the fact that this induced strain can affect the geometry of fractures in the rock, as discussed in Section 5.2. The effects of

changes in properties of the rock matrix (as opposed to the fractures) are assumed to have a negligible effect on UZ flow and transport (Section 5.2). In theory, the effects of a given fault displacement could be evaluated using process-level calculations for the effects of the induced stress and strain on fracture geometry. Then the effects of this change in fracture geometry on the fluid-flow properties of the fracture network could be evaluated. However, this method was not used in this analysis due to the large uncertainty and complexity of the problem.

Some of the effects of previous fault displacements at Yucca Mountain can be examined directly. Previous fault displacements have resulted in observable changes to the structure of the surrounding rock (Section 6.1.1). However, geologic observations are not adequate to assess the effects of some of the changes caused by fault displacements that could be important to UZ flow and transport. In particular, the effects of previous fault displacements on the present-day fracture apertures at Yucca Mountain are difficult to determine by observation. For example, it is difficult to determine by geologic observation that a given fracture with an effective hydraulic aperture of, say 200 : m, may have had an effective hydraulic aperture of 150 : m at some point in the past prior to a fault displacement event. In fact, it is difficult to determine the effective hydraulic apertures of the present-day fractures at Yucca Mountain by direct observation (Sonnenthal et al. 1997, Section 7.5.4). Fracture apertures at Yucca Mountain are determined through pneumatic flow tests (giving the fracture permeability) and a theoretical model relating fracture frequency (determined by observation of fractures), fracture permeability, and fracture aperture (Sonnenthal et al. 1997, Section 7.5.4).

### 6.2.1 Analysis Approach

In the absence of definitive, predictive process modeling or definitive geologic observational evidence, a bounding approach is used to assess the potential effects of fault displacement on potential repository performance. As a corollary to the assumptions in Section 5.2 and Section 5.3, the problem is assumed as bounded if large enough changes in fracture aperture are evaluated. Here, “large enough changes” are defined to be changes that can be justified as larger than any expected changes resulting from any fault displacements (in the vicinity of Yucca Mountain) that have an annual exceeding probability greater than  $10^{-8}$ . Given an assumed change in aperture, it is possible to estimate the change in fracture hydraulic properties using theoretical models that relate the changes in fracture properties to the changes in fracture aperture (see Section 6.2.1.3). The effects of the modified fracture properties on transport behavior between the potential repository and the water table can be evaluated using the UZ site-scale flow and transport models. Changes in transport are identified through the use of breakthrough curves (see Section 6.2.1.2) for a simulated non-diffusing, non-sorbing tracer as described in Section 5.4. If the identified changes in transport are small, then it can be concluded that the effects of fault displacement on potential radionuclide transport are negligible and can be excluded from further consideration in TSPA.

For such a method to be valid, the assumed changes in fracture aperture must be shown to represent a bounding change in fracture aperture for the effects of any fault displacement in the vicinity of Yucca Mountain. The justification that the assumed changes in fracture aperture bound the range of expected changes is given in Section 6.2.1.3.

The spatial distribution of changes to fracture aperture within the modeling domain is treated using two end-member scenarios (Section 5.5):

1. All fracture apertures are altered uniformly throughout the UZ model domain (both fault zones and fractured rock).
2. Only fracture apertures in the faults zones are altered.

The first scenario bounds the most widespread disturbance possible. The second scenario considers the possibility that the effects of fault displacement remain local to the fault zones. The second scenario is also used to investigate the potential sensitivity associated with an enhanced contrast in properties between the fault zones and the fractured rock.

Sensitivity calculations are performed for both the present-day (dry) climate and the long-term, glacial-transition (wetter) climate (CRWMS M&O 2000g). The average infiltration rates used in the TSPA-SR UZ flow model for the present-day mean climate is about 4.6 mm/year and for the glacial-transition mean climate is about 18 mm/year (CRWMS M&O 2000g).

The site-scale TSPA-SR model for UZ flow and radionuclide transport is based on a three-dimensional spatial domain. For illustrative purposes, due to their simplicity, one-dimensional and two-dimensional portions of the three-dimensional domain were also used in this study.

Several additional assumptions are also implicitly used in this modeling approach. These implicit assumptions, and the bases for these assumptions, are given in Sections 5.5 through 5.10.

#### **6.2.1.1 Dual-Permeability Concept**

The conceptual model for unsaturated flow and transport used in this analysis is called the dual-permeability model. In the version of the dual permeability model used in this analysis, there are two continua representing the fracture and matrix that overlap in the macroscopic flow continuum. At every macroscopic “point” we have separate hydrologic conditions, properties, and other factors, for the fracture continuum and for the matrix continuum. Therefore, at every macroscopic “point” there is also a defined flux of water (flow rate of water per unit area) in the fracture continuum and in the matrix continuum. Practically speaking, the macroscopic point (or length scale) is defined by the grid discretization. At the microscopic (or sub-grid) scale, the fractures and matrix are spatially distinct, with length scales that define the microscopic geometric arrangement of the fracture and matrix continua. Given this microscopic geometry of the continua and the properties and conditions defined in each continuum, a flux of fluid at each macroscopic point between the fracture and matrix continua is also defined. In other words, there is also an exchange of flow between the fracture and matrix continua as well as flow through each continuum at each macroscopic point.

Although the dual-permeability model has been described above in terms of a flow model, an analogous description can also be made for the transport model. That is, transport takes place at each macroscopic point in both the fracture and matrix continua (each continuum having its own transport properties and conditions), and there is, likewise, a transport exchange between the fracture and matrix continua.

The dual-permeability model for flow and transport can be used in three, two or one dimension. For example, a one-dimensional problem would have flow and transport in one linear direction only. This is easiest to understand for a problem in which flow occurs along one axis, say the  $z$ -axis. Assume that the rock properties and conditions at the boundaries of the model are independent of the remaining two spatial coordinates,  $x$  and  $y$ . Then the only spatial variations that could possibly occur in the problem are in the  $z$  direction. The spatial evolution of the problem can be completely described in terms of  $z$ . The  $x$  and  $y$  dimensions only enter the problem in a trivial sense to scale the total quantity of flow and transport that take place in the real three-dimensional domain. This simple scaling can be done after analyzing the spatial (and temporal) variations in the problem. Numerically, the one-dimensional dual-permeability model is configured using a stack of paired grid cells as shown in the one-dimensional connection diagram give in Figure 1. One stack represents the fracture continuum and one stack represents the matrix continuum. The dual-permeability connection diagram can be extended to two dimensions as shown in Figure 2. In three dimensions, the conceptual nature of the dual-permeability model (with overlapping continua) becomes more apparent in so far as a connection diagram is concerned. In this case, there is no “extra” dimension for the fracture/matrix node pairing, so the fracture/matrix node pairs must overlap spatially in a three-dimensional connection diagram.

#### **6.2.1.2 Active Fracture Concept**

The dual-permeability model used in this Rev 01 of the AMR differs from Rev 00 in that it employs the active fracture concept. The active-fracture-dual-permeability model (Liu et al. 1998; CRWMS M&O 2000f) takes into account of the possible situation where only a portion of the fracture network (conceptualized as a continuum in the dual-permeability model) is actively involved in conducting water, whereas other fractures can be bypassed. It conjectures that only a portion of the fracture network is hydraulically active and only this active portion is in hydraulic contact with the rock matrix. As a result of such conceptualization, capillary pressure and relative permeability for the entire fracture network are treated as equal to those for the active portion, and the geometric fracture-matrix interface area is scaled down to define an active fracture-matrix interface area for use in fracture-matrix interaction. Therefore, the mechanism of the active fracture model hinges upon how the active fracture network is defined. In the UZ flow model used for this AMR, the fraction of active fractures is defined as an exponential function of the effective water saturation for the entire fracture network, with the exponent being treated as a fitting parameter. Subsequently, the capillary pressure and the relative permeability functions for the entire fracture network are defined by using the effective water saturation of active fractures. In addition, the active fracture-matrix interface area is defined as the geometric fracture-matrix interface area multiplied by a power function of the effective water saturation of the active fractures.

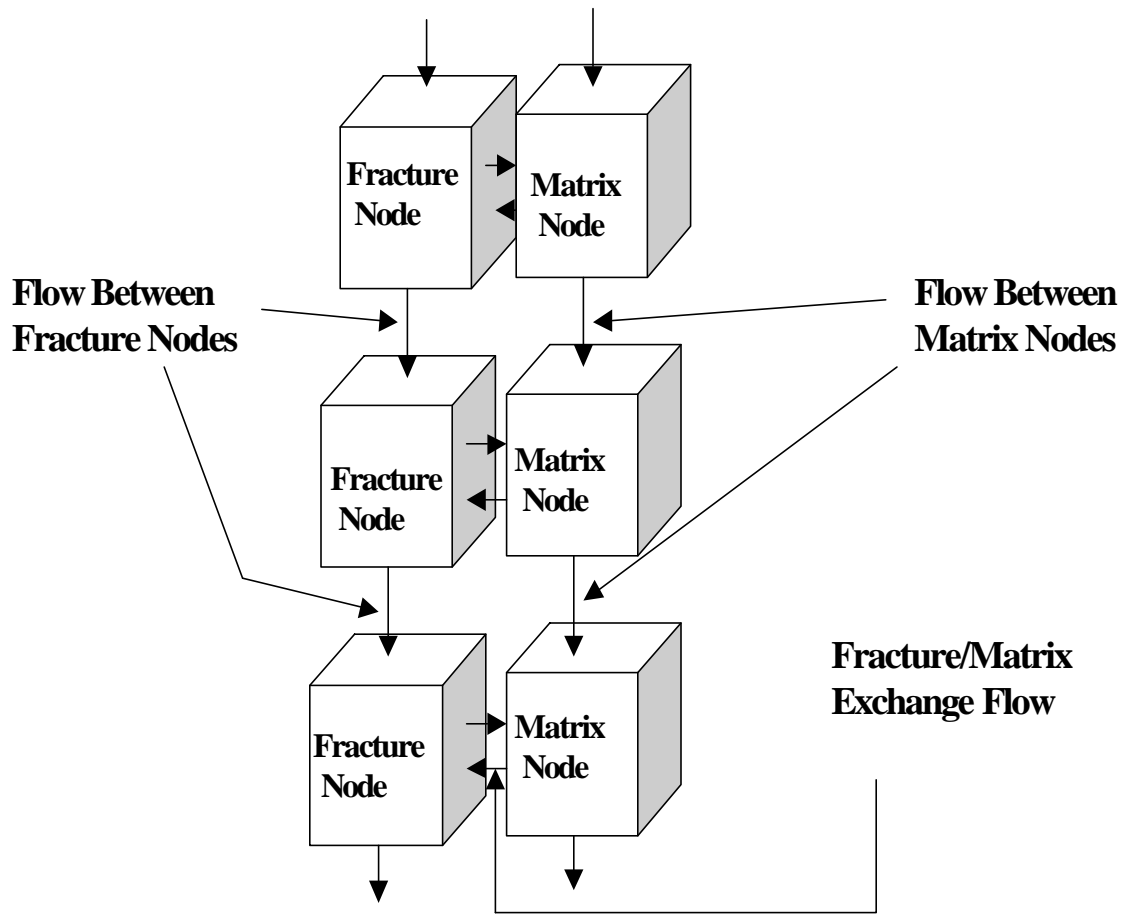


Figure 1. Conceptual Connection Diagram for a One-Dimensional Dual-Permeability Model

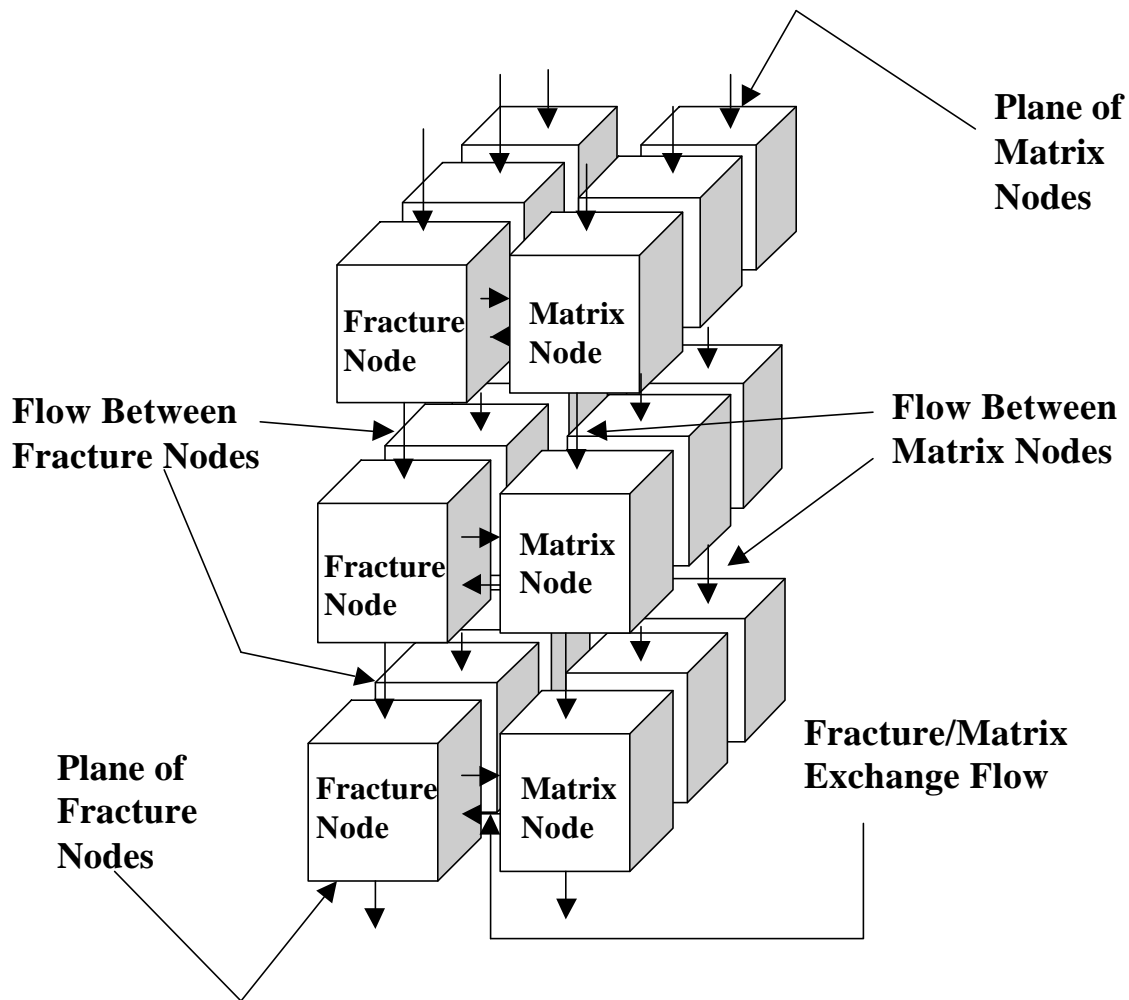


Figure 2. Conceptual Connection Diagram for a Two-Dimensional Dual-Permeability Model

### 6.2.1.2 Site-Scale Models for UZ Flow and Transport

The site-scale model for UZ flow uses the software TOUGH2 V1.4 (Wu et al. 1999). TOUGH2 is a multi-purpose numerical model that, among other problems, can solve fluid flow problems in geologic materials (Pruess 1991). The standard differential conservation equations describing flow are cast in an integrated form for the numerical solution methods used in TOUGH2. The solution to these conservation equations is obtained by discretization of problem in space and time. In this analysis, TOUGH2 is used to solve the equations for unsaturated flow in a fractured rock domain representative of Yucca Mountain. Unsaturated flow is defined to be the flow of water only in a geologic material with pore spaces partially filled with water and partially filled with air. In an unsaturated flow model (as opposed to a two-phase flow model), the air is assumed to be at static equilibrium. As discussed in Section 6.1.2.1, fractured rock is represented using an active-fracture-dual-permeability conceptual model.

The site-scale model for UZ transport uses the software FEHM V2.00 (Dash and Zyvoloski 1999). FEHM is a multi-purpose numerical model that, among other capabilities, can solve mass transport problems in geologic materials. The transport solution technique used in this analysis

is a particle tracking method based on a residence-time-transfer-function approach (Zyvoloski et al. 1995, Section 8.3.3.2). Particle tracking methods solve the transport problem by following the motions of simulated particles through geologic material. The motions of the particles are subject to the processes known to affect transport (i.e., flow, diffusion, sorption, and dispersion). However, rather than solving for the effects of these processes through the conservation equations, the effects are determined directly through the motion of particles over the spatial and temporal domain of the problem.

### 6.2.1.3 Breakthrough Curves

Breakthrough curves are used in this analysis to describe the behavior of radionuclide transport in the unsaturated zone. A breakthrough curve is generated by releasing particles uniformly over the fracture nodes of all the grid cells within the potential repository. Particles are only released to the fracture nodes because fractures are expected to be the main transport pathway at the repository horizon. Particles are released over some time period (short relative to the transport time of the problem), approximating an “instantaneous” release of the particles. For this analysis, the particles are released uniformly over a period of one year. The breakthrough curve shows the total mass that has arrived at the water table (over the entire model domain) relative to the total mass released as a function of time, as shown in Figure 3.

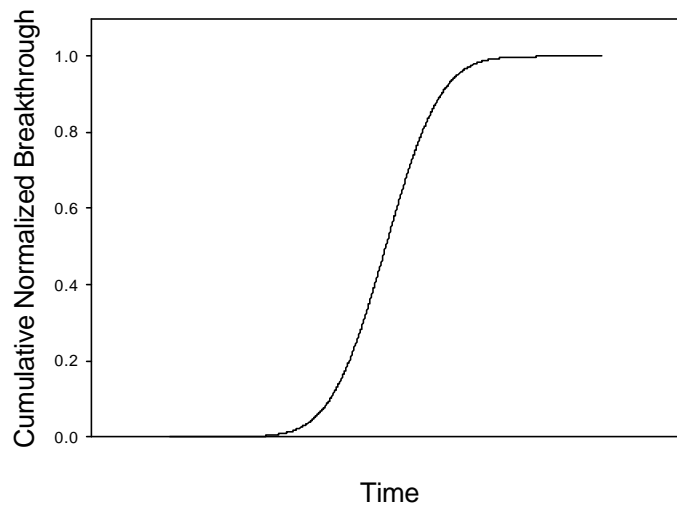
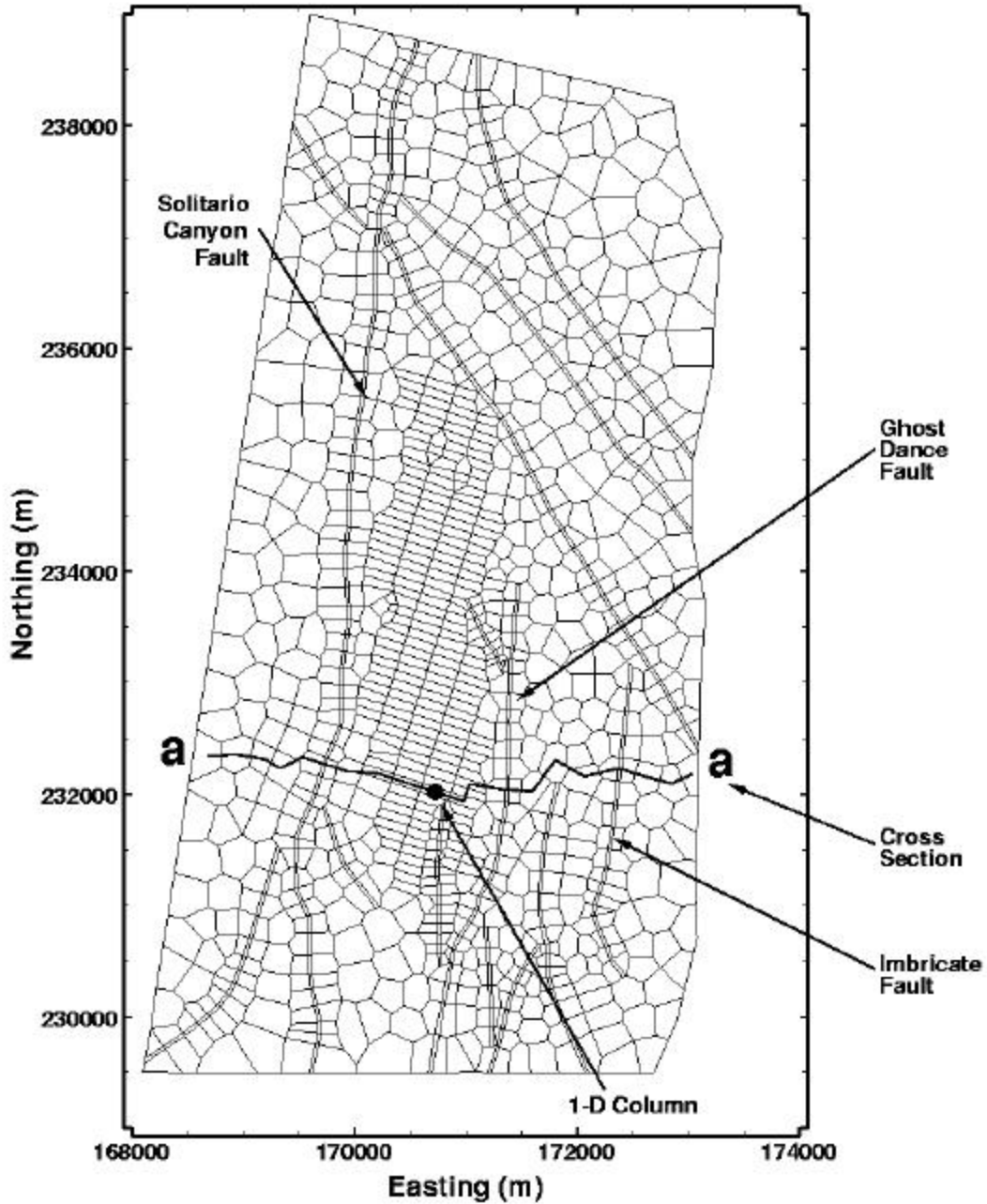


Figure 3. Schematic Diagram of a Breakthrough Curve

### 6.2.1.4 Problem Domain

The TSPA-SR site-scale UZ flow and transport model is shown in plan view in Figure 4 (CRWMS M&O 2000g). An east-west vertical cross-section and a one-dimensional column are extracted from this three-dimensional model for some sub-dimensional calculations. Figure 4 shows the locations of the 2-D vertical cross-section (a-a) and the column (C) within the three-dimensional UZ grid. The selected cross-section passes through three major faults in the region: counting from the west toward the east, the Solitario Canyon fault, Ghost Dance fault, and the Imbricate fault.



mView 2.20Q  
21 Jun 2009

Figure 4. Plan View of the Locations of the Two-Dimensional Cross Section and the Nearby Faults within the TSPA-SR UZ Grid. The Location of the One-Dimensional Column Is Shown with a '•' Symbol.

### 6.2.1.5 Bounds on the Change in Fracture Aperture

As discussed in Section 6.2.1, the approach used to investigate the effects of fault displacements is to evaluate the sensitivity of radionuclide transport in the UZ to changes in fracture apertures. This is investigated over a wide enough range to bound the potential changes in fracture aperture that could result from any fault displacement at Yucca Mountain with an annual exceeding probability of greater than  $10^{-8}$ . As discussed in Section 6.1.1, the largest fault movement close to the potential repository is likely to be along Solitario Canyon fault. The general topic of seismic hazard at Yucca Mountain has been investigated in detail in the report "Probabilistic Seismic Hazard Analyses for Fault Displacement and Vibratory Ground Motion at Yucca Mountain, Nevada" (CRWMS M&O 1998e). For Solitario Canyon fault, the hazard analysis shows fault displacement 5 m (CRWMS M&O 1998e, Figure 8.3) at an annual exceeding probability of  $10^{-8}$ . We use 10 m as an extremely conservative fault displacement for bounding analyses.

Geomechanical models used to investigate the amount of strain induced by fault movements in the rock at Yucca Mountain show that changes in strain extend several kilometers from a fault movement (Gauthier et al. 1995; National Research Council 1992, Appendix D). Using a three-dimensional elastic boundary element model of Yucca Mountain, Gauthier et al. (1995) investigated the effects of a right-lateral, strike-slip fault displacement on a fault dipping 60E. The fault movement was 1 meter along a 30 km section of the fault. The results show strains of 10 microns per meter (10 micro-strain, or  $10^{-5}$ ) up to 8 km from the fault. Geomechanics calculations were also performed in the National Research Council (1992, Appendix D) report. This calculation was for a normal displacement along a fault dipping 60E to the vertical. The simulated fault movement was 1 meter along 30 km section from the surface to a depth of 10 km. The results of this calculation show  $50^{-5}$  two kilometers from the fault plane and  $10^{-5}$  about 6 km from the fault plane. If these models were used for a 10 m fault movement instead of 1 m, the strains would be amplified proportionally because of the linearity of the elastic model. Therefore, for a bounding fault movement of 10 meters along Solitario Canyon fault, an elastic model would predict strains up to  $500^{-5}$  two kilometers from the fault and  $100^{-5}$  six kilometers from the fault. If the conservative assumption is made that all the strain accumulates in the fractures, then an estimate of the change in aperture can be made. First, assume a lower bound aperture of  $100^{-3}$  m in the present-day system (Sonnenthal et al. 1997, Table 7.12) and a fracture spacing of approximately 1 m (Sonnenthal et al. 1997, Table 7.7). Then a tensile strain of  $500^{-5}$  would result in a new fracture aperture of about  $600^{-3}$  m. For a compressive strain of  $500^{-5}$ , then the fractures would essentially be closed and the rock matrix would necessarily be compressed.

These results suggest that a factor of 10 change in aperture would bound the effects of tensile strain. In fact, because the average aperture at Yucca Mountain is approximately  $200^{-3}$  m (Sonnenthal et al. 1997, Table 7.12), a factor of 10 change would result in fractures with an average aperture of  $2000^{-3}$  m, or 2 mm. With regard to the reduction in aperture under compressive strain, other limitations constrain the change in fracture aperture. Attempts were made to use a factor of 10 reduction in aperture, however, convergence problems were encountered with the flow model. This is likely the result of insufficient bulk permeability in the

system to accommodate the imposed infiltration flow conditions. Therefore, reductions in aperture were limited to factors of 0.2, and in the case of a wetter climate, the lowest value that could be used was a factor of 0.5.

### 6.2.1.6 Affected Parameters

Given a change in aperture, theoretical models are available to quantitatively model the associated changes in fracture permeability, fracture capillary pressure, and fracture porosity. Fracture aperture enters flow and transport modeling in different ways. Aperture affects the permeability and capillary pressure used for steady-state unsaturated flow calculations. For radionuclide transport calculations, the fracture aperture affects the fracture porosity. Fracture aperture also affects matrix diffusion for radionuclide transport, but for these simulations the matrix diffusion coefficient was set to zero. The fracture apertures used in these different parameters are not necessarily the same because the theoretical models strictly apply to idealized “parallel plate” fractures. Therefore, the aperture for permeability, capillary pressure, and porosity are generally different values. However, we will assume that an increase or decrease in aperture will affect these physical characteristics in proportion to the functional dependence on aperture in the theoretical models.

The relationship for permeability, known as the cubic law, (Freeze and Cherry, Section 2.12; Sonnenthal et al., 1997, Section 7.5.4) is the following:

$$k = \bar{f} \frac{b^3}{12} \quad (\text{Eq. 1})$$

where  $\bar{f}$  is the average fracture frequency,  $k$  is the permeability, and  $b$  is the fracture aperture. As can be seen, the permeability is proportional to the cube of the fracture aperture.

The relationship for capillary pressure (van Genuchten 1980; Sonnenthal, et al. 1997, Section 7.5.5) is the following:

$$P_c = \frac{2\mathbf{t} \cos \mathbf{q}}{b\mathbf{r}g} [S_e^{-1/m} - 1]^{1/(1-m)} \quad (\text{Eq. 2})$$

where  $J$  is the surface tension of an air/water interface,  $2$  is the contact angle between the air/water interface and the mineral surface,  $D$  is the density of water,  $g$  is the acceleration of gravity,  $S_e$  is the effective water saturation (normalized for the residual and maximum saturations), and  $m$  is the shape parameter for the variation in capillary pressure with water saturation. The collection of terms,  $\frac{b\mathbf{r}g}{2\mathbf{t} \cos \mathbf{q}}$ , is known as the van Genuchten " parameter. The van Genuchten " parameter scales the overall capillary pressure in the system. The parameter  $m$  accounts for the distribution of fracture apertures that the air/water interface encounters as a function of water saturation. As can be seen, the van Genuchten " parameter is directly proportional to fracture aperture.

The relationship for porosity,  $N_f$ , is the following:

$$\mathbf{f}_f = fb \quad (\text{Eq. 3})$$

The porosity is also found to be proportional to the fracture aperture.

Now, assume  $b$  is changed to  $b^*$ , then correspondingly  $k$ ,  $\alpha$ , and  $N_f$  are changed to  $k^*$ ,  $\alpha^*$ , and  $N_f^*$ . These variables can be used to express the following relationships:

$$k^* = (b^*/b)^3 k \quad (\text{Eq. 4})$$

$$\mathbf{a}^* = (b^*/b)\mathbf{a} \quad (\text{Eq. 5})$$

$$\mathbf{f}_f^* = (b^*/b)\mathbf{f}_f \quad (\text{Eq. 6})$$

The factor of change in fracture aperture ( $b^*/b$ ) is then used to directly assign the new values of permeability, capillary pressure ( $\alpha$ ), and porosity.

In addition, the volumes for fracture and matrix elements should also be varied. Assume  $V_f$  and  $V_m$  as the original fracture and matrix element volumes, then the fracture and matrix element volumes varied due to fracture aperture change can be calculated as

$$V_f^* = V_f (\mathbf{f}_f^* / \mathbf{f}_f) \quad (\text{Eq. 7})$$

$$V_m^* = V_m (1 - \mathbf{f}_f^*) / (1 - \mathbf{f}_f) \quad (\text{Eq. 8})$$

Such variation in fracture and matrix element volumes only changes the partition of the bulk grid-cell volume (into either  $V_f$  and  $V_m$  or  $V_f^*$  and  $V_m^*$ ) which itself remains as a constant. Rev00 of this AMR differs from this Rev01 in that Rev00 ignores any matrix element volume changes while fracture element volumes are varied with fracture aperture changes.

### 6.2.1.7 Calculation Procedures

Each calculation involves two major computer programs: TOUGH2/version-1.4 (Pruess 1987, 1991; CRWMS M&O 2000g) and FEHM/version-2.0 (Dsay and Zyvoloski 1999; Zyvoloski et al. 1999). TOUGH2 with its EOS9 module (for single-phase unsaturated flow) is used for computing unsaturated flow fields. Through transient simulations, steady-state flow fields are obtained and used in subsequent transport simulations. FEHM performs specified particle-tracking calculations on the flow field calculated by TOUGH2. The software routine 't2fehm2\_v3x.f' is used for organizing TOUGH2 output into files ready for restarting FEHM particle-tracking calculations.

The matrix and fracture parameter values both for the hydrogeologic units and the faults are taken from the TSPA-SR base-case UZ flow model (CRWMS M&O 2000g) and treated as the base-case for this study. Sensitivity cases are conducted using fracture apertures modified as discussed in Sections 6.2.1, 6.2.1.5 and 6.2.1.6. Flow and transport modeling calculations are performed for present-day and glacial-transition climates. The UZ flow results from the base-

case UZ flow calculation are processed to obtain the initial condition for calculations involving cases affected by fault displacement.

The utility computer routines involved in the calculations include:

- (a) 'extract\_xd.f': For extracting sub-dimensional models out of the three-dimensional UZ model. The extraction is performed upon TOUGH2 MESH and GENER input sections. Other input sections for TOUGH2 are processed separately.
- (b) 'sr\_ini\_ext.f': For preparing the INCON section of the TOUGH2 input by extracting data from a previously converged TOUGH2 output file for a given grid. This is in essence the same as the routine 'va\_ini\_ext.f' used in Rev 00 of this AMR, except some differences to conform to the format used in TSPA-SR UZ flow model (CRWMS M&O 2000g).
- (c) 'alt\_tough2sr.f': For altering seismically affected parameters in a TOUGH2 input file, using the factor of change in fracture aperture as the primary parameter. For each selected factor, fracture porosity, permeability, and van Genuchten " parameters are changed in accordance with equations, (4), (5), and (6). The fracture and matrix element volumes used in the TOUGH2 input section, MESH, are changed, using equations (7) and (8). This is in essence similar to the routine 'alt\_tough2\_aper.f' used in Rev 00 of this AMR. This new routine allows the accommodation of locally altered fracture zones by using the symbol '&' in replacement of the symbol 'F' for the names of the altered fracture zones. Other differences are caused by the need to conform to the format used in the TSPA-SR UZ flow model (CRWMS M&O 2000g). The parameter for defining active fractures is kept as unchanged, which implies that changes in fracture apertures do not affect the distribution of active fractures.
- (d) 'fehm\_post.f': For processing FEHM particle-tracking results into concentration histories synthesized for the entire system outlet. This program is in essence the same as the program 'bkpm.f' (DTN: MO9807MWDOFEHM.000). Modifications were made mainly to make the program capable of handling multiple species with variable number of input particles (irrelevant to this study).
- (e) 't2fehm2\_v3x.f': For processing TOUGH2 output into FEHM readable files so that the latter can simulate the transport of radionuclides within the flow field described by the TOUGH2 output. This software routine is in essence the same as 't2fehm2\_v3.f' (CRWMS M&O 2000e). The modifications are for preparing the 'dmdp', 'rock', 'zone', and 'zone2' macros in such ways that localized perturbations to fracture zones can be accommodated.
- (f) 'mb\_tough2\_v1.4.f': For calculating the mass fluxes input to and output from the UZ model in order to examine the mass-balance condition. A steady state solution should have sufficient mass balance (negligible mass imbalance) for the whole system, i.e., the difference between the total mass flux input and the total mass flux output for the UZ domain should be sufficiently small.
- (g) 'post\_tough2sr.f': For extracting column data from TOUGH2 output files so that the distributions of flow variables along the selected columns can be plotted.

Further descriptions of these software routines, including the source code listings, are provided in Attachments I through VII.

The source listings of these software routines, together with the input and output files for the calculations presented in Section 6.2.2, are available from the technical database under the data tracking number: MO0006SPAUZT20.002.

### 6.2.2 Results

The next four subsections describe the effects of fracture aperture changes on flow in the unsaturated zone and mass releases at the water table. Results for cases in which the fracture apertures are varied are compared with the corresponding base cases. The first subsection, 6.2.2.1, describes the effects of changes in fracture aperture on the flow conditions and on transport. The one-dimensional modeling is carried out for illustrative purposes to examine changes in key flow variables and their implications on transport as a result of changes in fracture aperture. Only the present-day climate is used for the one-dimensional calculations. The second subsection, 6.2.2.2, describes the results for transport in a two-dimensional model when fracture apertures are changed uniformly throughout the modeling domain. These calculations are performed for present-day and the wetter, glacial-transition climates. The third subsection, 6.2.2.3, describes the results for transport in a three-dimensional model. The fourth subsection, 6.2.2.4, considers a three-dimensional model when fracture apertures are only changed in the fault zones, not in the fractured rock. These 3-D calculations are also performed for present-day and the glacial-transition climates. Mass transport calculations correspond to the continuous release of  $10^4$  particles at the potential repository for a period of one year.

#### 6.2.2.1 Fracture Apertures Altered Uniformly for the Model; One-Dimensional Calculations for Present-Day Climate

A one-dimensional model was extracted from the TSPA-SR three-dimensional model (CRWMS M&O 2000g; DTN: LB990701233129.001, LB990801233129.003) using the software routine 'extract\_xd.f'. The location of this one-dimensional column in the three dimensional model is shown in Figure 4. The total water influx to the model for the present-day climate is  $0.216 \times 10^{-2}$  kg/s, which, with the horizontal area of the column being  $2.17 \times 10^4$  m<sup>2</sup>, corresponds to an infiltration of about 3.14 mm/year. Flow calculations for the one-dimensional model were performed using TOUGH2 and these flow fields were converted to input files for FEHM using 't2fehm2\_v3x.f'. The breakthrough curves were computed using FEHM and post-processed using 'fehm\_post.f'. Calculations for altered fracture aperture cases were conducted by modifying the input data for TOUGH2 using the software routine 'alt\_tough2sr.f'. The initial condition for the TOUGH2 calculations for the altered aperture cases was obtained using the output of TOUGH2 for the base case, post-processed by the software routine 'sr\_ini\_ext.f' for use as input to TOUGH2. Mass balances were examined using the software routine 'mb\_tough2\_v1.4.f' to ensure steady-state solutions. Extraction of flow variables was conducted using the routine 'post\_tough2sr.f'.

Figure 5 shows the breakthrough curves at the water table for three cases. When compared with the base case, both of the altered cases show delayed initial breakthroughs, and except at the repository for the factor-of-0.2 case where majority of the particles transferred from the their

initial releasing fracture node to the corresponding matrix node almost instantly, there is no or little fracture-matrix inter-transport along the pathway as manifested in Figure 5 by the lack of bimodality. With the factor-of-0.2 case being matrix dominant and the factor-of-10 case being fracture dominant, for the majority of the particles, transport is delayed for the former and enhanced for the latter. This is significantly different from Rev 00 of this AMR. The differences can be attributed to the different ways in which the fracture network is conceptualized in Rev 00 and this version: the conventional dual-permeability model in Rev00 vs. the active-fracture-dual-permeability model in this Rev01. Other reasons may include differences in calibrated rock parameters, and in handling of the partition of bulk grid-cell volumes (see the comment following equations (7) and (8)).

The differences between the base case and the perturbed cases can be related to water saturation and flux distributions in the fractures and the matrix. Figures 6 and 7 show the water saturation distributions. Note that the potential repository is located at an approximate elevation of 1100 meters. When fracture apertures are altered from the base case, in general, for the factor-of-0.2 case, saturation for the fractures and the matrix is increased, whereas for the factor-of-10 case, the saturation is reduced.

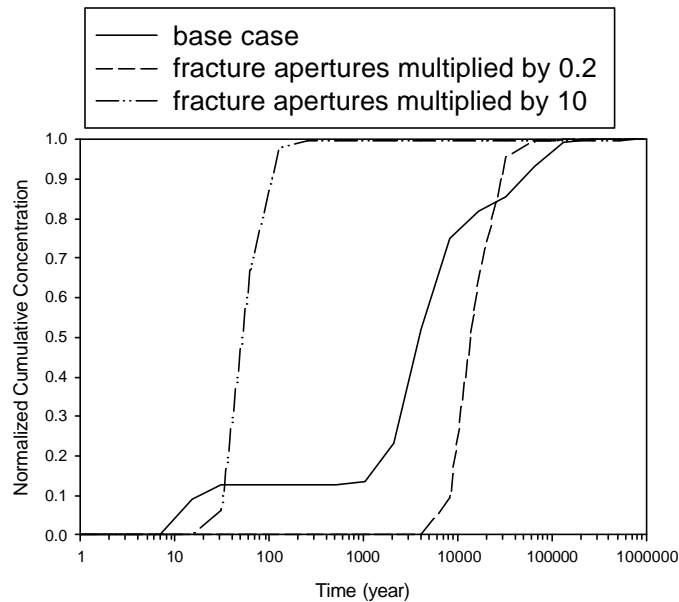


Figure 5. Breakthrough Curves for the One-Dimensional Column Model under Present-Day Infiltration. DTN: MO0006SPAUZT20.002.

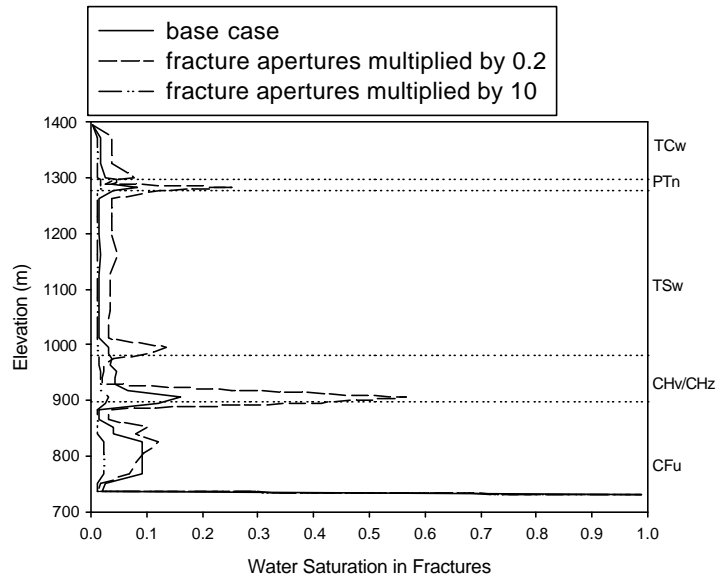


Figure 6. Water Saturation Distributions in the Fractures for the One-Dimensional Column Model under Present-Day Infiltration. DTN: MO0006SPAUZT20.002.

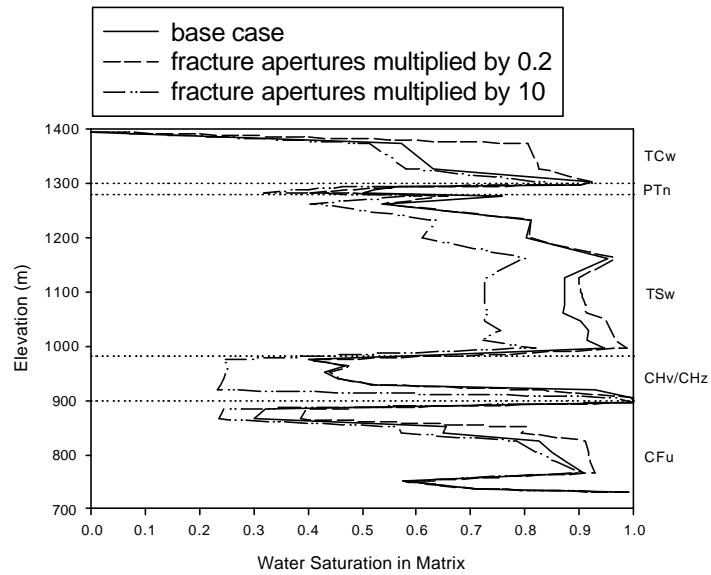


Figure 7. Water Saturation Distributions in the Matrix for the One-Dimensional Column Model under Present-Day Infiltration. DTN: MO0006SPAUZT20.002.

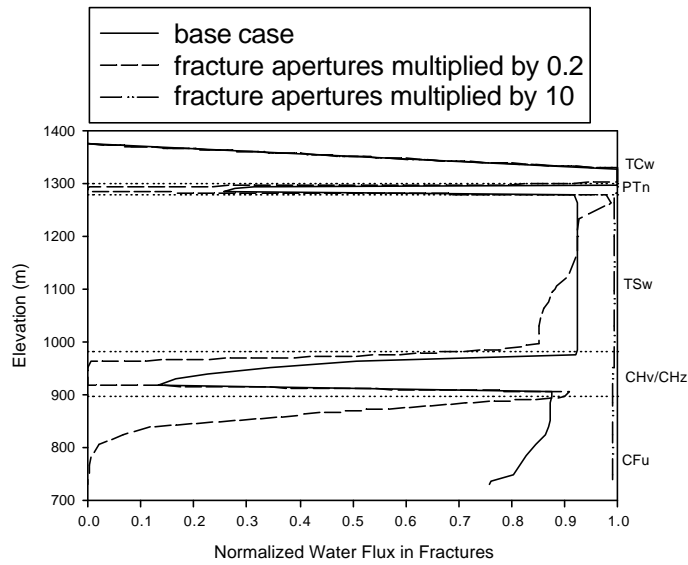


Figure 8. Normalized Water Flux Distributions in the Fractures for the One-Dimensional Column Model under Present-Day Infiltration. DTN: MO0006SPAUZT20.002.

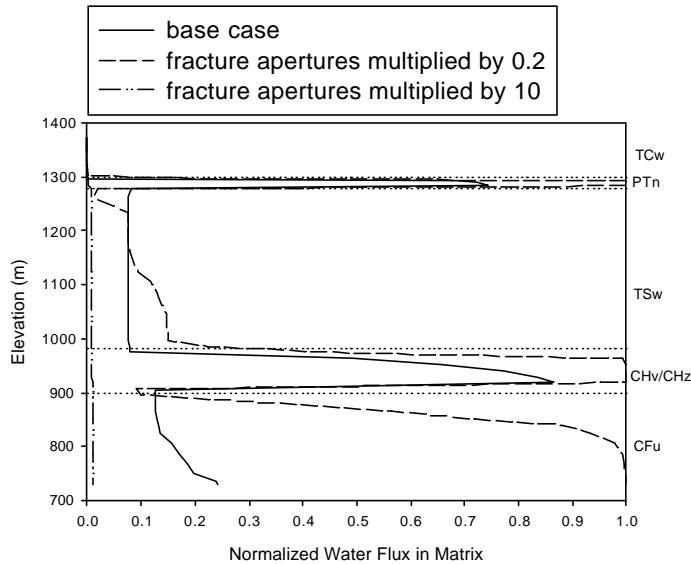


Figure 9. Normalized Water Flux Distributions in the Matrix for the One-Dimensional Column Model under Present-Day Infiltration. DTN: MO0006SPAUZT20.002.

Figures 8 and 9 show the water flux distributions along the column. From these figures one can see that for the base case, the matrix of the Calico Hills unit takes the majority of the total flux and thus controls the travel times of most particles. For the factor-of-0.2 case, the matrix of both

the Calico Hills and the Crator Flat undifferentiated units conduct most of the flux. For the factor-of-10 case, in contrast, essentially all the flux goes through the fractures.

The driving force for partition of flux between the fractures and the matrix is the capillary pressure difference between the two media. Figures 10 and 11 show the capillary pressure distributions in the fractures and the matrix. Note that the plots stop just short of the water table at a nonzero capillary pressure. Shown in Figure 12 (very similar to Figure 11 due to the dominance of matrix capillary pressure) is the capillary pressure in the matrix minus the capillary pressure in the fractures. For the factor-of-10 case, capillary pressure (absolute value) in the matrix increases whereas capillary pressure in the fractures decreases, when compared with the base case. The reverse is true for the factor-of-0.2 case. As a result, the capillary pressure difference between the matrix and the fractures increases for the factor-of-10 case and decreases for the factor-of-0.2 case, when compared with the base case. Specifically, for the factor-of-10 case, such increase in capillary pressure differential between matrix and fractures causes the delay in the initial arrival time, however, gravity assumes control very shortly afterwards.

In summary, when fracture aperture is decreased, fracture flux is decreased while matrix flux is increased, and when fracture aperture is increased, fracture flux is increased while matrix flux is decreased. For the factor-of-10 case using this particular 1-D column model, the fracture network takes almost the entire flux, leaving little possibility for fracture-matrix inter-flow. Due to differences in infiltration and layering compositions, however, other columns if taken as 1-D models would probably behave differently. This particular 1-D model only serves as an expedient to show the some of the typical hydraulic effects of varying fracture apertures.

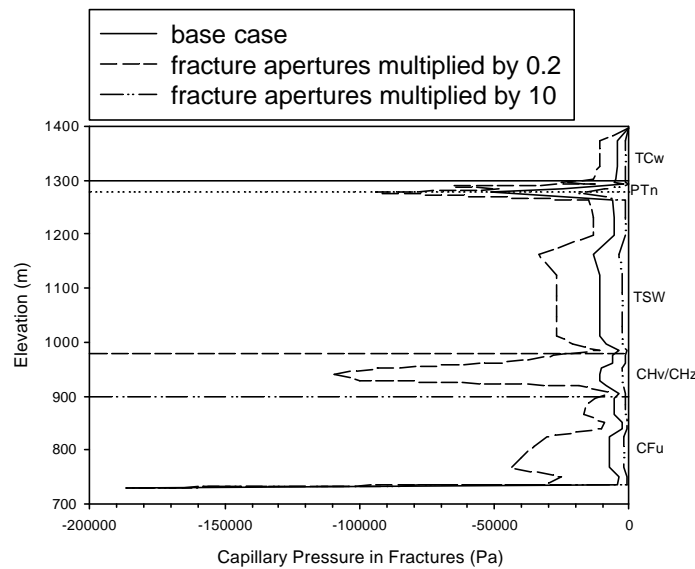


Figure 10. Capillary Pressure Distributions in the Fractures for the One-Dimensional Column Model under Present-Day Infiltration. DTN: MO0006SPAUZT20.002.

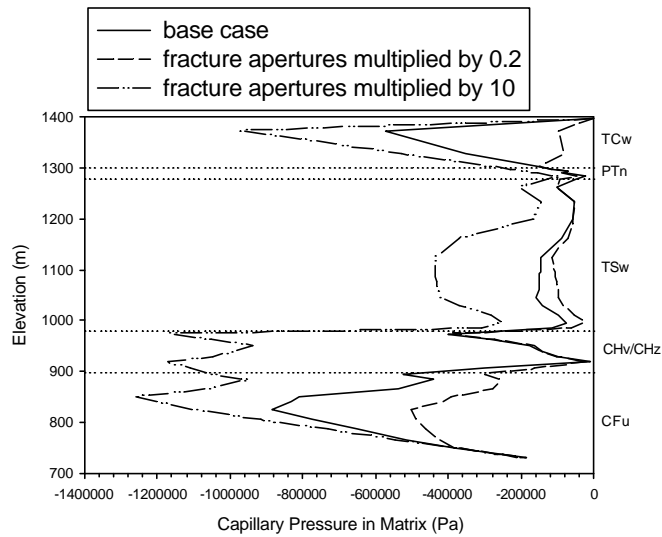


Figure 11. Capillary Pressure Distributions in the Matrix for the One-Dimensional Column Model under Present-Day Infiltration. DTN: MO0006SPAUZT20.002.

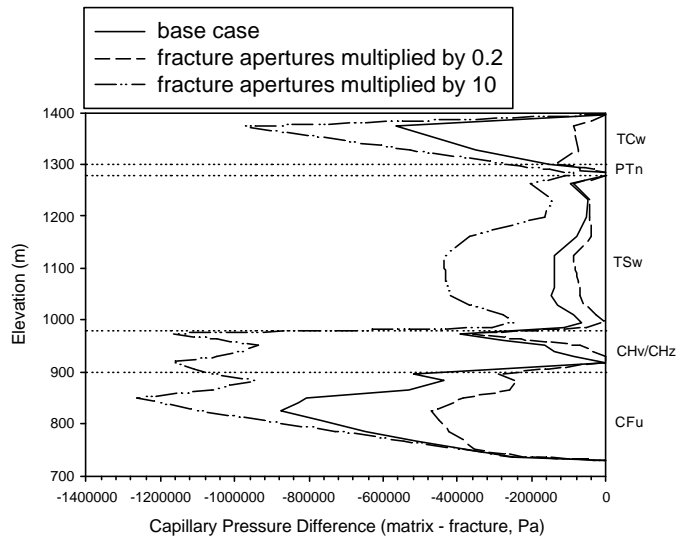


Figure 12. Capillary Pressure-Difference Distributions for the One-Dimensional Column Model under Present-Day Infiltration. DTN: MO0006SPAUZT20.002.

**6.2.2.2 Fracture Apertures Altered Uniformly Across the Repository Block; Two-Dimensional Calculations for Present-Day and Glacial-Transition Climates**

Calculations for flow and transport were also conducted for the two-dimensional, vertical cross-section identified in Figure 4. A two-dimensional model was extracted from the three-dimensional model (CRWMS M&O 2000g; DTN: LB990701233129.001, LB990801233129.003, LB990801233129.009) using the software routine ‘extract\_xd.f’. As for the one-dimensional model, the transport calculations were performed for non-sorbing, non-diffusing particles released into the fracture nodes of the repository elements over a one-year period. The total water influx to the two-dimensional model for the present-day climate is 0.0882 kg/s. Flow calculations for the two-dimensional model were performed using TOUGH2 and these flow fields were converted to input for FEHM using ‘t2fehm2\_v3x.f’. The breakthrough curves were computed using FEHM and post-processed using ‘fehm\_post.f’. Calculations for altered fracture aperture cases were conducted by modifying the input data for TOUGH2 using the software routine ‘alt\_tough2sr.f’. The initial condition for the TOUGH2 calculations for the altered aperture cases were obtained using the output of TOUGH2 for the base case, post-processed by the software routine ‘sr\_ini\_ext.f’ for use as input to TOUGH2. Mass balances for all the TOUGH2 runs were checked using the software routine ‘mb\_tough2\_v1.4.f’.

Shown in Figure 13 are the cumulative synthetic breakthrough curves of four cases. The results are very similar to the 1-D calculations, but obviously the degree of impact due to changes in fracture aperture has been reduced. Such behavior can be, in some degree, attributed to lateral migration and more fracture-matrix interchange; only in two- or three- dimensional models can the former mechanism be available and the latter mechanism enhanced.

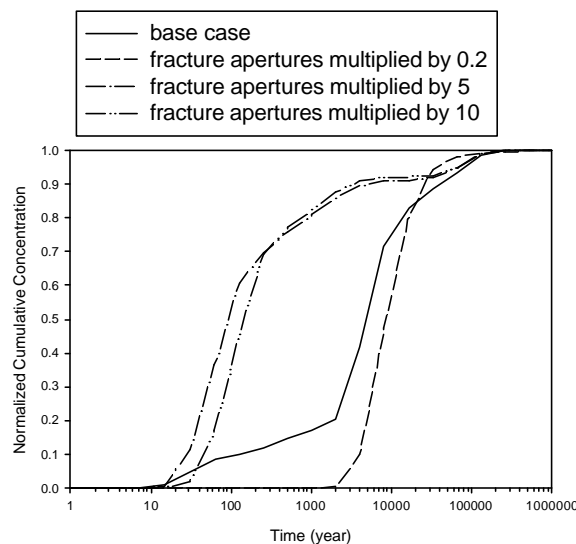


Figure 13. Breakthrough Curves for the Two-Dimensional Model under Present-Day Infiltration. DTN: MO0006SPAUZT20.002.

The total water influx to the model for the glacial-transition climate is 0.378 kg/s. As shown in Figure 14, due to the increase in water influx, the travel times have decreased from those for the present-day climate. The results for different fracture apertures are similar in nature to those for the present-day climate, but the initial breakthroughs occur earlier.

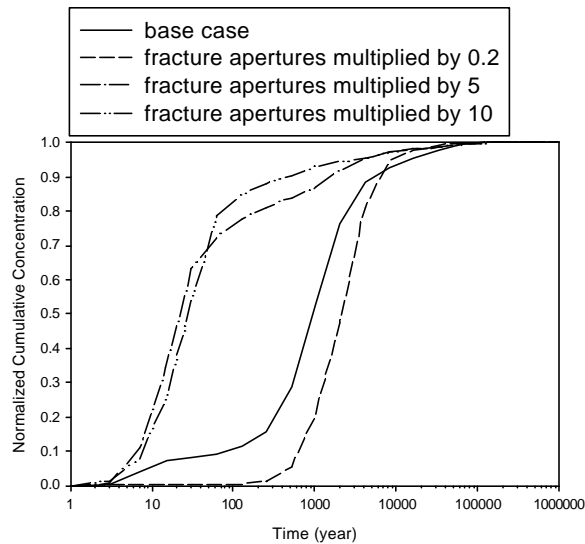


Figure 14. Breakthrough Curves for the Two-Dimensional Model under Glacial-Transition Infiltration. DTN: MO0006SPAUZT20.002.

### 6.2.2.3 Fracture Apertures Altered Uniformly Across the Repository Block; Three-dimensional Calculations for Present-Day and Glacial-Transition Climates

Calculations based on 3-D models are supposedly more realistic than 1-D or 2-D calculations. In this set of calculations, the 3-D flow and transport calculations described in this section were performed in exactly the same manner as described in Section 6.2.2.2. The breakthrough curves for the present-day and the glacial-transition climates are shown in Figures 15 and 16, respectively. Comparing with the 1-D and 2-D results presented in the two preceding sections, the 3-D results exhibit much reduced effect of changing fracture apertures on the synthetic mass releases at the water table. Specifically, for the factor-of-10 case, although the fracture transport clearly shows dominance, it at most (at about 50% arrival) only shortens the travel time by about one order of magnitude. The higher infiltration associated with the glacial-transition climate basically only causes the breakthrough curves shift toward earlier arrivals.

### 6.2.2.4 Fracture Apertures Altered in Fault Zones Only; Three-Dimensional Calculations for Present-Day and Glacial-Transition Climates

In this set of calculations, only the fracture apertures for the fault zones are changed by given factors. Otherwise, the flow and transport calculations described in this section were performed in exactly the same manner as described in Section 6.2.2.2.

As shown in Figures 17 and 18, respectively, for the present-day climate and the glacial-transition climate, the breakthroughs for the altered cases remain essentially unchanged from the base case. This indicates that if only the fault fracture apertures are affected by factors of 0.2 to 10, there would be virtually no impact to UZ flow and transport.

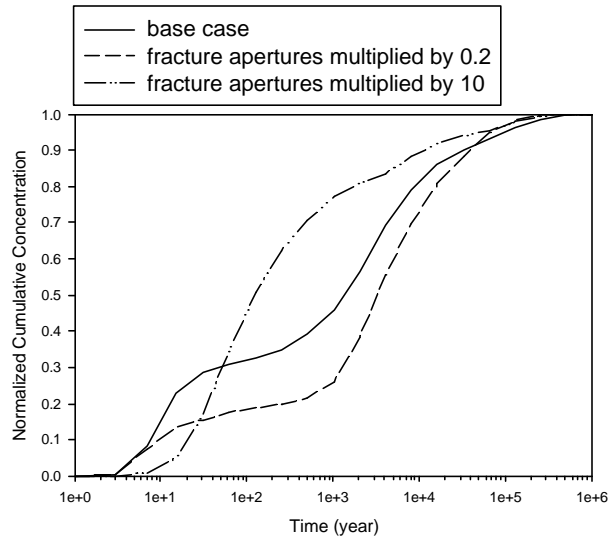


Figure 15. Breakthrough Curves for the Three-Dimensional Model under Present-Day Infiltration. DTN: MO0006SPAUZT20.002.

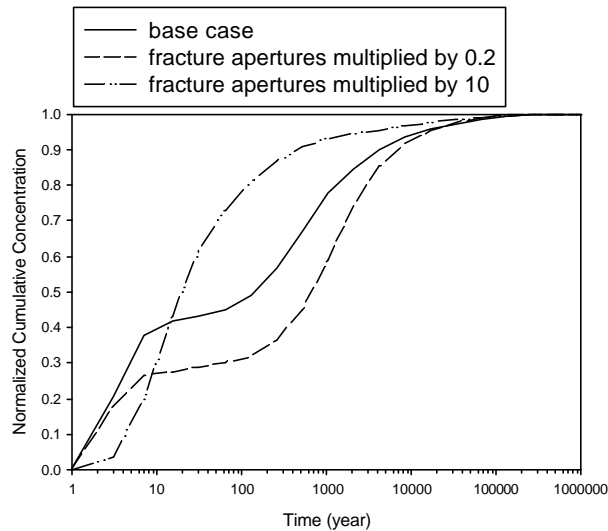


Figure 16. Breakthrough Curves for the Three-Dimensional Model under Glacial-Transition Infiltration. DTN: MO0006SPAUZT20.002.

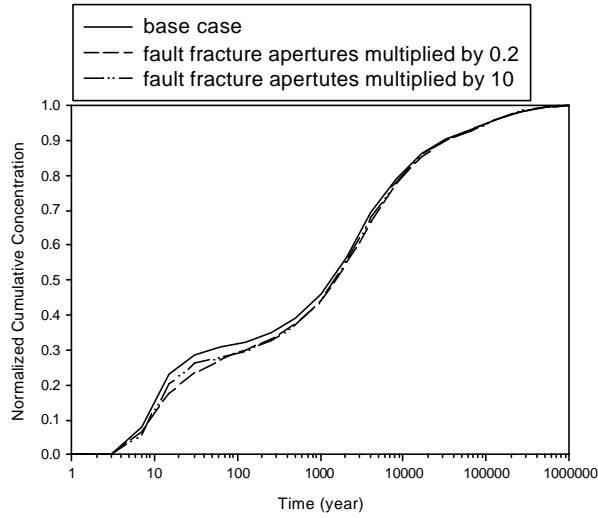


Figure 17. Breakthrough Curves for the Three-Dimensional Model under Present-day Infiltration when Fault Fractures Are Altered. DTN: MO0006SPAUZT20.002.

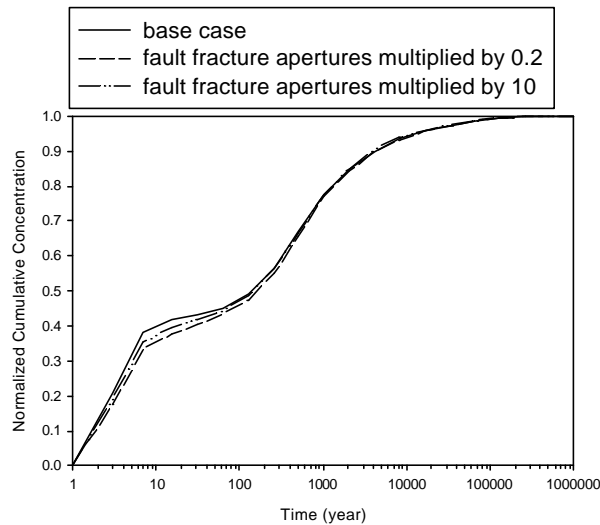


Figure 18. Breakthrough Curves for the Three-Dimensional Model under Glacial-Transition Infiltration when Fault Fractures Are Altered. DTN: MO0006SPAUZT20.002.

### 6.2.3 Discussion

The effect of changing fracture apertures on mass transport reflects the trend observed in the effect on flow; increased aperture leads to greater transport in fractures and shorter travel time to

the water table. This leads to a consistent trend for simulated tracer breakthrough profiles at the water table. If the fracture apertures are decreased (increased), the travel times of the majority of the particles are increased (decreased), causing delayed (earlier) breakthrough. In particular, when fracture apertures are increased, the travel times of some particles are (sometimes, significantly) decreased due to enhanced transport in the fractures.

The one- and two- dimensional models produced more significant early breakthroughs than the three-dimensional model, primarily because the three-dimensional model allows more lateral diversion and more fracture-matrix interaction. Since the TSPA-SR three-dimensional UZ flow model encompasses our current best understanding of the site and thus is believed to be the best available model, the general conclusion regarding fault-displacement effect on UZ transport should and will be drawn from the three-dimensional modeling results.

Capillary and gravity forces in the fractures of the dual-permeability model tend to work against fracture-matrix inter-flow and keep water flowing in the fractures. Note that fracture-matrix inter-flow is driven by the matrix-fracture capillary pressure difference. Assuming the inter-flow is from the fractures to the matrix, larger fracture apertures tend to promote fracture-to-matrix flow due to decreased fracture capillary pressure and increased matrix capillary pressure (i.e., increased matrix-fracture capillary pressure differential). On the other hand, however, as fracture aperture is increased, gravity exerts more effect to keep flow within the fractures. The decreased capillary pressure in the fractures is roughly inversely proportional to the fracture aperture. In addition, due to the use of upstream weighting of the relative permeability in the numerical scheme of TOUGH2, the fracture relative permeability is used with the matrix absolute permeability to estimate the effective permeability of the fracture/matrix interface for fracture to matrix flow. The fracture relative permeability is the effective permeability for the fracture system at the given flow rate divided by the absolute permeability of the fracture system (i.e. a saturated fracture system). Thus, when the fracture apertures are increased, the fracture relative permeability (for about the same amount of fracture flow) decreases roughly in proportion to the cube of the aperture ratio. This is due to the fact that the effective permeability is roughly set by the amount of flow and the saturated permeability is proportional to the cube of the fracture aperture (see equation 1). Therefore, the fracture/matrix interface effective permeability is also reduced by this ratio. This reduction of the fracture/matrix interface effective permeability leads toward greater flow and transport in the fractures when fracture apertures are increased. The above mechanism for enhanced fracture transport when fracture aperture is increased can be further promoted by the use of active-fracture-dual permeability model in this Rev01, as opposed to the conventional dual-permeability model used in Rev00. The active-fracture-dual-permeability model, among other things, scales the fracture-matrix interface areas using a function of water saturation in the fractures, and thus can further reduce fracture-to-matrix transport because fracture-matrix interface areas are reduced as a result of the generally reduced water saturation in the fractures.

## 7. CONCLUSIONS

This study attempts to address the potential effects of fault displacement on transport in the unsaturated zone using sensitivity analysis that is conducted by perturbing fracture parameters.

The degree of such perturbations are conservatively based on phenomenological assessment of the geological information of the site.

In the context of the TSPA-SR 3-D UZ flow and transport model, sensitivity studies for UZ flow and transport presented in this analysis suggest that transport between the potential repository and the water table is only weakly coupled to changes in fracture aperture. Overall, insignificant changes in transport behavior are found for large changes in fracture aperture. Changes in fracture aperture confined to the fault zones show virtually no effect on transport behavior. Some breakthrough is found to be at most only about one order of magnitude earlier than the base case (under the present-day or the glacial-transition climate), for an extremely conservative ten-fold increase in fracture aperture applied over the entire UZ domain. Effects of such magnitude on travel time are no more significant than those caused by some of the other uncertainties, such as those due to infiltration uncertainties (CRWMS M&O 2000a). Therefore, models for TSPA may exclude the effects of fault displacement on UZ transport.

This document may be affected by technical product input information that requires confirmation. Any changes to the document that may occur, as a result of completing the confirmation activities will be reflected in subsequent revisions. The status of the input information quality may be confirmed by review of the Document Input Reference System database.

The assumptions given in Section 5.9 and 5.10 are TBV. Confirmation of these assumptions depends on the qualification of the flow and transport models for TSPA-SR. These TBV assumptions, and the use of TBV input data (DTN: [LB990701233129.001](#), [LB990801233129.003](#), [LB990801233129.009](#)) for TOUGH2 make the resulting output of the calculations and conclusions stated here TBV. The data package for this AMR (DTN:MO0006PAUZT20.002) serves as the quantitative basis for the analysis conducted in this report, and should not be employed elsewhere without the same preconditions and assumptions as set forth in this report.

## 8. INPUT AND REFERENCES

Andrews, R.W. 2000. "AP-SV.1Q Control of the Electronic Management of Data Evaluation for Natural Systems Analysis/Model Reports." Letter from R.W. Andrews (CRWMS M&O) to S.P. Mellington (DOE/YMSCO), April 11, 2000, LA.PARWA.04/00-039, with enclosure. ACC: MOL.20000412.0785.

Anderson, R.E.; Bucknam, R.C.; Crone, A.J.; Haller, K.M.; Machette, M.N.; Personius, S.F.; Barnard, T.P.; Cecil, M.J.; and Dart, R.L. 1995. *Characterization of Quaternary and Suspected Quaternary Faults, Regional Studies, Nevada and California*. Open-File Report 95-599. Denver, Colorado: U.S. Geological Survey. ACC: MOL.19960924.0562.

Anderson, R.E.; Crone, A.J.; Machette, M.N.; Bradley, L-A.; and Diehl, S.F. 1995. *Characterization of Quaternary and Suspected Quaternary Faults, Amargosa Area, Nevada and California*. Open File Report 95-613. Denver, Colorado: U.S. Geological Survey. TIC: 246589.

CRWMS M&O 1998a. "Unsaturated Zone Hydrology Model." Chapter 2 of *Total System Performance Assessment – Viability Assessment (TSPA-VA) Analyses Technical Basis Document*. B00000000-01717-4301-00002 REV 01. Las Vegas, Nevada: CRWMS M&O. ACC: MOL.19981008.0002.

CRWMS M&O 1998b. "Unsaturated Zone Radionuclide Transport." Chapter 7 of *Total System Performance Assessment – Viability Assessment (TSPA-VA): Analyses Technical Basis Document*. B00000000-01717-4301-00007 REV 01. Las Vegas, Nevada: CRWMS M&O. ACC: MOL.19981008.0007.

CRWMS M&O 1998c. "Geology." Book 1 – Section 3 of *Yucca Mountain Site Description*. B00000000-01717-5700-00019 REV 00. Las Vegas, Nevada: CRWMS M&O. ACC: MOL.19980729.0049.

CRWMS M&O 1998d. *Cross Drift Geotechnical Predictive Report: Geotechnical Baseline Report*. BABEA0000-01717-5705-00002 REV 1. Las Vegas, Nevada: CRWMS M&O. ACC: MOL.19980806.0219.

CRWMS M&O 1999a. *Machine Readable Media Forms; Compact Disk YMP FEP Database Rev. 00C*. Las Vegas, Nevada: CRWMS M&O. ACC: MOL.19991214.0518.

CRWMS M&O 1999b. *Conduct of Performance Assessment*. Activity Evaluation, September 30, 1999. Las Vegas, Nevada: CRWMS M&O. ACC: MOL.19991028.0092.

CRWMS M&O 2000a. *Analysis of Base-Case Particle Tracking Results of the Base-Case Flow Fields*. ANL-NBS-HS-000024 REV 00. Las Vegas, Nevada: CRWMS M&O. ACC: MOL.20000207.0690

CRWMS M&O 2000b. *Features, Events, and Processes in UZ Flow and Transport*. ANL-NBS-MD-000001 Rev 00. Las Vegas, Nevada: CRWMS M&O. ACC: MOL.20000502.0240.

CRWMS M&O 2000c. *Features, Events, and Processes in Saturated Zone Flow and Transport*. Input Transmittal NEP-PA-00046T. Las Vegas, Nevada: CRWMS M&O. ACC: MOL.20000310.0342.

CRWMS M&O 2000d. *Fault Displacement Effects on Transport in the Unsaturated Zone*. TDP-NBS-HS-000018 Rev 03. Las Vegas, Nevada: CRWMS M&O. ACC: MOL.20000320.0399.

CRWMS M&O 2000e. *Abstraction of Flow Fields for RIP (ID: U0125)*. ANL-NBS-HS-000023 Rev 00. Las Vegas, Nevada: CRWMS M&O. ACC: MOL.20000127.0089.

CRWMS M&O 2000f. *Conceptual and Numerical Models for UZ Flow and Transport*. MDL-NBS-HS-000005 Rev 00. Las Vegas, Nevada: CRWMS M&O. ACC: MOL.19990721.0526.

CRWMS M&O 2000g. *UZ Flow Models and Submodels*. MDL-NBS-HS-000006 Rev 00. Las Vegas, Nevada: CRWMS M&O. ACC: MOL.19990721.0527.

Dash, Z. V. and Zyvoloski, G.A. 1999. *Software Design Document for the FEHM Application*. SC-194, STN: 10031-SDD-2.00-00. Los Alamos, New Mexico: Los Alamos National Laboratory. ACC: MOL.19990810.0036.

Day, W.C.; Potter, C.J.; Sweetkind, D.S.; and Keefer, W.R. 1996. "Structural Geology of the Central Block of Yucca Mountain." Chapter 2-I. of *Seismotectonic Framework and Characterization of Faulting at Yucca Mountain, Nevada*. Whitney, J.W., ed. Milestone 3GSH100M. Denver, Colorado: U.S. Geological Survey. TIC: 237980.

Day, W.C.; Potter, C.J.; Sweetkind, D.S.; Dickerson, R.P.; and San Juan, C.A. 1998a. *Bedrock Geologic Map of the Central Block Area, Yucca Mountain, Nevada*. Map MI-2601. Washington, D.C.: U.S. Geological Survey. TIC: 237019.

Day, W.C.; Dickerson, R.P.; Potter, C.J.; Sweetkind, D.S.; San Juan, C.A.; Drake, R.M., II; and Fridrich, C.J. 1998b. *Bedrock Geologic Map of the Yucca Mountain Area, Nye County, Nevada*. Geologic Investigations Series I-2627. Denver, Colorado: U.S. Geological Survey. ACC: MOL.19981014.0301.

DOE (U.S. Department of Energy) 2000. *Quality Assurance Requirements and Description*. DOE/RW-0333P, Rev. 10. Washington, D.C.: U.S. Department of Energy, Office of Civilian Radioactive Waste Management. ACC: MOL.20000427.0422.

Dyer, J.R. 1999. "Revised Interim Guidance Pending Issuance of New U.S. Nuclear Regulatory Commission (NRC) Regulations (Revision 01, July 22, 1999), for Yucca Mountain, Nevada." Letter from J.R. Dyer (DOE/YMSCO) to D.R. Wilkins (CRWMS M&O), September 3, 1999, OL&RC:SB-1714, with enclosure. "Interim Guidance Pending Issuance of New NRC Regulations for Yucca Mountain (Revision 01)." ACC: MOL.19990910.0079.

Freeze, R.A. and Cherry, J.A. 1979. *Groundwater*. Englewood Cliffs, New Jersey: Prentice-Hall, Inc. TIC: 217571.

Gauthier, J.H.; Wilson, M.L.; Borns, D.J.; and Arnold, B.W. 1995, *Impacts of seismic activity on long-term repository performance at Yucca Mountain*. SAND95-1917C. Albuquerque, New Mexico: Sandia National Laboratories. ACC: MOL.19960327.0356.

Liu, H. H.; Doughty, C.; and Bodvarsson, G.S. 1998. "An Active Fracture Model for Unsaturated Flow and Transport in Fractured Rocks." *Water Resources Research*, 34(10), 2633-2646. Washington, D.C.: American Geophysical Union. TIC: 243012.

Menges, C.M. and Whitney, J.W. 1996. "Distribution of Quaternary Faults in the Site Area." Chapter 4.2 of *Seismotectonic Framework and Characterization of Faulting at Yucca Mountain, Nevada*. Whitney, J.W., ed. Milestone 3GSH100M. Denver, Colorado: U.S. Geological Survey. ACC: MOL.19970129.0041.

Menges, C.M.; Taylor, E.M.; Vadurro, G.; Oswald, J.A.; Cress, R.; Murray, M.; Lundstrom, S.C.; Paces, J.B. and Mahan, S.A. 1997. *Logs and Paleoseismic Interpretations from Trenches 14C and 14D on the Bow Ridge Fault, Northeastern Yucca Mountain, Nye County, Nevada*. Miscellaneous Field Studies Map MF-2311. Denver, Colorado: U.S. Geological Survey. ACC: MOL.19980226.0591.

National Research Council 1992. *Ground Water at Yucca Mountain, How High Can it Rise?, Final Report of the Panel on Coupled Hydrologic/Tectonic/Hydrothermal Systems at Yucca Mountain*. Washington, D.C.: National Academy Press. TIC: 204931.

Piety, L.A. 1996. *Compilation of Known or Suspected Quaternary Faults Within 100 km of Yucca Mountain, Nevada and California*. Open File Report 94-112. Denver, Colorado: U.S. Geological Survey. ACC: MOL.19971009.0003.

Potter, C.J.; Day, W.C.; and Sweetkind, D.S. 1996a. "Structural Evolution of the Potential High-Level Nuclear Waste Repository Site at Yucca Mountain, Nevada." *Abstracts with Programs - Geological Society of America*, 28, (7), A-191. Boulder, Colorado: Geological Society of America. TIC: 233271.

Potter, C.J.; Day, W.C.; Sweetkind, D.S.; and Dickerson, R.P. 1996b. "Fault Styles and Strain Accommodation in the Tiva Canyon Tuff, Yucca Mountain, Nevada." *Eos, Transactions, American Geophysical Union*, 77, (17), S265. Washington, D.C.: American Geophysical Union. TIC: 234819.

Potter, C.J.; Dickerson, R.P.; and Day, W.C. 1999. *Nature and Continuity of the Sundance Fault*. Open-File Report 98-266. Denver, Colorado: U.S. Geological Survey. TIC: 246609.

Pruess, K. 1987. *TOUGH User's Guide*. NUREG/CR-4645. Washington, D.C.: U.S. Nuclear Regulatory Commission. TIC: 217275.

Pruess, K. 1991. *TOUGH2 - A General-Purpose Numerical Simulator for Multiphase Fluid and Heat Flow*. LBL-29400. Berkeley, California: Lawrence Berkeley National Laboratory. ACC: NNA.19940202.0088.

Ramelli, A.R.; Oswald, J.A.; Vadurro, G.; Menges, C.M.; and Paces, J.B. 1996. "Quaternary Faulting on the Solitario Canyon Fault." Chapter 4.7 of *Seismotectonic Framework and Characterization of Faulting at Yucca Mountain, Nevada*. Whitney, J.W., ed. Milestone 3GSH100M. Denver, Colorado: U.S. Geological Survey. TIC: 237980.

Scott, R.B. 1990. "Tectonic Setting of Yucca Mountain, Southwest Nevada." Chapter 12 of *Basin and Range Extensional Tectonics Near the Latitude of Las Vegas Nevada*. Wernicke, B.P., ed. Memoir 176. Boulder, Colorado: Geological Society of America. TIC: 222540.

Scott, R.B. and Bonk, J. 1984. *Preliminary Geologic Map of Yucca Mountain, Nye County, Nevada, with Geologic Sections*. Open-File Report 84-494. Denver, Colorado: U.S. Geological Survey. TIC: 203162.

Simonds, F.W.; Whitney, J.W.; Fox, K.F.; Ramelli, A.R.; Yount, J.C.; Carr, M.D.; Menges, C.M.; Dickerson, R.P.; and Scott, R.B. 1995. *Map Showing Fault Activity in the Yucca Mountain Area, Nye County, Nevada*. Map I-2520. Denver, Colorado: U.S. Geological Survey. TIC: 232483.

Sonnenthal, E.L.; Ahlers, C.F.; and Bodvarsson, G.S. 1997. "Fracture and Fault Properties for the UZ Site-Scale Flow Model". Chapter 7 of the *The Site-Scale Unsaturated Zone Model of Yucca Mountain, for the Viability Assessment*. Bodvarsson, G.S.; Bandurraga, T.M.; and Wu, Y.S., eds. LBNL-40376. Berkeley, California: Lawrence Berkeley National Laboratory. ACC: MOL.19971014.0232.

Sweetkind, D.S.; Barr, D.L.; Polacsek, D.K.; and Anna, L.O. 1997. *Administrative Report: Integrated Fracture Data in Support of Process Models, Yucca Mountain, Nevada*. Milestone SPG32M3. Denver, Colorado: U.S. Geological Survey. ACC: MOL.19971017.0726.

Sweetkind, D.S. and Williams-Stroud, S.C. 1996. *Characteristics of Fractures at Yucca Mountain, Nevada: Synthesis Report*. Administrative Report. Denver, Colorado: U.S. Geological Survey. ACC: MOL.19961213.0181.

Sweetkind, D.S.; Potter, C.J.; and Verbeek, E.R. 1996. "Interaction Between Faults and the Fracture Network at Yucca Mountain, Nevada." *Eos, Transactions*, S266. Washington, D.C.: American Geophysical Union. TIC: 236789.

USGS (U.S. Geological Survey) 1998. *Probabilistic Seismic Hazard Analyses for Fault Displacement and Vibratory Ground Motion at Yucca Mountain, Nevada*. Milestone SP32IM3, June 15, 1998. Three volumes. Oakland, California: U.S. Geological Survey. ACC: MOL.19980619.0640.

van Genuchten, M.T. 1980. "A Closed-Form Equation for Predicting the Hydraulic Conductivity of Unsaturated Soils." *Soil Science Society of America Journal*, 44, (5), 892-898. Madison, Wisconsin: Soil Science Society of America . TIC: 217327.

Wu, Y-S.; Haukwa, C.; and Mukhopadhyay, S. 1999. *TOUGH2 V1.4 and T2R3D V1.4 Verification and Validation Report*. Lawrence Berkeley National Laboratory. ACC: MOL.20000216.0111.

YMP (Yucca Mountain Site Characterization Project) 1998. *Q-List*. YMP/90-55Q, Rev. 5. Las Vegas, Nevada: Yucca Mountain Site Characterization Office. ACC: MOL.19980513.0132.

Zyvoloski, G.A.; Robinson, B.A.; Dash, Z.V.; and Trease, L.L. 1995. *Models and Methods Summary for the FEHM Application*. LA-UR-94-3787, Revision 1. Los Alamos, New Mexico: Los Alamos National Laboratory. ACC: TIC: 222337.

Zyvoloski, G.A.; Robinson, B.A.; Dash, Z.V.; and Trease, L.L. 1999. *User's Manual for the FEHM Application*. STN: 10031-UM-2.00-00. Los Alamos, New Mexico: Los Alamos National Laboratory. ACC: MOL.19990810.0038.

## **CODES, STANDARDS, AND REGULATIONS**

ASTM D 5718 – 95. 1995. *Standard Guide for Documenting a Ground-Water Flow Model Application*. West Conshohocken: American Society for Testing and Materials. TIC: 246012.

## **PROCEDURES**

QAP-2-0, *Conduct of Activities*, Rev 5, ICN 1, 11/9/99.

QAP-2-3, *Classification of Permanent Items*, Rev 10, 5/26/99.

AP-3.10Q, *Analyses and Models*, Rev 2, ICN 2, 6/19/00.

AP-SI.1Q, *Software Management*, Rev 2 ICN 4, 2/24/00.

AP-SV.1Q, *Control of the Electronic Management of Data Evaluation*, Rev 0 ICN 1, 5/15/00.

## **SOFTWARE**

Lawrence Berkeley National Laboratory 1/14/2000. *Software Code: TOUGH2 V1.4*. V1.4 Sun Workstation and DEC/ALPHA. 10007-1.4-01.

LANL (Los Alamos National Laboratory) 1999. *Software Code: FEHM V2.00*. V2.00. SUN Ultra Sparc. 10031-2.00-00.

Software Routine: 'extract\_xd.f' V1

Software Routine: 'sr\_ini\_ext.f' V1

Software Routine: 'alt\_tough2sr.f' V1

Software Routine: 'fehm\_post.f' V1

Software Routine: 't2fehm2\_v3x.f' V1

Software Routine: 'mb\_tough2\_v1.4.f' V1

Software Routine: 'post\_tough2sr.f' V1

## **SOURCE DATA**

LB990701233129.001. 3-D UZ Model Grids for Calculation of Flow Fields for PA for AMR U0000, "Development of Numerical Grids for UZ Flow and Transport Modeling". Submittal date: 09/24/1999.

LB990801233129.003. TSPA Grid Flow Simulations for AMR U0050, "UZ Flow Models and Submodels" (Flow Field #3). Submittal date: 11/29/1999.

LB990801233129.009. TSPA Grid Flow Simulations for AMR U0050, "UZ Flow Models and Submodels" (Flow Field #9). Submittal date: 11/29/1999.

**REFERENCE ONLY DATA**

GS990408314224.001. Detailed Line Survey Data for Stations 00+00.89 to 14+95.18, ECRB Cross Drift. Submittal Date: 9/9/99.

GS990408314224.002. Detailed Line Survey Data for Stations 15+00.85 to 26+63.85, ECRB Cross Drift. Submittal Date: 9/9/99.

GS990408314224.006. Full-Periphery Geologic Maps for Station 20+00 to 26+81, ECRB Cross Drift. Submittal Date: 9/9/99.

GS990408314224.003. Full-Periphery Geologic Maps for Station -0+10 to 10+00, ECRB Cross Drift. Submittal Date: 9/9/99.

**ATTACHMENT I**  
**SOFTWARE ROUTINE 'extract\_xd.f v.1'.**

## ATTACHMENT I

### Software routine 'extract\_xd.f v.1'

This routine is used for extracting sub-dimensional models out of the TSPA-SR three-dimensional UZ model. The extraction is performed upon TOUGH2 MESH and GENER input sections. Other input sections for TOUGH2 are processed separately. The code listing given below and files referred to in this Attachment may be found in the technical database under the data tracking number MO0006SPAUZT20.002.

(1) Code listing:

```

c
c   To extract a (e.g., 2-D) grid out of a given (e.g., 3-D) grid.
c
c   input files: MESH file for the given grid.
c                 GENER file for the given grid.
c   output files: MESH file for the extracted grid.
c                 GENER file for the extracted grid.
c
c   kode   =1, start extraction using two parameters: rloc & bound.
c           =2, start extraction from a given file of 'column indicators':
c             'zx_*.txt'.
c           =3, start extraction from a given (1-D) column indicator:
c             colc & coln.
c
c   double precision VOLX
c   parameter(kode=2, rloc=2.32e05, bound=100.0)
c   character dumele*5,EL*3,MA1*3,MA2*2,EL1*3,EL2*3
c   character ELG*3,SL*3,TYPE*4,ITAB*1,charx*75
c   character colc*1
c   data colc/'h'/,coln/18/
c   input files:
c     open(11,file='3d2kpa_pc1.mesh',status='old')
c     open(21,file='pchml_inf.dat',status='old')
c     if(kode.eq.2) open(31,file='zx_sr.txt',status='old')
c   output files:
c     open(12,file='MESH.2d')
c     open(13,file='MESH.tmp2d')
c     open(14,file='GENER.2d')
c
c     read(11,'(a5)') dumele
c     write(12,'(a5)') dumele
50  read(11,'(a5)') dumele
c     if(dumele.eq.'CONNE') then
c       write(13,'(a3)') '+++'
c       goto 120
c     endif
c
c     if(dumele.ne.'CONNE') backspace(11)
c     read(11,100) EL,NE,NSEQ,NADD,MA1,MA2,VOLX,AHTX,X,Y,Z
100  FORMAT(A3,I2,2I5,A3,A2,2E10.4,10X,3f10.3)
c     if(kode.eq.1) then
c       if(abs(Y-rloc).le.bound) then

```

## Fault Displacement Effects on Transport in the Unsaturated Zone

---

```
        write(12,100)EL,NE,NSEQ,NADD,MA1,MA2,VOLX,AHTX,X,Y,Z
        write(13,100)EL,NE,NSEQ,NADD,MA1,MA2,VOLX,AHTX,X,Y,Z
    endif
    goto 50
endif
if(kode.eq.2) then
    rewind (31)
102  read(31,'(A3,I2)') EL1,NE1
    if(EL1.eq.'+++') goto 50
    if(EL1(3:3).eq.EL(3:3).and.NE1.eq.NE) then
        write(12,100)EL,NE,NSEQ,NADD,MA1,MA2,VOLX,AHTX,X,Y,Z
        write(13,100)EL,NE,NSEQ,NADD,MA1,MA2,VOLX,AHTX,X,Y,Z
        goto 50
    endif
    goto 102
endif
if(kode.eq.3) then
    if(EL(3:3).eq.colc.and.NE.eq.coln) then
        write(12,100)EL,NE,NSEQ,NADD,MA1,MA2,VOLX,AHTX,X,Y,Z
        write(13,100)EL,NE,NSEQ,NADD,MA1,MA2,VOLX,AHTX,X,Y,Z
    endif
    goto 50
endif

120  write(12,*)
    write(12,'(a5)') dumele
150  read(11,200) EL1,NE1,EL2,NE2,NSEQ,NAD1,NAD2,ISOT,D1,D2,
+    AREAX,BETAX,ifm
200  FORMAT(A3,I2,A3,I2,4I5,4E10.4,I5)
    if(EL1.eq.'+++') then
        write(12,*)
        goto 360
    endif
    kodel=0
    kode2=0
    rewind(13)
250  read(13,100) EL,NE,NSEQ,NADD,MA1,MA2,VOLX,AHTX,X,Y,Z
    if(EL.eq.'+++') goto 150
    if(EL.eq.EL1.and.NE.eq.NE1) kodel=1
    if(EL.eq.EL2.and.NE.eq.NE2) kode2=1
    if(kodel.eq.1.and.kode2.eq.1) then
        write(12,200) EL1,NE1,EL2,NE2,NSEQ,NAD1,NAD2,ISOT,
+        D1,D2,AREAX,BETAX,ifm
        goto 150
    endif
    goto 250

360  read(21,'(a75)') charx
    write(14,'(a75)') charx
380  READ(21,400) ELG,NEG,SL,NS,NSEQ,NADD,NADS,LTAB,TYPE,ITAB,GX,EX,HX
400  FORMAT(A3,I2,A3,I2,4I5,5X,A4,A1,3E10.4)
    if(ELG.eq.'+++') then
        write(14,*)
        close (12)
        close (14)
        stop
    endif
endif
```

```

rewind(13)
420  read(13,100) EL,NE,NSEQ,NADD,MA1,MA2,VOLX,AHTX,X,Y,Z
      if(EL.eq.'+++') goto 380
      if(ELG.eq.EL.and.NEG.eq.NE) then
        write(14,400)ELG,NEG,SL,NS,NSEQ,NADD,NADS,LTAB,TYPE,ITAB,GX,EX,HX
        goto 380
      endif
      goto 420

      end

```

(2) Example Input Files:

(a) '3d2kpa\_pc1.mesh' (renamed as 'MESH.3d' in DTN: MO0006SPAUZT20.002)

A TOUGH2 MESH file for the TSPA-SR 3-D UZ grid, containing ELEM and CONNE sections for element and connection definitions.

```

ELEME
Faa 1          tcwF10.6530E+040.1000E+01          169399.101236623.643 1626.0963
Maa 1          tcwM10.2267E+060.0000E+00          169398.601236623.643 1626.0963
Fba 1          tcwF20.6488E+050.1000E+01          169399.101236623.643 1606.4657
Mba 1          tcwM20.3179E+070.0000E+00          169398.601236623.643 1606.4657
...
Faa24         tcwF20.4528E+050.1000E+01          171803.703232305.813 1259.4992
Maa24         tcwM20.2219E+070.0000E+00          171803.203232305.813 1259.4992
Fba24         tcwF20.4528E+050.1000E+01          171803.703232305.813 1227.5282
Mba24         tcwM20.2219E+070.0000E+00          171803.203232305.813 1227.5282
...

CONNE
Fea 1Fda 1     30.8477E+010.3796E+010.8857E+05-.1000E+01 1
Mea 1Mda 1     30.8477E+010.3796E+010.8857E+05-.1000E+01
Fda 1Fca 1     30.3796E+010.1831E+020.8857E+05-.1000E+01 1
Mda 1Mca 1     30.3796E+010.1831E+020.8857E+05-.1000E+01
...
Fea24Fda24     30.3319E+010.1173E+010.7080E+05-.1000E+01 1
Mea24Mda24     30.3319E+010.1173E+010.7080E+05-.1000E+01
Fda24Fca24     30.1173E+010.1743E+010.7080E+05-.1000E+01 1
Mda24Mca24     30.1173E+010.1743E+010.7080E+05-.1000E+01
...

```

(b) 'pchm1\_inf.dat'

A TOUGH2 GENER file for the TSPA-SR present-day climate, renamed from the GENER section in the original file, 'pa\_pchm1.dat', under DTN: LB990801233129.003.

```

GENER
...
Faa22          COM1 0.2046E-020.7561E+05
Faa23          COM1 0.1015E-020.7561E+05
Faa24          COM1 0.2309E-020.7561E+05
Faa25          COM1 0.5936E-020.7561E+05
Faa26          COM1 0.5750E-020.7561E+05
...

```

(c) 'zx\_sr.txt'

List of grid-blocks containing column identifiers for the 2-D cross section (Figure 4) sub-model to be extracted from the TSPA-SR 3-D UZ grid.

TPb48  
 TPa66  
 TPe82  
 TPk52  
 TPF93  
 TPB58  
 TPf92  
 TPb73  
 TPh34  
 TPh35  
 TPh36  
 TPh37  
 TPh41  
 Tpd20  
 TPA42  
 Tpd21  
 TPc69  
 TPa24  
 TPc96  
 Tpd69  
 TPA67  
 Tpd70  
 TPa98  
 TPa47  
 TPb29  
 +++

(3) Example Output Files:

(a) 'MESH.2d'

A TOUGH2 MESH file for the extracted 2-D sub-model (Figure 4).

```
ELEME
Faa24    0    0tcwF20.4528E+050.1000E+01    171803.703232305.813    1259.499
Maa24    0    0tcwM20.2219E+070.0000E+00    171803.203232305.813    1259.499
Fba24    0    0tcwF20.4528E+050.1000E+01    171803.703232305.813    1227.528
Mba24    0    0tcwM20.2219E+070.0000E+00    171803.203232305.813    1227.528
...
```

```
CONNE
Fea24Fda24    0    0    0    30.3319E+010.1173E+010.7080E+05-.1000E+01    1
Mea24Mda24    0    0    0    30.3319E+010.1173E+010.7080E+05-.1000E+01    0
Fda24Fca24    0    0    0    30.1173E+010.1743E+010.7080E+05-.1000E+01    1
Mda24Mca24    0    0    0    30.1173E+010.1743E+010.7080E+05-.1000E+01    0
...
```

(b) 'GENER.2d'

A TOUGH2 GENER file for the extracted 2-D sub-model. Contained as the GENER section in the present-day TOUGH2 input files, such as 'tough2.inp2d\_pchm1', under the DTN: MO0006SPAUZT20.002.

```
GENER
Faa24    0    0    0    0    0    COM1 0.2309E-020.7561E+050.0000E+00
Faa47    0    0    0    0    0    COM1 0.1072E-020.7561E+050.0000E+00
Faa66    0    0    0    0    0    COM1 0.1089E-010.7561E+050.0000E+00
Faa98    0    0    0    0    0    COM1 0.3110E-030.7561E+050.0000E+00
```

...

(4) Verification:

'Faa24', 'Fea24Fda24' and their associated data in the output file 'MESH.2d' are picked up by the program from the input file 'MESH.3d', because the column identifier 'a24' exists in the input file 'zx\_sr.txt'.

'Faa24' and its associated data in the output file 'GENER.2d' are picked up by the program from the input file 'pchm1\_inf.dat', because the column identifier 'a24' exists in the input file 'zx\_sr.txt'.

Similar observations can be made for other column identifiers in the input file 'zx\_sr.txt'. Therefore, the program has been verified to be correct.

(5) Range of Validation:

This software routine is valid for extracting 2D cross-sectional or 1D column models from any 3D TOUGH2 MESH or GENER files.

**ATTACHMENT II**

**SOFTWARE ROUTINE 'sr\_ini\_ext.f v.1'.**

## ATTACHMENT II

### Software routine 'sr\_ini\_ext.f v.1'

This routine is used for preparing the INCON section of the TOUGH2 input by extracting data from a previously converged TOUGH2 output file (e.g., an output from TSPA-SR), for a given grid. The code listing given below and files referred to in this Attachment may be found in the technical database under the data tracking number MO0006SPAUZT20.002.

#### (1) Code listing:

```

c
c   To get INCON by using a SR TOUGH2 output file.
c   Note that SR tough2 output uses a format different from VA.
c
parameter(por_tp=0.20,por_bt=0.28)
character*20 file_va,file_ini,file_mesh,file_va_trx
character ele_name*5, ele_dum*8, dum*1, dum_char*80, ele_name*5
logical file13

write(*,*) 'kode=3, 3D model, no truncation'
write(*,*) 'kode=1 or 2, 1D or 2D model, need truncation'
read(*,*) kode
if(kode.ne.3) then
  write(*,*) 'MESH file for the truncated model: file_mesh'
  read(*,'(a20)') file_mesh
  open(14,file=file_mesh)
  write(*,*) 'truncated INCON: file_va_trx'
  read(*,'(a20)') file_va_trx
  open(15,file=file_va_trx)
endif

write(*,*) '3D INCON file to be generated: file_ini'
write(*,*) '(if already exist, still input the file name)'
read(*,'(a20)') file_ini
inquire(file=file_ini,exist=file13)
if(file13.and.kode.ne.3) then
  open(13,file=file_ini,status='old')
  goto 400
endif
if(file13.and.kode.eq.3) stop

c
c generate INCON for the 3D model using VA TOUGH2 output:
c
open(13,file=file_ini)
write(13,'(a5)') 'INCON'

write(*,*) 'VA TOUGH2 output file: file_va'
read(*,'(a20)') file_va
open(12,file=file_va,status='old')

100 read(12,'(a8)') ele_dum
if(ele_dum.ne.' ELEM.') goto 100
read(12,*)
read(12,*)

```

```

150  read(12,'(a8)') ele_dum
    if(ele_dum.eq.' @@@@') then
        write(13,*)
        close(12)
        if(kode.ne.3) goto 400
        stop
    endif

    if(ele_dum(4:8).eq.'ELEM.') then
        read(12,*)
        read(12,*)
        read(12,180) dum,ele_name,ind,pre,sat
cc   Write(*,180) dum,ele_name,ind,pre,sat
    else
        backspace(12)
        read(12,180) dum,ele_name,ind,pre,sat
    endif
180  format(A1,A5,I12,2E12.5)

    por=0.
    if(ele_name(1:2).eq.'TP') por=por_tp
    if(ele_name(1:2).eq.'BT') por=por_bt
    if(abs(sat-1.0).le.1e-05) sat=0.999
    if(ele_name.ne.' ') write(13,200) ele_name,por,sat,0,0,0
200  FORMAT(A5,10X,E15.8/(5E20.13))
    goto 150

c
c truncation:
c
400  read(14,*)
    write(15,'(a5)') 'INCON'
450  read(14,'(a5)') ele_name

    if(ele_name.eq.' ') then
        write(15,*)
        close(13)
        close(14)
        close(15)
        stop
    endif
    rewind(13)
    read(13,*)
500  read(13,'(a5)') ele_namex
    if(ele_namex.eq.' ') goto 450
    if(ele_namex.eq. ele_name) then
        backspace(13)
        read(13,'(a80)') dum_char
        write(15,'(a80)') dum_char
        read(13,'(a80)') dum_char
        write(15,'(a80)') dum_char
        goto 450
    else
        read(13,*)
        goto 500
    endif
    endif

end

```



```
Mba24          0.00000000E+00
 0.7544000148773E+00 0.00000000000000E+00 0.00000000000000E+00 0.00000000000000E+00
...
```

(b) 'INCON.2d'

A TOUGH2 INCON file generated for the extracted 2-D model.

```
INCON
Faa24          0.00000000E+00
 0.1374199986458E-01 0.00000000000000E+00 0.00000000000000E+00 0.00000000000000E+00
Maa24          0.00000000E+00
 0.7467100024223E+00 0.00000000000000E+00 0.00000000000000E+00 0.00000000000000E+00
Fba24          0.00000000E+00
 0.1375500019640E-01 0.00000000000000E+00 0.00000000000000E+00 0.00000000000000E+00
Mba24          0.00000000E+00
 0.7544000148773E+00 0.00000000000000E+00 0.00000000000000E+00 0.00000000000000E+00
...
```

(4) Verification:

The contents of the output files have been checked against the source file 'pa\_pchm1.out' and are found to be correct. As examples, 'Faa 1' and its associated data in the output file 'INCON.3d' are picked up by the program from the input file 'pa\_pchm1.out' correctly, and 'Faa 24' and its associated data in the output file 'INCON.2d' are picked up by the program from the input file 'pa\_pchm1.out' correctly because 'Faa 24' is in the input file 'MESH.2d'.

Similar observations can be made with regard to other components in 'INCON.3d' and 'INCON.2d'. Thus, the program has been verified to accomplish what is intended.

(5) Range of Validation:

This software routine is valid for preparing a TOUGH2 INCON file in 1D, 2D, or 3D from any TOUGH2 - EOS9 3D output files.

**ATTACHMENT III**  
**SOFTWARE ROUTINE 'alt\_tough2sr.f v.1'.**

### ATTACHMENT III

#### Software routine 'alt\_tough2sr.f v.1'

This routine is used for altering seismically affected parameters in a TOUGH2 input file, using the factor of change in fracture aperture as the primary parameter. For each selected factor, fracture porosity, permeability, and van Genuchten air-entry scaling parameters are changed in accordance with equations, (4) to (6) in Section 6.2.1.6. The fracture and matrix element volumes in the TOUGH2 MESH section are also changed using equations, (7) and (8) in Section 6.2.1.6. The code listing given below and files referred to in this Attachment may be found in the technical database under the data tracking number MO0006SPAUZT20.002.

#### (1) Code Listing:

```

c
c   To alter hydrologic parameters for TOUGH2,
c       due to changes in fracture apertures.
c
c   note:
c   - set the parameters properly before each run;
c   - for 1-D model, the column has to be identified as
c       a fake fault in the input file 'file_alt'.
c
c   input files:
c   - tough2 input file, containing 'ROCKS' section of data.
c   - parameter file, containing the material names and the fault block
c       identifiers that determine the materials and the regions where
c       fracture apertures are to be altered.
c   - original tough2 mesh file.
c   - altered tough2 mesh file.
c
c   output files:
c   - altered tough2 input file, containing altered 'ROCKS' section.
c   - altered tough2 mesh file, containing altered fracture material
c       identifiers and volumes.
c
c   parameters:
c   - kodm = 1, use '&' in the altered fracture names in replacement
c           of 'F', also retain the original fractures names;
c           must be used if the impact zones occupy only portions
c           of the model domain.
c           = 2, no change to fracture names even though their parameters
c           have been altered; useful only if the entire model
c           domain is impacted.
c   - kodv = 1, no change in fracture or matrix element volumes
c           (option 1/2 for flow calculations);
c           = 2, change fracture and matrix element volumes according
c           to fracture porosity changes
c           (the selection for transport calculations);
c           = 3, change volumes by the specified v_factor, for specified
c           blocks only (current setup: fracture, fault, zeolite;
c           option 2/2 for easier-to-converge flow calculations).
c           = 4, change volumes by the specified v_factor, for all
c           blocks.

```

## Fault Displacement Effects on Transport in the Unsaturated Zone

---

```
c      - mxmat_alt: maximum number of materials to be altered.
c      - mrock: maximum number of rocks, including the materials in the
c          altered region.
c      - cdist: the radius limit (same unit as the coordinates in MESH)
c          with respect to the specified fault
c          locations (variable by layers; the fractures within this radius of
c          the specified fault locations are to be altered
c          for the specified materials).
c      - v_factor: the factor for increasing volumes for specified blocks.
c      - mfaub: maximum number of fault blocks that define the region
c          to be altered.
c      - mlay: maximum number of layers for a fault column.
c
```

```
parameter (mxmat_alt=200,mrock=200,mlay=80)
parameter (cdist=1.e10,kodv=2,kodm=1,v_factor=10000.0,mfaub=100)
double precision VOLX
character dumele*5,MATR*5,EL1*3,EL2*3,faub(mfaub)*3,MAT0*5
character*5 rmat(mxmat_alt),MAT(mrock),
+      charx,chary,MATY,MATZ,char0(mfaub,mlay)
character*80 dum_char
character*40 file_in,file_out,file_alt,file_mesh,file_mesh_alt
dimension DM(mrock),POR(mrock),PER(3,mrock),
+      CWET(mrock),SH(mrock),NAD(mrock)
dimension COM(mrock),EXPAN(mrock),CDRY(mrock),
+      TORT(mrock),GK(mrock),perf(3,mrock),perf_old(mrock)
dimension RP(7,mrock),CP(7,mrock),IRP(mrock),ICP(mrock)
dimension factor(mxmat_alt),x0(mfaub,mlay),y0(mfaub,mlay),
+      klayer(mfaub)

write(6,*) 'Altered parameter file: file_alt'
read(5,'(a40)') file_alt
write(6,*) 'TOUGH2 input file containing ROCKS: file_in'
read(5,'(a40)') file_in
write(6,*) 'Altered TOUGH2 input file: file_out'
read(5,'(a40)') file_out
write(6,*) 'Original MESH file for the model: file_mesh'
read(5,'(a40)') file_mesh
write(6,*) 'Altered MESH file: file_mesh_alt'
read(5,'(a40)') file_mesh_alt

open(11,file=file_in, status='old')
open(12,file=file_alt, status='old')
open(13,file=file_out, status='unknown')
open(14,file=file_mesh, status='old')
open(15,file=file_mesh_alt, status='unknown')

open(30,file='alt_tmp.out', status='unknown')

read(12,'(a80)') dum_char
read(12,*) nmat_alt
do i=1,nmat_alt
  read(12,*) rmat(i),factor(i)
enddo
read(12,'(a80)') dum_char
read(12,*) nfau_alt
do i=1,nfau_alt
  read(12,'(a3)') faub(i)
```

```

        enddo

        read(11,'(a80)') dum_char
        write(13,'(a80)') dum_char
        read(11,'(a80)') dum_char
        write(13,'(a80)') dum_char

c***** Begin generating the altered tough2 input file:

c***** Read Rock Parameters, Generate Altered Rocks and Their Parameters:
        NM=1
300   READ(11,200) MAT(NM),NAD(NM),DM(NM),POR(NM),(PER(I,NM),I=1,3),
+     CWET(NM),SH(NM)
200   FORMAT(A5,I5,7E10.3)
        IF(MAT(NM).EQ.'      ') GOTO 450

        COM(NM)=0.D0
        EXPAN(NM)=0.D0
        CDRY(NM)=0.D0
        TORT(NM)=0.D0
        GK(NM)=0.D0
        IRP(NM)=0
        ICP(NM)=0
        perf(1,nm)=0.0
        perf(2,nm)=0.0
        perf(3,nm)=0.0

        IF(NAD(NM).GE.1) then
        READ(11,220) COM(NM),EXPAN(NM),CDRY(NM),TORT(NM),GK(NM),
+ (perf(i,nm),i=1,3)
        ENDIF
220   FORMAT(8E10.3)

        IF(NAD(NM).LE.1) GOTO 280
        READ(11,260) IRP(NM),(RP(I,NM),I=1,7)
        READ(11,260) ICP(NM),(CP(I,NM),I=1,7)
260   FORMAT(I5,5X,7E10.3)

        write(13,200) MAT(NM),NAD(NM),DM(NM),POR(NM),(PER(I,NM),I=1,3),
+     CWET(NM),SH(NM)
        WRITE(13,220) COM(NM),EXPAN(NM),CDRY(NM),TORT(NM),GK(NM),
+     (perf(i,nm),i=1,3)
        write(13,260) IRP(NM),(RP(I,NM),I=1,7)
        write(13,260) ICP(NM),(CP(I,NM),I=1,7)
        perf_old(NM)=perf(3,NM)

280   NM=NM+1
        GOTO 300

450   NM=NM-1
        NMR=0
        do i=1, nmat_alt
        do k=1,NM
        if(MAT(k).eq.rmat(i)) then
        NMR=NMR+1
        NMX=NM+NMR
        MAT(NMX)=MAT(k)

```

```

    if(kodm.eq.1) then
      ind=index(MAT(k),'F')
      MAT(NMX)(ind:ind)='&'
    endif
    NAD(NMX)=NAD(k)
    DM(NMX)=DM(k)
    POR(NMX)=POR(k)
    COM(NMX)=COM(k)
    EXPAN(NMX)=EXPAN(k)
    CDRY(NMX)=CDRY(k)
    TORT(NMX)=TORT(k)
    GK(NMX)=GK(k)
    CWET(NMX)=CWET(k)
    SH(NMX)=SH(k)
    IRP(NMX)=IRP(k)
    ICP(NMX)=ICP(k)
    do m=1,7
      RP(m,NMX)=RP(m,k)
      CP(m,NMX)=CP(m,k)
    enddo
    do m=1,2
      perf(m,NMX)=perf(m,k)
    enddo
    perf(3,NMX)=perf(3,k)*factor(i)
    CP(3,NMX)=CP(3,k)*factor(i)
    do j=1,3
      PER(j,NMX)=PER(j,k)*(factor(i)*factor(i)*factor(i))
    enddo
  endif
enddo
enddo

if(kodm.eq.2) then
  do i=NM+1,NMX+2
    do j=1,4
      backspace(13)
    enddo
  enddo
  do i=NM-2,NM-1
    write(13,200) MAT(i),NAD(i),DM(i),POR(i),(PER(J,i),J=1,3),
+   CWET(i),SH(i)
    WRITE(13,220) COM(i),EXPAN(i),CDRY(i),TORT(i),GK(i),
+   (perf(j,i),j=1,3)
    write(13,260) IRP(i),(RP(J,i),J=1,7)
    write(13,260) ICP(i),(CP(J,i),J=1,7)
  enddo
endif

do i=NM+1,NMX
  write(13,200) MAT(i),NAD(i),DM(i),POR(i),(PER(J,i),J=1,3),
+   CWET(i),SH(i)
  WRITE(13,220) COM(i),EXPAN(i),CDRY(i),TORT(i),GK(i),
+   (perf(j,i),j=1,3)
  write(13,260) IRP(i),(RP(J,i),J=1,7)
  write(13,260) ICP(i),(CP(J,i),J=1,7)
enddo
write(13,200) MAT(NM),NAD(NM),DM(NM),POR(NM),(PER(J,NM),J=1,3),

```

## Fault Displacement Effects on Transport in the Unsaturated Zone

---

```
+      CWET(NM),SH(NM)
write(13,*)
500  read(11,'(a80)') dum_char
write(13,'(a80)') dum_char
if (dum_char(1:5).eq.'ENDCY') then
  write(13,*)
  close(11)
  close(12)
  close(13)
  goto 600
endif
goto 500

c***** End of generating the altered tough2 input file.

c***** Begin generating the altered tough2 mesh file:

600  read(14,'(a5)') dumele
do i=1,nfau_alt
  klayer(i)=0
enddo
900  read(14,'(a5)') dumele
if(dumele.eq.'CONNE') goto 990
backspace(14)
read(14,910) charx,NSEQ,NADD,MATR,VOLX,AHTX,X,Y,Z
910  FORMAT(A5,2I5,A5,2E10.4,10X,3f10.3)
if(index(MATR,'F').ne.0) then
  do i=1,nfau_alt
    if(charx(3:5).eq.faub(i)) then
      klayer(i)=klayer(i)+1
      ki=klayer(i)
      x0(i,ki)=X
      y0(i,ki)=Y
      char0(i,ki)=charx
    endif
  enddo
endif
goto 900

990  rewind(14)
write(30,*) '*** (x,y) locations, element names of the faults:'
write(30,'(2f12.2,4x,a5)')
+    ((x0(i,ki),y0(i,ki),char0(i,ki),ki=1,klayer(i)),i=1,nfau_alt)
write(30,*) 'number of layers for each of the faults ='
write(30,'(10i5)') (klayer(i),i=1,nfau_alt)
read(14,'(a5)') dumele
write(15,'(a5,a9,e10.1)') dumele,' cdist= ',cdist
write(30,*) '*** elements, original & new rock names, distances:'
50  read(14,'(a5)') dumele
if(dumele.eq.'CONNE') then
  backspace(15)
  write(15,*)
  goto 120
endif
backspace(14)
read(14,910) charx,NSEQ,NADD,MATR,VOLX,AHTX,X,Y,Z
MAT0=MATR
```

```

do i=1,NMR
  ind=index(MAT(NM+i),'&')
  if(MAT(NM+i)(1:ind-1).eq.MATR(1:ind-1).and.
+MAT(NM+i)(ind+1:5).eq.MATR(ind+1:5).and.MATR(ind:ind).eq.'F') then
    do j=1,nfau_alt
      do n=1,klayer(j)
        if(charx(1:2).eq.char0(j,n)(1:2)) then
          rdist=sqrt((X-x0(j,n))**2+(Y-y0(j,n))**2)
          if(rdist.le.cdists) then
            MATR=MAT(NM+i)
            write(30,75) charx,MAT0,MATR,rdist
75          format(3(a5,2x),f10.2)
            goto 80
          endif
        endif
      enddo
    enddo
  endif
enddo

80  goto(110,90,85,82),kodv

82  VOLX=VOLX*v_factor
    goto 110

85  if(charx(1:1).eq.'F'.or.MAT0(5:5).eq.'f'.or.MAT0(5:5).eq.'z')
+  VOLX=VOLX*v_factor
    goto 110

90  if(charx(1:1).eq.'F') then
      do i=1, nmat_alt
        if(MAT0.eq.rmat(i).and.index(MATR,'&').ne.0) then
          VOLX=VOLX*factor(i)
          goto 110
        endif
      enddo
    elseif(charx(1:1).eq.'M') then
      rewind(30)
91    read(30,'(a80)') dum_char
      if(index(dum_char,'distances').eq.0) goto 91
93    read(30,75,end=110) chary,MATY,MATZ,dist
      if(charx(2:5).eq.chary(2:5)) then
        do k=NM+1,NMX
          if(MATZ.eq.MAT(k)) then
            do j=1,NM
              if(MAT(j).eq.MATY) goto 95
            enddo
95          ratio=(1.-perf(3,k))/(1.-perf_old(j))
            VOLX=VOLX*ratio
            goto 110
          endif
        enddo
      endif
      goto 93
    endif
  endif
enddo

110  write(15,910) charx,NSEQ,NADD,MATR,VOLX,AHTX,X,Y,Z

```

## Fault Displacement Effects on Transport in the Unsaturated Zone

---

```
      goto 50

120  write(15,'(a5)') dumele
150  read(14,700) EL1,NE1,EL2,NE2,NSEQ,NAD1,NAD2,ISOT,D1,D2,
+    AREAX,BETAX,ifm
700  FORMAT(A3,I2,A3,I2,4I5,4E10.4,I5)
      write(15,700) EL1,NE1,EL2,NE2,NSEQ,NAD1,NAD2,ISOT,D1,D2,
+    AREAX,BETAX,ifm
      if(EL1.eq.'+++'.or.EL1.eq.'  ') then
          backspace(15)
          write(15,*)
          close(14)
          close(15)
          stop
      endif
      goto 150
c***** End of generating the altered tough2 mesh file.

      end
```

### (2) Example Input Files:

#### (a) 'tough2.inp2d\_pchm1'

A TOUGH2 input file for the base case 2-D model.

```
Mean inf conceptual #1 input ysw/6/3/99
ROCKS from inversion "itough2 binfLlxi binfLlx 9" Date: 2-Jun-99 15:27
tcwM1  2 2.500    0.2530    0.3855E-140.3855E-140.3855E-14 1.000    1000.
          1.0000
          7    0.4704    0.7000E-01 1.000          1.000
          7    0.4704    0.7000E-010.3998E-040.1000E+11 1.000
tcwM2  2 2.500    0.8200E-010.2742E-180.2742E-180.2742E-18 1.000    1000.
          1.0000
          7    0.2407    0.1900    1.000          1.000
          7    0.2407    0.1900    0.1806E-040.1000E+11 1.000
tcwM3  2 2.500    0.2030    0.9227E-160.9227E-160.9227E-16 1.000    1000.
          1.0000
          7    0.3979    0.3100    1.000          1.000
          7    0.3979    0.3100    0.3443E-050.1000E+11 1.000
...
tcwF1  2 2.500    1.000     0.2410E-110.2410E-110.2410E-11 1.000    1000.
          1.0000
          7    0.6265    0.1000E-01 1.000          1.000
          7    0.6265    0.1000E-010.3152E-020.1000E+11 1.000    0.3016
tcwF2  2 2.500    1.000     0.1000E-090.1000E-090.1000E-09 1.000    1000.
          1.0000
          7    0.6132    0.1000E-01 1.000          1.000
          7    0.6132    0.1000E-010.2131E-020.1000E+11 1.000    0.3016
tcwF3  2 2.500    1.000     0.5420E-110.5420E-110.5420E-11 1.000    1000.
          1.0000
          7    0.6068    0.1000E-01 1.000          1.000
          7    0.6068    0.1000E-010.1261E-020.1000E+11 1.000    0.3016
...
```

#### (b) 'MESH.2d'

A TOUGH2 MESH file for the base case 2-D model. See Attachment I.

(c) 'alt\_tough2sr.dat0.2s'

A factor-of-0.2 change in fracture apertures prescribed for the UZ model.

altered units and factors of alteration:

```

41
tcwF1      0.200
tcwF2      0.200
tcwF3      0.200
ptnF1      0.200
ptnF2      0.200
ptnF3      0.200
ptnF4      0.200
ptnF5      0.200
ptnF6      0.200
tswF1      0.200
tswF2      0.200
tswF3      0.200
tswF4      0.200
tswF5      0.200
tswF6      0.200
tswF7      0.200
tswF8      0.200
tswF9      0.200
ch1Fv      0.200
ch2Fv      0.200
ch3Fv      0.200
ch4Fv      0.200
ch5Fv      0.200
ch1Fz      0.200
ch2Fz      0.200
ch3Fz      0.200
ch4Fz      0.200
ch5Fz      0.200
ch6Fz      0.200
pp4Fz      0.200
pp3Fd      0.200
pp2Fd      0.200
pp1Fz      0.200
bf3Fd      0.200
bf2Fz      0.200
tr3Fd      0.200
tr2Fz      0.200
tcwFf      0.200
ptnFf      0.200
tswFf      0.200
chnFf      0.200
***** fault gridblocks:
1
B58
    
```

(3) Example Output Files:

(a) 'tough2.inp2d0.2grid'

The TOUGH2 input file with its fracture hydrological parameters being altered in accordance with equations, (4) to (6) when fracture apertures are multiplied by a factor of 0.2.

```

Mean inf conceptual #1 input ysw/6/3/99
ROCKS from inversion "itough2 binfLlxi binfLlx 9" Date: 2-Jun-99 15:27
tcwM1      2 .250E+01 .253E+00 .385E-14 .385E-14 .385E-14 .100E+01 .100E+04
.000E+00 .000E+00 .100E+01 .000E+00 .000E+00 .000E+00 .000E+00 .000E+00
    
```

## Fault Displacement Effects on Transport in the Unsaturated Zone

---

7		.470E+00	.700E-01	.100E+01	.000E+00	.100E+01	.000E+00	.000E+00
7		.470E+00	.700E-01	.400E-04	.100E+11	.100E+01	.000E+00	.000E+00
tcwM2	2	.250E+01	.820E-01	.274E-18	.274E-18	.274E-18	.100E+01	.100E+04
		.000E+00	.100E+01	.000E+00	.000E+00	.000E+00	.000E+00	.000E+00
7		.241E+00	.190E+00	.100E+01	.000E+00	.100E+01	.000E+00	.000E+00
7		.241E+00	.190E+00	.181E-04	.100E+11	.100E+01	.000E+00	.000E+00
tcwM3	2	.250E+01	.203E+00	.923E-16	.923E-16	.923E-16	.100E+01	.100E+04
		.000E+00	.100E+01	.000E+00	.000E+00	.000E+00	.000E+00	.000E+00
7		.398E+00	.310E+00	.100E+01	.000E+00	.100E+01	.000E+00	.000E+00
7		.398E+00	.310E+00	.344E-05	.100E+11	.100E+01	.000E+00	.000E+00
...								
tcwF1	2	.250E+01	.100E+01	.241E-11	.241E-11	.241E-11	.100E+01	.100E+04
		.000E+00	.100E+01	.000E+00	.000E+00	.000E+00	.000E+00	.280E-01
7		.627E+00	.100E-01	.100E+01	.000E+00	.100E+01	.000E+00	.000E+00
7		.627E+00	.100E-01	.315E-02	.100E+11	.100E+01	.302E+00	.000E+00
tcwF2	2	.250E+01	.100E+01	.100E-09	.100E-09	.100E-09	.100E+01	.100E+04
		.000E+00	.100E+01	.000E+00	.000E+00	.000E+00	.000E+00	.200E-01
7		.613E+00	.100E-01	.100E+01	.000E+00	.100E+01	.000E+00	.000E+00
7		.613E+00	.100E-01	.213E-02	.100E+11	.100E+01	.302E+00	.000E+00
tcwF3	2	.250E+01	.100E+01	.542E-11	.542E-11	.542E-11	.100E+01	.100E+04
		.000E+00	.100E+01	.000E+00	.000E+00	.000E+00	.000E+00	.150E-01
7		.607E+00	.100E-01	.100E+01	.000E+00	.100E+01	.000E+00	.000E+00
7		.607E+00	.100E-01	.126E-02	.100E+11	.100E+01	.302E+00	.000E+00
...								
topbd	2	.230E+04	.200E+00	.603E-10	.603E-10	.603E-10	.166E+01	.100E+31
		.000E+00	.166E+01	.000E+00	.000E+00	.000E+00	.000E+00	.000E+00
1		.200E+00	.300E+00	.700E+00	.800E+00	.000E+00	.000E+00	.000E+00
1		.000E+00	.000E+00	.100E+01	.000E+00	.000E+00	.000E+00	.000E+00
botbd	2	.230E+04	.280E+00	.537E-17	.537E-17	.537E-17	.135E+01	.100E+31
		.000E+00	.156E+01	.000E+00	.000E+00	.000E+00	.000E+00	.000E+00
7		.390E+00	.000E+00	.100E+01	.000E+00	.000E+00	.000E+00	.000E+00
7		.390E+00	.000E+00	.580E-06	.100E+13	.100E+01	.000E+00	.000E+00
tcw&1	2	.250E+01	.100E+01	.193E-13	.193E-13	.193E-13	.100E+01	.100E+04
		.000E+00	.100E+01	.000E+00	.000E+00	.000E+00	.000E+00	.560E-02
7		.627E+00	.100E-01	.100E+01	.000E+00	.100E+01	.000E+00	.000E+00
7		.627E+00	.100E-01	.630E-03	.100E+11	.100E+01	.302E+00	.000E+00
tcw&2	2	.250E+01	.100E+01	.800E-12	.800E-12	.800E-12	.100E+01	.100E+04
		.000E+00	.100E+01	.000E+00	.000E+00	.000E+00	.000E+00	.400E-02
7		.613E+00	.100E-01	.100E+01	.000E+00	.100E+01	.000E+00	.000E+00
7		.613E+00	.100E-01	.426E-03	.100E+11	.100E+01	.302E+00	.000E+00
tcw&3	2	.250E+01	.100E+01	.434E-13	.434E-13	.434E-13	.100E+01	.100E+04
		.000E+00	.100E+01	.000E+00	.000E+00	.000E+00	.000E+00	.300E-02
7		.607E+00	.100E-01	.100E+01	.000E+00	.100E+01	.000E+00	.000E+00
7		.607E+00	.100E-01	.252E-03	.100E+11	.100E+01	.302E+00	.000E+00
...								

### (b) 'MESH.2d0.2grid'

The TOUGH2 MESH file corresponding to the case when fracture apertures are multiplied by a factor of 0.2.

ELEME	cdist=	.1E+11						
Faa24	0	0tcw&2	.9056E+04	.1000E+01	171803.703232305.813	1259.499		
Maa24	0	0tcwM2	.2255E+07	.0000E+00	171803.203232305.813	1259.499		
Fba24	0	0tcw&2	.9056E+04	.1000E+01	171803.703232305.813	1227.528		
Mba24	0	0tcwM2	.2255E+07	.0000E+00	171803.203232305.813	1227.528		
...								

```

CONNE
Faa24Fda24    0    0    0    3 .3319E+01 .1173E+01 .7080E+05-.1000E+01    1
Maa24Mda24    0    0    0    3 .3319E+01 .1173E+01 .7080E+05-.1000E+01    0
Faa24Fca24    0    0    0    3 .1173E+01 .1743E+01 .7080E+05-.1000E+01    1
Maa24Mca24    0    0    0    3 .1173E+01 .1743E+01 .7080E+05-.1000E+01    0
...

```

(4) Verification:

The contents of the two output files, 'tough2.inp2d0.2grid' and 'MESH.2d0.2grid', have been checked against the input files and confirmed to be in accord with the intended purpose of the software routine. Examples are as follows:

In 'tough2.inp2d0.2grid', the permeability ( $m^2$ ), porosity (dimensionless), and van Genuchten  $\alpha$  (1/Pa) for the fracture identifier 'tcw&1' are:  $.193E-13$ ,  $.560E-02$ ,  $.630E-03$ , respectively. Note that 'tcw&1' is perturbed from 'tcwF1' according to equations (4) through (6) in Section 6.2.1.6. These parameter values for 'tcw&1' are calculated from these equations, i.e., they are the products of the corresponding parameter values for 'tcwF1',  $.241E-11$ ,  $.280E-01$ ,  $.315E-02$ , and  $(0.2)^3$ ,  $0.2$ ,  $0.2$ , respectively, as dictated by the perturbation parameter 0.2 specified in the input file 'alt\_tough2sr.dat0.2s'.

The material identifier for the fracture element 'Faa24' has been changed from 'tcwF2' in the input file 'MESH.2d' to 'tcw&2' in the output file 'MESH.2d0.2grid', while the material identifier for the matrix element 'Maa24' in the output file 'MESH.2d0.2grid' remains the same as in the input file 'MESH.2d'.

With the fracture element 'Faa24' having a volume of  $.4528E05 m^3$  and the matrix element 'Maa24' having  $.2219E+07 m^3$  in the input file 'MESH.2d', the volumes ( $m^3$ ) for 'Faa24' and 'Maa24' in the output file 'MESH.2d0.2grid' are calculated from equations (7) and (8) in Section 6.2.1.6: for 'Faa24',  $.9056E+04 = .4528E+05 * (0.4E-02 / 0.2E-01)$ ; for 'Maa24',  $.2255E+07 = .2219E+07 * (1 - 0.4E-02) / (1 - 0.2E-01)$ .

Similar observations to these examples can be made for all other intended changes in the output files, which verifies the program to be correct for its intended purpose.

(5) Range of Validation:

This software routine is valid for modifying any TOUGH2 input file using the active-fracture-dual-permeability model with the van Genuchten capillary pressure and relative permeability functions to account for a change in fracture aperture by some multiplicative scaling factor.

**ATTACHMENT IV**  
**SOFTWARE ROUTINE 'feh<sub>m</sub>\_post.f v.1'**

## ATTACHMENT IV

### Software routine 'fehm\_post.f v.1'

This routine is used for processing FEHM particle-tracking results into cumulative breakthrough histories synthesized for the entire system outlet. Modifications were made mainly to make the program capable of handling multiple species with variable number of input particles (irrelevant to this study). The code listing given below and files referred to in this Attachment may be found in the technical data base under the data tracking number MO0006SPAUZ20.002.

#### (1) Code Listing:

```

parameter(cmin=1.e-10,max_spec=10)
character*80 line,prx*5,cidx*5,title*31
character*60 outfile,fout*10,dfile*30,ctmp
real*8 time,time_old(max_spec)
double precision total(max_spec),conc,rate_const(max_spec)
integer entered,cur_in,left,tot_entered,decayed
integer left_old(max_spec)
character*6 spacer2
do i=1,max_spec
time_old(i)=0.
left_old(i)=0.
rate_const(i)=0.
enddo
ifehm=2
prx='spec_'
title='Particle Tracking ==> Species: '
dfile='fehmn.files'
open(ifehm,file=dfile,status='old',iostat=iofehm)
if(iofehm.eq.0)then
do ip=1,4
read(ifehm,*)outfile
end do
else
write(*,*) 'name of FEHM output file: '
read(*,'(a60)') outfile
endif
9 write(*,*)'decay (1) or conservative (2)? '
read(*,*) iflag
if(abs(iflag).gt. 2 ) then
write(*,*) 'Bad input, Try again'
goto 9
endif
write(*,*) 'total mass (in mass unit): '
read(*,*) totmass
write(*,*) 'time_sim (in years):'
read(*,*) time_sim

call prefix(outfile,leng)
open(7,file=outfile)

c determine number of particles in problem
1 read(7,'(a80)') line

```

```

        if (line(12:16).eq.'Years') read(7,*) time
        if(abs(time-time_sim).le.1.0) then
            numspec=0
901      read(7,'(a80)',end=99) line
            if (line(16:22).eq.'Entered') then
                numspec=numspec+1
                read(line,72) spacer2,total(numspec)
72       format(1a30,i11)
            endif
            goto 901
        endif
        goto 1
99      write(6,*) 'total number of particles: '
        write(6,*) (i,total(i),i=1,numspec)
        if(iflag.eq.1) then
            write(*,*) 'rate_const (in 1/year):'
            read(*,*) (rate_const(i),i=1,numspec)
        endif
C
        rewind(7)
        write(6,*)''
        ist=0
2       read(7,'(a80)',end=999) line
        if (line(12:16).eq.'Years') then
            read(7,*) time
            ist=ist+1
            iout=20
            idx=0
        else
            if(line(24:54).eq.title)then
                read(line,59) ctmp,cidx
59      format(A54,a5)
                iout=iout+1
                idx=idx+1
                if(ist.eq.1)then
                    do i=1,5
                        if(cidx(i:i).ne.' ') then
                            jj=i
                            goto 777
                        endif
                    enddo
777      fout=prx//cidx(jj:5)
                open(iout,file=fout)
                write(6,*) 'Output Data Stored in File: ',fout
            endif
            read(7,'(a80)') line
            if (line(16:22).eq.'Entered') then
                read(line,72) spacer2,entered
                read(7,'(a80)') line
                read(line,72) spacer2,cur_in
                read(7,'(a80)') line
                read(line,72) spacer2,left
                read(7,'(a80)') line
                read(line,72) spacer2,decayed
                left_this = left - left_old(idx)
                delta_time = time - time_old(idx)
                if(delta_time.ne.0.)then

```

```

        if(iflag.eq.1) then
            conc = exp(-rate_const(iout-20)*time)*real(left_this)
        else
            conc = real(left_this)
        end if
        cnorm=conc/total(iout-20)
        conc = (totmass/total(iout-20))*conc/delta_time
        if(conc.le.cmin) conc=cmin
        left_old(idx) = left
        time_old(idx) = time
        write(iout,100) time,conc,cnorm,left/total(iout-20)
    endif
endif
endif
endif
goto 2

999  write(6,*) ' '
     write(6,*) 'Finished'

100  format(1x,g13.3,3x,g13.6,2(3x,f7.4))
     end
     subroutine prefix(fname,length)
     character*60 fname
     do length=1,60
         if(fname(length:length).eq.'.')goto 100
     end do
100  length=length-1
     return
     end

```

(2) Example Input File:

'fnpt3d.out10grid'

An output file from FEHM V2.00 for the 3-D factor-of-10 case when the entire fracture grid is affected by fault displacement.

FEHM V2.00 99-06-11 07/17/2000 10:45:05

File purpose - Variable - Unit number - File name

control	- iocntl	- 1	- fnpt3d.files
input	- inpt	- 11	- fnpt3d.dat
geometry	- incoor	- 12	- fnpt3d.grid
zone	- inzone	- 13	- fnpt3d.zone
output	- iout	- 14	- fnpt3d.out
initial state	- iread	- 15	- fnpt3d.ini
final state	- isave	- 16	- fnpt3d.fin
time history	- ishisp	- 17	- fnpt3d.hisp
time his.(tr)	- istr	- 18	- fnpt3d.tr
contour plot	- iscon	- 19	- fnpt3d.con
con plot (dp)	- iscon1	- 0	- not using
fe coef stor	- isstor	- 21	- fnpt3d.stor
input check	- ischk	- 22	- fnpt3d.chk

Value provided to subroutine user: not using

ptrk read from optional input file: fnpt3d.ptrk

# Fault Displacement Effects on Transport in the Unsaturated Zone

Mean inf conceptual #1 input ysw/6/3/99

File purpose - Variable - Unit number - File name

```
control      - iocntl - 1 - fnpt3d.files
input        - inpt   - 11 - fnpt3d.dat
geometry     - incoor - 12 - fnpt3d.grid
zone        - inzone - 13 - fnpt3d.zone
output      - iout   - 14 - fnpt3d.out
initial state - iread  - 15 - fnpt3d.ini
final state  - isave  - 16 - fnpt3d.fin
time history - ishisp - 17 - fnpt3d.hisp
time his.(tr) - istrc - 18 - fnpt3d.trc
contour plot - iscon  - 19 - fnpt3d.con
con plot (dp) - isconl - 0 - not using
fe coef stor - isstor - 21 - fnpt3d.stor
input check  - ischk  - 22 - fnpt3d.chk
```

Value provided to subroutine user: not using

```
**** input title : coor **** incoor = 12 ****
**** input title : elem **** incoor = 12 ****
**** input title : stop **** incoor = 12 ****
**** input title : zone **** inzone = 13 ****
**** input title : stop **** inzone = 13 ****
**** input title : dpdp **** inpt = 11 ****
dpdp read from optional input file: fnpt3d.dpdp
**** input title : perm **** inpt = 11 ****
**** input title : rlp  **** inpt = 11 ****
**** input title : rock **** inpt = 11 ****
rock read from optional input file: fnpt3d.rock
**** input title : flow **** inpt = 11 ****
**** input title : time **** inpt = 11 ****
**** input title : ctrl **** inpt = 11 ****
**** input title : iter **** inpt = 11 ****
**** input title : sol  **** inpt = 11 ****
**** input title : rflo **** inpt = 11 ****
**** input title : air  **** inpt = 11 ****
**** input title : node **** inpt = 11 ****
**** input title : zone **** inpt = 11 ****
zone read from optional input file: fnpt3d.zone2
**** input title : ptrk **** inpt = 11 ****
ptrk read from optional input file: fnpt3d.ptrk
**** input title : stop **** inpt = 11 ****
```

```
!!!!!!!!!!!!!!!!!!!!!!!!!!!!!!
Coefficients read from *.stor file
!!!!!!!!!!!!!!!!!!!!!!!!!!!!!!
```

storage for geometric coefficients      391475 in common(nr)      391475

no particle tracking on restart file

```
storage needed for ncon            439139 available      439139
storage needed for nop            439139 available      476641
storage needed for a matrix       6263584 available     6263584
storage needed for b matrix       6263584 available     7626256
storage needed for gmres           7816896 available     7816896
storage available for b matrix resized to                    1<<<<<<
```

time for reading input, forming coefficients      24.2

# Fault Displacement Effects on Transport in the Unsaturated Zone

---

\*\*\*\* analysis of input data on file fnpt3d.chk \*\*\*\*

note>>h.t. solution stopped after time step 1

note>>tracer solution started on time step 1

Species: 1

at time: 0.9999999999999999

rest: 0.0000000000000000 0.0000000000000000

\*\*\*\*\*

Time Step 1

### Timing Information

Years	Days	Step Size (Days)
0.100000E+01	0.365250E+03	0.365250E+03

Heat and Mass Solution Disabled

\*\*\*\*\*

Particle Tracking ==> Species: 1

Number Having Entered System: 9900

Number Currently In System : 9900

Number Having Left System : 0

Number Having Decayed : 0

Node	Concentration	# of Particles
1	0.000000E+00	0
47665	0.000000E+00	0

Species: 1

at time: 3.0000000000000000

rest: 2.0000000000000000 0.0000000000000000

\*\*\*\*\*

...

\*\*\*\*\*

Time Step 7

### Timing Information

Years	Days	Step Size (Days)
0.127000E+03	0.463868E+05	0.233760E+05

Heat and Mass Solution Disabled

\*\*\*\*\*

Particle Tracking ==> Species: 1

Number Having Entered System: 9900

Number Currently In System : 4916

Number Having Left System : 4984

Number Having Decayed : 0

Node	Concentration	# of Particles
1	0.000000E+00	0
47665	0.000000E+00	0

Species: 1

at time: 255.00000000000000

rest: 1195.0000000000000 0.0000000000000000

\*\*\*\*\*

...

# Fault Displacement Effects on Transport in the Unsaturated Zone

```
*****
Time Step          20

                    Timing Information
                    Years          Days          Step Size (Days)
                    0.100000E+07    0.365250E+09    0.173754E+09
Heat and Mass Solution Disabled

                    *****
                    Particle Tracking ==> Species: 1
Number Having Entered System:      9900
Number Currently In System :       0
Number Having Left System :       9900
Number Having Decayed :            0

Node   Concentration   # of Particles
  1    0.000000E+00      0
47665 0.000000E+00      0

simulation ended: days 3.653E+08 timesteps 20

total N-R iterations =          0
total solver iterations =        0

total code time(timesteps) =      5.130001

****-----****
**** This program for ****
**** Finite Element Heat and Mass Transfer in porous media ****
****-----****
****                               Version : FEHM V2.00 99-06-11 ****
****                               End Date : 07/17/2000 ****
****                               Time : 10:45:44 ****
****-----****
```

### (3) Example Output File:

'pt.3d10grid'

Corresponding to the input file 'fnpt3d.out', this output file contains histories of the concentration, normalized concentration, and accumulative normalized concentration synthesized at the water table for the 3-D factor-of-10 case when the entire fracture grid is affected by fault displacement.

1.00	0.100000E-09	0.0000	0.0000
3.00	0.101010E-03	0.0002	0.0002
7.00	0.227273E-02	0.0091	0.0093
15.0	0.518939E-02	0.0415	0.0508
31.0	0.773990E-02	0.1238	0.1746
63.0	0.533775E-02	0.1708	0.3455
127.	0.246843E-02	0.1580	0.5034
255.	0.943024E-03	0.1207	0.6241
511.	0.343277E-03	0.0879	0.7120
0.102E+04	0.115807E-03	0.0593	0.7713
0.205E+04	0.373856E-04	0.0383	0.8096
0.410E+04	0.135634E-04	0.0278	0.8374
0.819E+04	0.974096E-05	0.0399	0.8773

## Fault Displacement Effects on Transport in the Unsaturated Zone

---

0.164E+05	0.499379E-05	0.0409	0.9182
0.328E+05	0.120221E-05	0.0197	0.9379
0.655E+05	0.425397E-06	0.0139	0.9518
0.131E+06	0.391488E-06	0.0257	0.9775
0.262E+06	0.125615E-06	0.0165	0.9939
0.524E+06	0.227341E-07	0.0060	0.9999
0.100E+07	0.212334E-09	0.0001	1.0000

### (4) Verification

This software routine has been verified before in TSPA-VA related calculations, and has been verified for this AMR by checking its output files manually. As an example: In the output file 'pt.3d10', the synthetic cumulative normalized concentration at the water is '0.5034' at the time of '127.' years. As intended by this program, this value is calculated by dividing the 'Number Having Left System: 4984' with 'Number Having Entered System: 9990' in the input file 'fnpt3d.out'.

### (5) Range of Validation:

This software routine is valid for constructing cumulative breakthrough histories from FEHM output at any given downstream boundary given a pulse input of any solute.

**ATTACHMENT V**  
**SOFTWARE ROUTINE 't2feh2\_v3x.f v.1'**

## ATTACHMENT V

### Software routine 't2fehm2\_v3x.f v.1'

The is a software routine in essence the same as described in (CRWMS M&O 2000e), except some minor modifications to accommodate the possibility of localized perturbations to rock parameters in TOUGH2 files. More specifically, the modifications are to allow the use of the character '&' in replacement of the character 'F' to represent altered rock zones. This routine and related data can be found in the database under DTN: MO0006SPAUZ20.002.

#### (1) Code Listing:

```

c      t2fehm2_v3x.f
C*****
c      Modified to accomodate altered material types in the 'dmdp' and
c      'rock' macros.
c          y.xiang, 4/12/2000.
c
c      Modified to accomodate altered material types in the 'zone' and
c      'zone2' macros.
c          y.xiang, 4/6/2000.
c
c      This program creates column formatted files from TOUGH2.OUT
c      files of EOS3 simulations.
c      Files MESH, TOUGH2.INP, and TOUGH2.OUT must be present.
c      The format of the output files are amenable for an FEHM
c      restart.
c
c          C.K.Ho 5/27/97
c      This version now re-formats TOUGH2.OUT files in either EOS3 or
c      EOS9 format. Multidimensional files can be post-processed. This
c      version assumes that the elements listed in ELEME alternate
c      between fractures and matrix, starting with a fracture element.
c      This can be generalized in the loop (do 3000...) by knowing how
c      how the fracture and matrix elements were listed and by arranging
c      the arrays accordingly. I started this by asking the user to
c      specify the ordering, but I didn't do much with it in this version.
c      So for now, the elements should be listed alternately starting with
c      a fracture element. Also, the matrix materials are assumed to be listed
c      first in the ROCKS card.
c
c          C.K.Ho
c          9/2/97-9/12/97,9/19/97
c      This version (oplpostv3.f) is tailored specifically for LBL site-scale
c      runs. The previous version (optionlpostv2.f) is still good for SNL
c      TOUGH2 simulations of flow fields. The major revisions include reading
c      information from external files (MESH, GENER). In MESH, the material
c      identifier is a 5-character name--not an integer, which was assumed in
c      the previous version. The coordinates will have to be
c      read from MESH. Changes will have to be made for recognizing
c      fracture or matrix materials to accomodate all the materials (there
c      are greater than 100 materials) in the site-scale model. The dimensions
c      will have to be greatly increased to accommodate the 80,000 element
c      site-scale model.

```

## Fault Displacement Effects on Transport in the Unsaturated Zone

---

```
c      C.K.Ho
c      10/23/97
c
c      This version (oplpostv4.f) does not assume any ordering in the ROCKS
c      card.  There can be different numbers of matrix and fracture
c      materials written to the FEHM zone macro.  Also, this version can read
c      in a file containing repository element names to create a separate zone.
c      Another assumption is that the active elements are listed before any
c      boundary elements ('TP' or 'BT') in ELEME.
c      C.K.Ho
c      11/5/97
c
c      A few things have been cleaned up and it appears to work for the LBNL
c      3-D site scale model.  The current version is 't2fehm2.f'.
c      C.K.Ho
c      11/6/97
c
c      This version accommodates new output formatting used by LBNL.  The
c      index field in the output has been changed from i6 to i12.  Also,
c      the flux output has been shifted to the left a bit, and nlin3 is now equal
c      to 3 instead of 4 (this is the amount of header lines inserted in the flux
c      output periodically).
c      The liquid pressure now appears where the gas pressure used to appear in
c      the output file.  To calculate the gas pressure:  $P_g = P_l - P_c$ 
c      C.K.Ho
c      3/9/99
c
c      This version allows the user to calculate the primary volumes as the
c      sum of the fracture and matrix volumes listed in the TOUGH2 ELEME card.
c      This eliminates the need to divide the fracture volume in the ELEME
c      card by the fracture porosity in the ROCKS card, which in the SR
c      base-case runs have in some instances been tranformed to matrix
c      porosities for perched water materials, yielding incorrect primary
c      volumes.
c      C.K.Ho
c      10/10/99
c*****
c23456789012345678901234567890123456789012345678901234567890123456789012
C
      implicit double precision (a-h,o-z)
      DIMENSION X(99000),Y(99000),z(99000),SL(99000),vol(99000)
      dimension PG(99000)
      dimension gelem(99000),ifm(99000)
      dimension fluxl(990000),fmlfm(99000),ncord(99000)
      dimension icon2(990000),flol2(990000),istrw(990000)
      dimension drok(500),por(500),nelmdg(99000),ncon2(99000)
      double precision lblpor
      CHARACTER*22 BLOCK
      CHARACTER*5  ELEMN(99000),ELEM1(490000),ELEM2(490000),ELEMX
      character*5  genname,matname(500),matb,mat(99000)
      character*80 header
      character*40 filen,control,dat,grid,ini,stor,dpdp,rock,zone
      character*40 filein,fileout,meshfile,repfile,zone2,check
      character*1  char2
      character*5  repname(1003)
      common/int/  ncon(99000),icon(99000,35)
      common/flux/ flol(99000,35)
```

C

```

write(*,*) 'This program will re-format TOUGH2 output files'
write(*,*) 'for FEHM restart files. The following files'
write(*,*) 'must be present: input, output, and MESH.'
write(*,*) 'The MESH file should contain 5-character material'
write(*,*) 'names.'
write(*,*)
write(*,*) 'What is the name of the input file?'
read(*,*) filein
write(*,*) 'What is the name of the output file?'
read(*,*) fileout
write(*,*) 'What is the name of the MESH file?'
read(*,*) meshfile
write(*,4)
4   format('What type of run is this?'/,'1) SNL EOS3'/,'2) SNL EOS9?'/
& , '3) LBNL EOS9'/,'4) LBNL EOS9 SR/LA')
read(*,*) neos
write(*,*) 'What reference name would you like to use for the'
write(*,*) 'FEHM restart files? (no spaces in the name)'
read(*,*) filen
write(*,*) 'In ELEME, how are the elements listed?'
write(*,*) '(1) Alternatively with matrix first'
write(*,*) '(2) Alternatively with fracture first'
write(*,*) '(3) All matrix, then all fractures'
write(*,*) '(4) All fractures, then all matrix'
read(*,*) norder
write(*,*) 'For fracture-matrix connections, which element is'
write(*,*) 'listed first: (1) Fracture or (2) Matrix?'
read(*,*) nfmc
write(*,*) 'What is the print-out time (sec) of interest?'
read(*,*) tsec
write(*,*) 'Would you like to calculate primary volumes as the'
write(*,*) 'sum of the fracture & matrix volumes in ELEME?'
write(*,*) '(1=yes, 0=no)'
read(*,*) nprimary
volscale=1.
if(nprimary.eq.1) go to 6
write(*,*) 'The fracture volumes will be used as the primary'
write(*,*) 'control volume for each element. Have they been'
write(*,*) 'modified in TOUGH2.INP? (1=yes, 0=no)'
read(*,*) nvol
if(nvol.eq.1) then
  write(*,*) 'What is the scaling factor to retrieve correct',
& ' primary volumes from fracture volumes?'
  read(*,*) volscale
end if
6   write(*,7)
7   format('What is the geometry?'/,'0) 3-D'/,'1) X-Y Plane'/
& , '2) X-Z Plane'/,'3) Y-Z Plane')
read(*,*) icnl
write(*,*) 'Is there a file with repository element names?'
write(*,*) '1 = yes, 0 = no'
read(*,*) nrepans
if(nrepans.eq.1) then
  write(*,9)
9   format('What is the name of the file with repository elements?')
  read(*,*) repfile

```

```
write(*,*)'Would you like to modify the 2nd character of the'  
write(*,*)'element name? 1=yes, 0=no'  
read(*,*) n2nd  
if(n2nd.eq.1) then  
  write(*,*)'What character would you like to use?'  
  read(*,'(a1)') char2  
end if  
open(19,file=repfile,status='old')  
end if  
  
if(norder.eq.1.or.norder.eq.2) then  
  nalt=2  
else  
  nalt=1  
end if
```

c...Define FEHM restart files based on reference name

```
kend=index(filn,' '  
control=filn(1:kend-1)//'.files'  
dat=filn(1:kend-1)//'.dat'  
grid=filn(1:kend-1)//'.grid'  
ini=filn(1:kend-1)//'.ini'  
stor=filn(1:kend-1)//'.stor'  
dpdp=filn(1:kend-1)//'.dpdp'  
rock=filn(1:kend-1)//'.rock'  
zone=filn(1:kend-1)//'.zone'  
zone2=filn(1:kend-1)//'.zone2'  
check=filn(1:kend-1)//'.check'  
  
if(neos.eq.1) then  
  nlin1=5  
  nlin2=3  
  nlin3=3  
elseif(neos.eq.2) then  
  nlin1=6  
  nlin2=4  
  nlin3=4  
elseif(neos.eq.3) then  
  nlin1=6  
  nlin2=3  
  nlin3=4  
elseif(neos.eq.4) then  
  nlin1=6  
  nlin2=3  
  nlin3=3  
end if  
  
write(*,*) 'Thank You! Please wait while I work...'  
open(1,file=meshfile,status='old')  
open(2,file=fileout,status='old')  
open(3,file=filein,status='old')  
open(11,file=control,status='unknown')  
open(12,file=dat,status='unknown')  
open(13,file=grid,status='unknown')  
open(14,file=ini,status='unknown')  
open(15,file=stor,status='unknown')  
open(16,file=dpdp,status='unknown')
```

```
open(17,file=rock,status='unknown')
open(18,file=zone,status='unknown')
open(22,file=check,status='unknown')
open(23,file=zone2,status='unknown')

c....Data
  spht=1.e3
  per1=1.e-15
  per2=1.e-15
  per3=1.e-15
  day=365.25e0
  tims=365.25e6
  nstep=100
  iprtout=1
  iyear=1997
  month=10
  maxit=-10
  epm=1.e-4
  north=40
  ja=1
  jb=0
  jc=0
  igauss=1
  as=1.
  grav=3.
  upwgt=1.
  iamm=5
  aiaa=2.
  daymin=1.e-10
  daymax=1.e10
  lda=1
  g1=1.e-5
  g2=1.e-5
  g3=1.e-5
  tmch=-1.e-4
  overf=1.2
  irdof=0
  islord=0
  iback=0
  icoupl=0
  rnmax=14400.
  ntt=1
  intg=-1
  zero=1.d-10
  ra=287.
  rv=461.52

C
c...Read header from TOUGH2.INP
  read(3,'(a80)') header

c
c...Write information to .dat file
  write(12,510) header
510  format(a80/'# Particle tracking for TOUGH2 flow field')

c...Write dpdp macro
  write(12,516) dpdp
```

## Fault Displacement Effects on Transport in the Unsaturated Zone

---

```
516  format('dmdp'/'file'/a)

c...Write perm macro
    write(12,518) per1,per2,per3
518  format('perm'/'1 0 0 ',3e10.3/)

c...Write rlp macro
    write(12,520)
520  format('rlp'/'1 0. 0. 1. 1. 0. 1.'/'1 0 0 1'/)

c...Write rock macro
    write(12,522) rock
522  format('rock'/'file'/a)

c...Write flow macro
    write(12,524)
524  format('flow'/)

c...Write time macro
    write(12,526) day,tims,nstep,iprtout,iyear,month
526  format('time'/2e13.5,4i8/)

c...Write ctrl macro
    write(12,528) maxit,epm,north,ja,jb,jc,igaus,as,grav,upwgt,
    & iamm,aiaa,daymin,daymax,icnl,lda
528  format('ctrl'/i8,e10.2,i8/4i8/'0'/3f10.2/i8,3e10.2/2i8)

c...Write iter macro
    write(12,530) g1,g2,g3,tmch,overf,irdof,islord,iback,icoupl,
    & rnmax
530  format('iter'/5e10.2/4i8,e10.2)

c...Write sol macro
    write(12,532) ntt,intg
532  format('sol'/2i8)

c...Write rflo macro
    write(12,534)
534  format('rflo'/'air'/'-1'/'20.0 0.1')

c...Write node macro
    write(12,536)
536  format('node'/'1'/'1')

c...Write zone macro that corresponds to the repository nodes
    write(12,515) zone2
515  format('zone'/'file'/a)

c...Write ptrk macro
    write(12,538) filen(1:kend-1)
538  format('ptrk'/'file'/a,'.ptrk')

c...Write stop
    write(12,540)
540  format('stop')
c
```

---

```

c...Write information to control file
  write(11,501) dat,grid,zone,filen(1:kend-1),ini,filen(1:kend-1)
  &,filen(1:kend-1),filen(1:kend-1),filen(1:kend-1),stor,
  &filen(1:kend-1)
501  format(a/a/a/a,'.out'/a/a,'.fin'/a,'.his'/a,'.trc'/a,'.con'//
  & a/a,'.chk'/'all'/'0')

c...Read in repository element names
  if(nrepans.eq.1) then
    read(19,*) nrepelem
    numrep=nrepelem
    do i=1,nrepelem
      read(19,'(a5)') repname(i)
      repname(i)(1:1)='F'
      if(n2nd.eq.1) repname(i)(2:2)=char2
    end do
  end if

c...Read in grid information from MESH
  nbelm=0
  nbmat=0
  matb=' '
  N=1
  read(1,1000) block
1000 format(a22)
99  read(1,65) elemn(n),mat(n),vol(n),x(n),y(n),z(n)
65  format(a5,10x,a5,e10.4,20x,3e10.4)
  if(elemn(n).eq.' ') go to 98
  if(elemn(n)(4:4).eq.'0') elemn(n)(4:4)=' '
c...Count number of boundary elements, nbelm, and number of boundary
c...materials, nbmat.
  if(elemn(n)(1:2).eq.'TP'.or.elemn(n)(1:2).eq.'BT') then
    nbelm=nbelm+1
    if(mat(n).ne.matb) then
      nbmat=nbmat+1
      matb=mat(n)
    end if
  end if
  N=N+1
  GO TO 99
98  CONTINUE
  NMAX = N - 1
c...NMAX is the total number of elements read from MESH
  write(*,107) nmax
107  format('Have read in ',i8,' elements from MESH...')
c...nnodes is the total number of active nodes
  nnodes=nmax-nbelm

c...Find maximum number of materials used in ROCKS (nmat)
c  nmat=0
c  do i=1,nmax
c    nmat=max(mat(i),nmat)
c  end do
c  write(*,222) nmat
c222 format('Maximum number of active materials = ',i8,'...')

c...nfmat is the number of fracture materials

```

## Fault Displacement Effects on Transport in the Unsaturated Zone

---

```
c      nformat=(nmat-nbmat)/2

c...Read in connection information from MESH
      N=1
      READ(1,1500) BLOCK
1500  FORMAT(A22,3X,25X,E10.4)
199   read(1,1502) elem1(n),elem2(n),ifm(n)
c...ifm(n) is a flag in the 75th column of the CONNE card that Yu-Shu has
c...specified as equal to '2' for fracture-matrix connections
1502  format(2a5,64x,i1)
      IF(elem1(n)(1:5).EQ.'      '.OR.elem1(n)(1:3).EQ.'+++') GO TO 198
      if(elem1(n)(4:4).eq.'0') elem1(n)(4:4)=' '
      if(elem2(n)(4:4).eq.'0') elem2(n)(4:4)=' '
      N=N+1
      GO TO 199
198   CONTINUE
      NCMAX = N - 1
c...NCMAX is the total number of connections read from MESH
      write(*,203) ncmx
203   format('Have read in ',i8,' connections from MESH...')

c...Read in ROCKS information from TOUGH2 input file
18   read(3,1000) block
      if(block(1:5).ne.'ROCKS') go to 18

      i=1
      nformat=0
      nmmat=0
408  read(3,410) matname(i),drok(i),por(i)
410  format(a5,5x,2e10.4)
      if(matname(i).eq.'REFCO') go to 408
      if(matname(i).eq.'      ') then
c...ntotmat is the total number of materials in the ROCKS card
c...nmat is the number of materials associated with non-boundary
c...elements
          ntotmat=i-1
          nmat=ntotmat-nbmat
          go to 27
      end if
c...LBNL uses columns 71-80 in the second line of each material card to
c...identify the fracture porosity
      read(3,415) lblpor
415  format(70x,e10.4)
c...nformat is the total number of fracture materials
c
c Modified to accomodate altered fracture names as identified by
c the character '&' in replacement of 'F':
      if(matname(i)(3:3).eq.'&'.or.matname(i)(4:4).eq.'&') then
          nformat=nformat+1
          if(neos.eq.3.or.neos.eq.4) por(i)=lblpor
          if(por(i).eq.0.) por(i)=1.1d-5
          endif
          if(matname(i)(3:3).eq.'F'.or.matname(i)(4:4).eq.'F') then
              nformat=nformat+1
              if(neos.eq.3.or.neos.eq.4) por(i)=lblpor
c...The perched water fractures do not have porosities listed in ROCKS.
c...Yu-Shu said that they have the same porosity as the zeolitic fractures,
```

## Fault Displacement Effects on Transport in the Unsaturated Zone

---

```
c...which is 1.1e-5 (phone message 10/31/97).
      if(por(i).eq.0.) por(i)=1.1d-5
      end if
c...nmmat is the total number of matrix materials
      if(matname(i)(3:3).eq.'M'.or.matname(i)(4:4).eq.'M') nmmat=nmmat+1
      read(3,*)
      read(3,*)
      i=i+1
      go to 408

27    continue

c...10/27/97  Ho

c...Write grid macro file
      write(13,202) nnodes/2
202   format('coor'/i8)
c...This assumes that all boundary elements ('TP' and 'BT') are listed
c...after the active elements in ELEME
      do i=1,nnodes/2
          write(13,204) i,x(i*nalt),y(i*nalt),z(i*nalt)
204   format(i8,3(3x,f10.2))
      end do
      write(13,206)
206   format('/'elem''/2  1''/1  2  1''/'stop')

c...Initialize generation array
      do i=1,nmax
          gelem(i)=0.
      end do

c...Read in generation information from TOUGH2.INP
      i=1
33   read(3,1000,end=299) block
      if(block(1:5).ne.'GENER') go to 33
74   read(3,75) genname,g
75   format(a5,35x,e10.4)
      if(genname.eq.'    ') go to 77
      if(genname(4:4).eq.'0') genname(4:4)=' '
      do ik=1,nmax
          if(genname.eq.elemln(ik)) then
c...Assign a generation term for each element (flow into an element
c...is defined as negative)
c...The method used here is different than in v3.  It eliminates a
c...separate do-loop and the need for arrays igen and g.
              gelem(ik)=-g
              i=i+1
              go to 74
          end if
      end do
      write(*,*)'Could not find element name for generation'
      write(*,79) i,genname
79   format('element ',i8,': ',a5)
      stop

299  write(*,*)'***Warning*** No generation card in TOUGH2.INP'
```

```

77   ngentot=i-1

c...Write zone macro
      ntotin=0
      write(18,'(a4)') 'zone'
      write(23,'(a4)') 'zone'
      do i=1,ntotmat
        write(18,512) i,matname(i)
        write(23,512) i,matname(i)
512   format(i4,5x,'#',a5)
        write(18,'(a4)') 'nnum'
        write(23,'(a4)') 'nnum'
        nin=1
        do j=1,nmax
c...Match nodes to respective materials. This assumes that the
c...fractures and matrix elements are listed alternately in ELEME
c...starting with the fractures first
c...If element is a boundary element, go to next element
c
c Modified by yxiang to accomodate altered material types as identified
c by the character '&' in replacement of the character 'F':
c
          if(elemn(j)(1:2).eq.'TP'.or.elemn(j)(1:2).eq.'BT') goto 517
          if(mat(j).eq.matname(i)) then
            if(mat(j)(3:3).eq.'&'.or.mat(j)(4:4).eq.'&') then
              ncord(nin)=(j+1)/nalt
              nin=nin+1
              go to 517
            end if
            if(mat(j)(3:3).eq.'F'.or.mat(j)(4:4).eq.'F') then
              ncord(nin)=(j+1)/nalt
              nin=nin+1
              go to 517
            end if
            if(mat(j)(3:3).eq.'M'.or.mat(j)(4:4).eq.'M') then
              ncord(nin)=j/nalt+nnodes/2.
              nin=nin+1
            end if
          end if
517   end do
        nin=nin-1
        ntotin=ntotin+nin
        write(18,'(i10)') nin
        write(23,'(i10)') nin
        if(nin.gt.0) write(18,'(8i10)') (ncord(k),k=1,nin)
        if(nin.gt.0) write(23,'(8i10)') (ncord(k),k=1,nin)
      end do
      write(18,*)
      write(18,'(a4)') 'stop'

c...Now write zones for nodes corresponding to repository elements
      nrp=1
      do i=1,nmax
        do j=1,numrep
          if(elemn(i).eq.repname(j)) then
            ncord(nrp)=(i+1)/nalt
            nrp=nrp+1
          end if
        end do
      end do

```

```

        go to 527
    end if
end do
527 end do

nrp=nrp-1
write(23,*) '500 #fracture repository nodes'
write(23,'(a4)') 'nnum'
write(23,'(i10)') nrp
if(nrp.gt.0) write(23,'(8i10)') (ncord(k),k=1,nrp)
write(23,*) '501 #matrix repository nodes'
write(23,'(a4)') 'nnum'
write(23,'(i10)') nrp
do i=1,nrp
    ncord(i)=ncord(i)+nnodes/2.
end do
if(nrp.gt.0) write(23,'(8i10)') (ncord(k),k=1,nrp)
write(23,*)
write(23,'(a4)') 'stop'

c...Now write some additional information to the zone file
write(18,*)
write(23,*)
write(18,514) ntotin,nbmat,nbelm
write(23,514) ntotin,nbmat,nbelm
514 format(/'#Total number of nodes = ',i8/'#Total number of',
& ' active boundary materials = ',i8/'#Total number of active',
& ' boundary nodes = ',i8/)

c...Write dpdp macro file
write(16,550)
550 format('dpdp'/'1')
c...Loop over the materials and print out fracture porosities
c
c Modified by yxiang to accomodate altered fracture names as identified
c by the character '&' in replacement of 'F':
do i=1,ntotmat
if(matname(i)(3:3).eq.'&'.or.matname(i)(4:4).eq.'&') then
write(16,552) -i,jb,jc,por(i)
end if
if(matname(i)(3:3).eq.'F'.or.matname(i)(4:4).eq.'F') then
write(16,552) -i,jb,jc,por(i)
552 format(3i8,5x,e10.4)
end if
end do
write(16,554) ja,jb,jc
554 format(/,3i8,5x,'99.'/'/'stop')

c...Write rock macro file
write(17,556)
556 format('rock')
do i=1,ntotmat
porock=por(i)
if(matname(i)(3:3).eq.'F'.or.matname(i)(4:4).eq.'F')porock=1.
c Modified to accomodate altered fracture names as identified by
c the character '&' in replacement of 'F':
if(matname(i)(3:3).eq.'&'.or.matname(i)(4:4).eq.'&')porock=1.

```

## Fault Displacement Effects on Transport in the Unsaturated Zone

---

```
        write(17,558) -i,jb,jc,drok(i),spht,porock
558      format(3i8,5x,e10.4,5x,e10.4,5x,e10.4)
        end do
        write(17,559)
559      format(/'stop')

c...Search for "TOTAL TIME" in TOUGH2.OUT and then read in variables
89      READ(2,1000,END=90) BLOCK
        IF(BLOCK(1:12).NE.' TOTAL TIME') GO TO 89
        READ(2,1001) TIME
        if(time.ne.tsec.and.tsec.gt.0) go to 89
1001    FORMAT(E13.5)
        do nl=1,nlin1
            READ(2,1000) BLOCK
        end do

C
c23456789012345678901234567890123456789012345678901234567890123456789012

c...Read in state variables from TOUGH2.OUT
115    N1=1
        N2=MIN(NMAX,45)
        DO 2000 I=N1,N2
            if(neos.eq.1) then
c...      This is EOS3 format
                READ(2,1002) PG(I),SL(I)
1002    FORMAT(12x,e12.5,24x,7e12.5)
            elseif(neos.eq.2.or.neos.eq.3) then
c...      This is EOS9 format
                read(2,118) pg(i),sl(i)
118      format(12x,2e12.5)
            elseif (neos.eq.4) then
c...      This is EOS9 format with new index formatting of i12
                read(2,119) pl,sl(i),pc
                pg(i)=pl-pc
119      format(18x,3e12.5)
            end if
2000    CONTINUE

C
2100    CONTINUE

c...Check to see if we've read in all the element variables
        IF(N2.EQ.NMAX) GO TO 91
        N1=N2+1
        N2=MIN(NMAX,N1+56)
        do nl=1,nlin2
            READ(2,1000) BLOCK
        end do
        DO 2010 I=N1,N2
            if(neos.eq.1) then
c...      This is EOS3 format
                READ(2,1002) PG(I),SL(I)
            elseif(neos.eq.2.or.neos.eq.3) then
c...      This is EOS9 format
                read(2,118) pg(i),sl(i)
            elseif (neos.eq.4) then
c...      This is EOS9 format with new index formatting of i12
                read(2,119) pl,sl(i),pc
                pg(i)=pl-pc
```

```

        end if
2010  CONTINUE
        GO TO 2100
C
91    CONTINUE
C
c...Write saturations to .ini file (fractures saturations first followed
c...by matrix saturations)
        write(14,302) header
302  format(a80/'This is a .ini file with saturations, pressures',
        & ' and mass flux values.'/'0.'/'air'/'ptrk'/'nstr'/
        & 'dmdp'/'ndua')
        write(14,304) (sl(i),i=1,nnodes,2),(sl(i),i=2,nnodes,2)
304  format(4g16.8)

c...Write pressures to .ini file in MPa (fractures first, then matrix)
        write(14,304) (pg(i)*1.d-6,i=1,nnodes,2),
        & (pg(i)*1.d-6,i=2,nnodes,2)

        write(*,*)'Have read in state variables from output file...'
C
c...Read in flux variables from TOUGH2.OUT
289  READ(2,1500,END=190) BLOCK
        if(neos.lt.4) then
            IF(BLOCK(11:22).NE.'ELEM1  ELEM2') GO TO 289
        elseif (neos.eq.4) then
            IF(BLOCK(7:18).NE.'ELEM1  ELEM2') GO TO 289
        end if
        READ(2,1500) BLOCK
        READ(2,1500) BLOCK
C
c...Read in mass flow liquid for each connection pair
        N1=1
        N2=MIN(NCMAX,53)
        DO 1600 I=N1,N2
            if(neos.eq.1) then
                READ(2,1003) fluxl(I)
1003  FORMAT(80x,4e13.5)
            elseif (neos.eq.2.or.neos.eq.3) then
                read(2,121) fluxl(i)
121  format(29x,e13.5)
            elseif (neos.eq.4) then
                read(2,122) fluxl(i)
122  format(31x,e13.5)
            end if
1600  CONTINUE
C
2150  CONTINUE
        IF(N2.EQ.NCMAX) GO TO 191
        N1=N2+1
        N2=MIN(NCMAX,N1+56)
        do nl=1,nlin3
            READ(2,1500) BLOCK
        end do
        DO 2020 I=N1,N2
            if(neos.eq.1) then
                READ(2,1003) fluxl(I)

```

```

        elseif (neos.eq.2.or.neos.eq.3) then
            read(2,121) fluxl(i)
        elseif (neos.eq.4) then
            read(2,122) fluxl(i)
        end if
2020 CONTINUE
        GO TO 2150
C
191 CONTINUE

C
190 CONTINUE

c...Check
        write(*,*)'Have read in flux variables from output file...'

c...Check
c        do i=1,ncmax
c            write(15,444) i,elem1(i),elem2(i),fluxl(i)
c444        format(i8,2x,2(a5,2x),e10.4)
c        end do
c        stop
c...End check
C
c...Loop over all elements to determine connections and fluxes for each
c...element
        nmlfm=1
c...nmlfm is the total number of fracture-matrix connections
        DO 3000 I=1,NMAX

            if(mod(i,1000).eq.0) write(*,472) i
472        format('Still working... Element ',i8)

c...fmlfm(i) is the flow (kg/s) between fracture and matrix
        fmlfm(i)=0.d0

c...jj is the number of connections for each element
        do jj=1,35
            flol(i,jj)=0.d0
c...icon(i,jj) is the node number of the element for connection jj to element
i
            icon(i,jj)=0
        end do

        ELEMN=ELEMN(I)

c...If element is a boundary element, go to next element
        if(elemx(1:2).eq.'TP'.or.elemx(1:2).eq.'BT') go to 3000

c...Write the element number and the number of connections for that element
        if(i.gt.1) write(22,*) i-1,ncon(i-1)
c


---


c...For each element, loop over all connections to determine if
c...the element is either the first or second element in each connection
c...nc is the number of connections per element

        nc=1
    
```

## Fault Displacement Effects on Transport in the Unsaturated Zone

---

```
DO 3001 J=1,NCMAX

c...Say element is the first element in the connection
  if(elem1(j).eq.elemx) then
    nsign=-1
c...If connecting element is the top boundary, go to next connection
  if(elem2(j)(1:2).eq.'TP') go to 3001
c...If connecting element is the bottom boundary, treat the flow to the
c...bottom boundary as a sink/source term and move on to the next connection
  if(elem2(j)(1:2).eq.'BT') then
    gelem(i)=fluxl(j)*nsign
    go to 3001
  end if
c...What is the second element in the connection?
  do ii=1,nmax
    if(elem2(j).eq.eleml(ii)) then
      k2nd=ii
c...Determine if the connection is between a fracture and matrix element
c...If it is a fracture-matrix connection (both elements have the same
c...coordinates, or ifm=2), store this flux separately from fracture-fracture
c...or matrix-matrix fluxes.
      dx=dabs(x(k2nd)-x(i))
      dy=dabs(y(k2nd)-y(i))
      dz=dabs(z(k2nd)-z(i))
      if(dx.le.zero.and.dy.le.zero.and.dz.le.zero.or.
      & ifm(j).eq.2) then
c...If the first element of f-m connection is a fracture, then process this
        if(nfmc.eq.1) then
          go to 3017
        else
          go to 3001
        end if
      end if
      icon(i,nc)=ii
      flol(i,nc)=fluxl(j)*nsign
      nc=nc+1
      go to 3002
    endif
  end do
  write(*,7001) elemx,j,elem2(j),elem2(j-1),elem2(j+1)
7001  format('***Could not find 2nd element in connection for',
  & ' first element ',a5,'***'/'Connection index = ',i8/
  & 'Second element = ',a5/'j-1= ',a5/'j+1= ',a5)
  stop
end if

c...If no match in first element of connection, try second element
  if(elem2(j).eq.elemx) then
    nsign=1
c...If connecting element is the top boundary, go to next connection
  if(elem1(j)(1:2).eq.'TP') go to 3001
c...If connecting element is the bottom boundary, treat the flow to the
c...bottom boundary as a sink/source term and move on to the next connection
  if(elem1(j)(1:2).eq.'BT') then
    gelem(i)=fluxl(j)*nsign
    go to 3001
  end if
```

```

c...What is the first element in the connection?
  do ii=1,nmax
    if(elem1(j).eq.elemn(ii)) then
      k2nd=ii
c...Determine if the connection is between a fracture and matrix element
c...If it is a fracture-matrix connection (both elements have the same
c...coordinates), store this flux separately from fracture-fracture or
c...matrix-matrix fluxes.
      dx=dabs(x(k2nd)-x(i))
      dy=dabs(y(k2nd)-y(i))
      dz=dabs(z(k2nd)-z(i))
      if(dx.le.zero.and.dy.le.zero.and.dz.le.zero.or.
&      ifm(j).eq.2) then
c...If the second element of f-m connection is a fracture, then process this
      if(nfmc.eq.2) then
        go to 3017
      else
        go to 3001
      end if
    end if
    icon(i,nc)=ii
    flol(i,nc)=fluxl(j)*nsign
    nc=nc+1
    go to 3002
  end if
end do
write(*,7000) elemx,j,elem1(j)
7000 format('***Could not find 1st element in connection for',
& ' second element ',a5,'***/'Connection index = ',i8/
& '1st element = ',a5)
  stop
end if

c...If neither element 1 or 2 for connection j is equal to elemx, then
c...go on to the next connection
  goto 3001

3002  continue

c


---


c...go to next connection
  go to 3001

c


---


c...Come here if this is a fracture-matrix connection AND the element
c...being considered (elemx=elemn(i)) is a fracture
c...Consider outflow to be positive and
c...that the first element in the connection is a fracture
3017  continue
      fmlfm(nmlfm)=nsign*fluxl(j)
      nmlfm=nmlfm+1

c...Go to next connection
c


---


3001  continue

c...ncon(i) is the total number of connections for node i
      ncon(i)=nc-1

```

```

C
c...Check
c      write(15,446) i,ncon(i),(icon(i,j),j=1,ncon(i))
c446   format(10(i8,2x))
c      write(15,448) i,ncon(i),(flol(i,j),j=1,ncon(i))
c448   format(2(i8,2x),8(e10.4,2x))
c...End check

c...Go to next element
3000  CONTINUE

c...nmlfm is the total number of fracture-matrix connections
      nmlfm=nmlfm-1

c...Add connection for each element to itself using generation array
c...nmfluxval is the total number of mass flux values
c...Note: nodes 1-nnodes are still assumed to alternative between
c...fractures and matrix. This will be adjusted later in the print-out
c...to the FEHM files.
      nmfluxval=0
      do i=1,nnodes
        ncon(i)=ncon(i)+1
        icon(i,ncon(i))=i
        flol(i,ncon(i))=gelem(i)
        nmfluxval=nmfluxval+ncon(i)
c...Check
c      write(15,448) i,ncon(i),flol(i,ncon(i)),nmfluxval
c448   format(2(i8,2x),e10.4,2x,i8)
c...End check
c...nmfluxval is the total number of flux values for fracture and matrix
c...elements excluding f-m fluxes
      end do

c...Call sort subroutine to sort the necessary arrays in ascending order
c...of elements for each connection pair of a given element

      call sort(nnodes)
C
c...Create 1-D arrays containing icon and flol information. The arrays
c...will be icon2 and flol2. This assumes that the fractures and matrix
c...elements alternate in ELEME and fractures are listed first.
      k=1
      jj=1
      ncont1=0
c...ncont1 is the total number of connections for each continuum
c...do the fracture continuum first
      do i=1,nnodes,2
        do j=1,ncon(i)
c...The index k+nnodes/2+1 accounts for the leading pointer information
          icon2(k+nnodes/2+1)=(icon(i,j)+1)/2
          flol2(k)=flol(i,j)
          k=k+1
        end do
        ncont1=ncont1+ncon(i)
c...ncon2(jj) is the number of connections for fracture node jj, where jj is
c...now incremented 1,2,3...nnodes/2
        ncon2(jj)=ncon(i)

```

```

        jj=jj+1
    end do

c...Now do the matrix continuum
    do i=2,nnodes,2
        do j=1,ncon(i)
            flol2(k)=flol(i,j)
            k=k+1
        end do
    end do
c...ntotmfv is the total number of connections. This can be compared to
c...nmfluxval as a cross-check to see if they're equal.
    ntotmfv=k-1

c...Write mass flux values to .ini file
    write(14,602) nmlfm+nmfluxval,ntotmfv,nnodes,nmlfm
602  format('mass flux values'/i8,5x,'#ntotmfv=',i8,', nnodes=',i8,
    & ', number of f-m connections= ',i8)
    write(14,604) (flol2(i),i=1,ntotmfv),(fmlfm(i),i=1,nmlfm)
604  format(5g15.8)

c...Write .stor file
    write(15,702) header
702  format(a80/'This is a .stor file with dummy area coefficients')

c...Add the pointer information (number of fracture nodes+1) to ncont1
    neq=nnodes/2
    ncont=ncont1+(neq+1)
    iwtotl=ncont-(neq+1)

    write(15,704) iwtotl,neq,ncont,1
704  format(4(i8,2x))

c...Write primary volume for each node to .stor
c...If this is an LBNL run, check to see how user wants calculation performed
c...If nprimary=1, simply sum the fracture and matrix volumes in ELEME to get
c...the primary volume. If not, then divide the fracture volumes by the
c...fracture porosity, since the volumes in ELEME were multiplied by
c...the fracture porosity.
    if(nprimary.eq.1) then
        do i=1,nnodes,2
            vol(i)=vol(i)+vol(i+1)
        end do
        go to 835
    end if
    if(neos.eq.3.or.neos.eq.4) then
        do i=1,nnodes,2
            do j=1,ntotmat
                if(mat(i).eq.matname(j)) then
                    vol(i)=vol(i)/por(j)
                    go to 833
                end if
            end do
        end do
833  end do
    end if
c...If the fracture volumes were globally modified, multiply the volume
c...by a scaling factor, volscale, specified by the user to get the original

```

## Fault Displacement Effects on Transport in the Unsaturated Zone

---

```
c...volume back.
835  write(15,706) (vol(i)*vol*scale,i=1,nnodes,2)
706  format(1p5e16.8)

c...Compile and write ncon and pointer information
c...Fill the icon2(i) array from i=1,neq+1 (recall that icon2(i) has
c...already been filled from neq+2 to ncont1 (the total number of connections
c...for the fracture continuum
      icon2(1)=neq+1
      do i=2,neq+1
        icon2(i)=icon2(i-1)+ncon2(i-1)
      end do
      write(15,708) (icon2(i),i=1,ncont)
708  format(5(i8,2x))

c...Compile and write istrw information to .stor file
      do i=1,ncont
        if(i.le.iwtotl) then
          istrw(i)=i
        else
          istrw(i)=0
        end if
      end do
      write(15,708) (istrw(i),i=1,ncont)

c...Compile and write nelmdg information to .stor file
      do i=1,neq
        do j=icon2(i)+1,icon2(i+1)
          if(icon2(j).eq.i) nelmdg(i)=j
        end do
      end do
      write(15,708) (nelmdg(i),i=1,neq)

c...Write dummy area coefficients to .stor file
      do i=1,3
        write(15,706) (-1.0,j=1,iwtotl)
      end do
c


---


      write(*,1153) time
1153 format('Finished processing printout at ',e12.4,' sec')
      go to 722
C
90  CONTINUE
      write(*,*)'***Did not find desired print-out time in TOUGH2.OUT***'
C
722  write(*,*) 'Done!!!'

      stop
      END

      subroutine sort(nnodes)
c


---


c  This subroutine sorts variables using a multipass method.
c    C.K.Ho
c    9/8/97
```

c

```
implicit double precision (a-h,o-z)
common/int/ ncon(99000),icon(99000,35)
common/flux/ flol(99000,35)
```

c...The objective here is to arrange the connections in ascending order  
c...of connecting node number. The associated flux should also be sorted.

```
nsort=1
do i=1,nnodes
5   if(nsort.eq.1) then
      nsort=0
      do j=1,ncon(i)-1
          if(icon(i,j).gt.icon(i,j+1)) then
              itempicon=icon(i,j)
              icon(i,j)=icon(i,j+1)
              icon(i,j+1)=itempicon
              tempflol=flol(i,j)
              flol(i,j)=flol(i,j+1)
              flol(i,j+1)=tempflol
          nsort=1
          end if
      end do
      go to 5
    end if
    nsort=1
end do
return
end
```

### (2) Example Input Files:

#### (a) 't2fehm2\_v3.inp3d'

Mater input file for 't2fehm2\_v3x.f'. Among other parameters, this file contains the names for these files: a primary input file and a MESH input file for and an output file from TOUGH2 V1.4, a file that lists the repository nodes in the fracture domain of the dual-permeability grid, and the file designator for the FEHM V2.00 input files to be generated from executing 't2fehm2\_v3x.f'. The particular listing below corresponds to the 3-D factor-of-10 case when the entire fracture grid is affected by fault displacement.

```
tough2.inp3d10grid
tough2.inp3d10grid.out
MESH.3d10grid
4
fnpt3d
2
1
0
1
0
1
SR-repo-nodes
0
```

## Fault Displacement Effects on Transport in the Unsaturated Zone

---

### (b) 'tough2.inp3d10grid'

The primary input file to TOUGH2 V1.4 for the 3-D factor-of-10 case when the entire fracture grid is affected by fault displacement.

```

Mean inf conceptual #1 input ysw/6/3/99
ROCKS from inversion "itough2 binfL1xi binfL1x 9" Date: 2-Jun-99 15:27
tcwM1 2 0.250E+01 0.253E+00 0.385E-14 0.385E-14 0.385E-14 0.100E+01 0.100E+04
0.000E+00 0.000E+00 0.100E+01 0.000E+00 0.000E+00 0.000E+00 0.000E+00 0.000E+00
7 0.470E+00 0.700E-01 0.100E+01 0.000E+00 0.100E+01 0.000E+00 0.000E+00
7 0.470E+00 0.700E-01 0.400E-04 0.100E+11 0.100E+01 0.000E+00 0.000E+00
tcwM2 2 0.250E+01 0.820E-01 0.274E-18 0.274E-18 0.274E-18 0.100E+01 0.100E+04
0.000E+00 0.000E+00 0.100E+01 0.000E+00 0.000E+00 0.000E+00 0.000E+00 0.000E+00
7 0.241E+00 0.190E+00 0.100E+01 0.000E+00 0.100E+01 0.000E+00 0.000E+00
7 0.241E+00 0.190E+00 0.181E-04 0.100E+11 0.100E+01 0.000E+00 0.000E+00
...
tcwF1 2 0.250E+01 0.100E+01 0.241E-11 0.241E-11 0.241E-11 0.100E+01 0.100E+04
0.000E+00 0.000E+00 0.100E+01 0.000E+00 0.000E+00 0.000E+00 0.000E+00 0.280E-01
7 0.627E+00 0.100E-01 0.100E+01 0.000E+00 0.100E+01 0.000E+00 0.000E+00
7 0.627E+00 0.100E-01 0.315E-02 0.100E+11 0.100E+01 0.302E+00 0.000E+00
tcwF2 2 0.250E+01 0.100E+01 0.100E-09 0.100E-09 0.100E-09 0.100E+01 0.100E+04
0.000E+00 0.000E+00 0.100E+01 0.000E+00 0.000E+00 0.000E+00 0.000E+00 0.200E-01
7 0.613E+00 0.100E-01 0.100E+01 0.000E+00 0.100E+01 0.000E+00 0.000E+00
7 0.613E+00 0.100E-01 0.213E-02 0.100E+11 0.100E+01 0.302E+00 0.000E+00
...
tcw&1 2 0.250E+01 0.100E+01 0.241E-08 0.241E-08 0.241E-08 0.100E+01 0.100E+04
0.000E+00 0.000E+00 0.100E+01 0.000E+00 0.000E+00 0.000E+00 0.000E+00 0.280E+00
7 0.627E+00 0.100E-01 0.100E+01 0.000E+00 0.100E+01 0.000E+00 0.000E+00
7 0.627E+00 0.100E-01 0.315E-01 0.100E+11 0.100E+01 0.302E+00 0.000E+00
tcw&2 2 0.250E+01 0.100E+01 0.100E-06 0.100E-06 0.100E-06 0.100E+01 0.100E+04
0.000E+00 0.000E+00 0.100E+01 0.000E+00 0.000E+00 0.000E+00 0.000E+00 0.200E+00
7 0.613E+00 0.100E-01 0.100E+01 0.000E+00 0.100E+01 0.000E+00 0.000E+00
7 0.613E+00 0.100E-01 0.213E-01 0.100E+11 0.100E+01 0.302E+00 0.000E+00
...
GENER Mean Flux (mm/yr)= 4.5956 from file inf99_a.dat
Faa 1 COM1 0.1724E-010.7561E+05
Faa 2 COM1 0.4398E-020.7561E+05
...
Fak60 COM1 0.2806E-020.7561E+05
Fak61 COM1 0.2927E-020.7561E+05
ENDCY

```

### (c) 'tough2.inp3d10grid.out'

Output file from TOUGH2 V1.4 for the 3-D factor-of-10 case when the entire fracture grid is affected by fault displacement.

```

...
ELEM. INDEX PRES S(liq) PCAP K(rel) DIFFUS. DL
(KG/M**3) (PA) (PA) (M^2/S)

```

## Fault Displacement Effects on Transport in the Unsaturated Zone

```

Faa 1      1  0.91586E+05  0.12041E-01  -.41379E+03  0.73504E-08  0.16766E-08
0.99716E+03
Maa 1      2  -.72806E+06  0.11206E+00  -.82006E+06  0.89255E-07  0.33580E-10
0.99716E+03
Fba 1      3  0.90809E+05  0.10644E-01  -.11907E+04  0.17516E-09  0.16027E-07
0.99716E+03
Mba 1      4  -.54658E+06  0.55890E+00  -.63858E+06  0.59074E-04  0.12566E-11
0.99716E+03

```

...

ELEM1	ELEM2	INDEX	FLO(LIQ.)	VEL(LIQ.)	FLO(fract)	VEL(fract)
FLO(matrx)	VEL(matrx)		(KG/S)	(M/S)	(KG/S)	(M/S)
(KG/S)	(M/S)					
Fea 1	Fda 1	1	0.16905E-01	0.92969E-07	0.16905E-01	0.92969E-07
0.00000E+00	0.00000E+00					
Mea 1	Mda 1	2	-0.48420E-05	-0.50944E-12	-0.48420E-05	-0.50944E-12
0.48420E-05	-0.50944E-12					
Fda 1	Fca 1	3	0.17047E-01	0.90667E-07	0.17047E-01	0.90663E-07
0.00000E+00	0.00000E+00					
Mda 1	Mca 1	4	0.20182E-07	0.50774E-14	0.20182E-07	0.50774E-14
0.20182E-07	0.50774E-14					

...

### (d) 'MESH.3d10grid'

MESH file for TOUGH2 V1.4 for the 3-D factor-of-10 case when the entire fracture grid is affected by fault displacement. Note that the fracture and matrix volumes have been changed according to equations (7) and (8) in Section 6.2.1.6.

```

ELEME  cdist=      .1E+11
Faa 1    0    0tcw&1 .6530E+05 .1000E+01          169399.094236623.641  1626.096
Maa 1    0    0tcwM1 .1679E+06 .0000E+00          169398.594236623.641  1626.096
Fba 1    0    0tcw&2 .6488E+06 .1000E+01          169399.094236623.641  1606.466
Mba 1    0    0tcwM2 .2595E+07 .0000E+00          169398.594236623.641  1606.466

```

...

```

CONNE
Fea 1Fda 1    0    0    0    3 .8477E+01 .3796E+01 .8857E+05-.1000E+01    1
Mea 1Mda 1    0    0    0    3 .8477E+01 .3796E+01 .8857E+05-.1000E+01    0
Fda 1Fca 1    0    0    0    3 .3796E+01 .1831E+02 .8857E+05-.1000E+01    1
Mda 1Mca 1    0    0    0    3 .3796E+01 .1831E+02 .8857E+05-.1000E+01    0

```

...

### (e) 'SR-repo-nodes'

List of fracture nodes at the potential repository within the TSPA-SR UZ grid.

```

275
Fph 2
Foh 3
Fph 4

```

...

Fsk59  
Fsk60  
Ftk61  
+++++

(3) Example Output Files:

(a) 'fnpt3d.files'

Mater input file for FEHM V2.00, obtained by 't2fehm2\_v3x.f' from using the file designator 'fnpt3d' prescribed in the input file 't2fehm2\_v3.inp3d'.

fnpt3d.dat  
fnpt3d.grid  
fnpt3d.zone  
fnpt3d.out  
fnpt3d.ini  
fnpt3d.fin  
fnpt3d.his  
fnpt3d.trc  
fnpt3d.con

fnpt3d.stor  
fnpt3d.chk  
all  
0

(b) 'fnpt3d.dat'

Primary input file for FEHM V2.00, containing various input macros. This file is obtained by 't2fehm2-v3x.f' from using the specified file designator 'fnpt3d' and some parameter values internally set within 't2fehm2\_v3x.f'.

```
Mean inf conceptual #1 input ysw/6/3/99
# Particle tracking for TOUGH2 flow field
dpdp
file
fnpt3d.dpdp
perm
1 0 0 0.100E-14 0.100E-14 0.100E-14

rlp
1 0. 0. 1. 1. 0. 1.

1 0 0 1

rock
file
fnpt3d.rock
flow

time
0.36525E+03 0.36525E+09 100 1 1997 10

ctrl
-10 0.10E-03 40
1 0 0 1
0
1.00 3.00 1.00
5 0.20E+01 0.10E-09 0.10E+11
```

## Fault Displacement Effects on Transport in the Unsaturated Zone

---

```

      0      1
iter
  0.10E-04  0.10E-04  0.10E-04 -0.10E-03  0.12E+01
      0      0      0      0  0.14E+05
sol
  1      -1
rflo
air
-1
20.0  0.1
node
1
1
zone
file
fnpt3d.zone2
ptrk
file
fnpt3d.ptrk
stop

```

### (c) 'fnpt3d.grid'

Grid file for FEHM V2.00, obtained by 't2fehm2\_v3x.f' from processing the MESH file 'MESH.3d10grid' for TOUGH2 V1.4.

```

coor
  47664
    1    169398.59    236623.64    1626.10
    2    169398.59    236623.64    1606.47
    3    169398.59    236623.64    1569.84
    4    169398.59    236623.64    1547.73
...
  47661    170319.48    233610.05    793.11
  47662    170319.48    233610.05    775.09
  47663    170319.48    233610.05    757.05
  47664    170319.48    233610.05    739.02
...
elem
2  1
1  2  1
stop

```

### (d) 'fnpt3d.zone'

The 'zone' input macro for FEHM V2.00, obtained by 't2fehm2\_v3x.f' from processing the MESH file 'MESH.3d10grid' for TOUGH2 V1.4.

```

zone
  1      #tcwM1
nnum
  278
  47665    47840    47934    47987    48081    48110    48186    48220
  48434    48493    48548    48608    48637    48687    48716    48833
  49175    49373    49440    49466    49527    49586    49890    50000
...
49      #tcwF1

```

## Fault Displacement Effects on Transport in the Unsaturated Zone

---

```
nnum
      0
...
99   #tcw&1
nnum
     278
      1      176      270      323      417      446      522      556
     770      829      884      944      973     1023     1052     1169
    1511     1709     1776     1802     1863     1922     2226     2336
```

```
...
stop
```

```
#Total number of nodes =      95328
#Total number of active boundary materials =      2
#Total number of active boundary nodes =     2648
```

### (e) 'fnpt3d.ini'

The '.ini' file for FEHM V2.00, obtained by 't2fehm2\_v3x.f' from processing the output file 'tough2.inp3d10grid.out' from TOUGH2 V1.4.

```
Mean inf conceptual #1 input ysw/6/3/99
This is a .ini file with saturations, pressures and mass flux values.
0.
air
ptrk
nstr
dpdp
ndua
  0.12041000E-01  0.10644000E-01  0.10645000E-01  0.18717000E-01
  0.14629000E-01  0.22061000E-01  0.19274000E-01  0.17005000E-01
  0.16948000E-01  0.25263000E-01  0.15287000E-01  0.10431000E-01
  0.10417000E-01  0.10416000E-01  0.10568000E-01  0.10379000E-01
...
  0.91999790E-01  0.91999700E-01  0.92000200E-01  0.92000300E-01
  0.92000000E-01  0.92000000E-01  0.91999760E-01  0.91999800E-01
  0.91999600E-01  0.92000000E-01  0.92000000E-01  0.92000100E-01
  0.91999800E-01  0.91999900E-01  0.92000200E-01  0.91999700E-01
...
mass flux values
  830612      #ntotmfv= 782948, nnodes= 95328, number of f-m connections= 47664
-0.17240000E-01  0.17251000E-01-0.21898000E-04  0.10959000E-04-0.17251000E-01
  0.0000000      0.16989000E-01-0.14991000E-03  0.26188000E-03  0.15043000E-03
-0.16989000E-01  0.0000000      0.17047000E-01-0.37864000E-03  0.18100000E-03
  0.13922000E-03-0.17047000E-01  0.0000000      0.16905000E-01-0.53015000E-04
...

```

### (f) 'fnpt3d.dpdp'

The 'dmdp' input macro for FEHM V2.00, obtained by 't2fehm2\_v3x.f' from processing the MESH file 'MESH.3d10grid' and the primary input file 'tough2.inp3d10grid' for TOUGH2 V1.4.

```
dmdp
1
  -49      0      0      0.2800E-01
  -50      0      0      0.2000E-01
  -51      0      0      0.1500E-01
  -52      0      0      0.1100E-01
...
  -136     0      0      0.4400E+00
  -137     0      0      0.1600E+00
  -138     0      0      0.3600E+00
  -139     0      0      0.1600E-01
      1      0      0      99.
stop
```

(g) 'fnpt3d.rock'

The 'rock' macro input file for FEHM V2.00, obtained by 't2fehm2\_v3x.f' from processing the primary input file 'tough2.inp3d10grid' for TOUGH2 V1.4.

```
rock
  -1      0      0      0.2500E+01      0.1000E+04      0.2530E+00
  -2      0      0      0.2500E+01      0.1000E+04      0.8200E-01
  -3      0      0      0.2500E+01      0.1000E+04      0.2030E+00
  -4      0      0      0.2500E+01      0.1000E+04      0.3870E+00
...
  -136     0      0      0.2510E+04      0.1000E+04      0.1000E+01
  -137     0      0      0.2330E+04      0.1000E+04      0.1000E+01
  -138     0      0      0.2520E+04      0.1000E+04      0.1000E+01
  -139     0      0      0.2460E+04      0.1000E+04      0.1000E+01
stop
```

(h) 'fnpt3d.stor'

The '.stor' input file for FEHM V2.00, obtained by 't2fehm2\_v3x.f' from processing the MESH file 'MESH.3d10grid' for TOUGH2 V1.4.

```
Mean inf conceptual #1 input ysw/6/3/99
This is a .stor file with dummy area coefficients
 391474      47664      439139      1
 2.33200000E+05  3.24380000E+06  3.24380000E+06  6.72360000E+05  1.50220000E+06
 1.23795000E+06  2.91930000E+06  2.68340000E+06  2.68340000E+06  1.07056000E+06
...
 47665      47669      47675      47681      47688
 47694      47700      47706      47712      47718
...
```

# Fault Displacement Effects on Transport in the Unsaturated Zone

---

```
-1.00000000E+00 -1.00000000E+00 -1.00000000E+00 -1.00000000E+00 -1.00000000E+00  
-1.00000000E+00 -1.00000000E+00 -1.00000000E+00 -1.00000000E+00 -1.00000000E+00
```

...

## (i) 'fnpt3d.zone2'

The '.zone' macro for FEHM V2.00 containing the specified repository nodes, obtained by 't2fefm2\_v3x.f' from processing the input file 'SR-repo-nodes' together with the MESH file 'MESH.3d10grid' for TOUGH2 V1.4.

```
zone  
  1      #tcwM1  
nnum  
  278  
  47665    47840    47934    47987    48081    48110    48186    48220  
  48434    48493    48548    48608    48637    48687    48716    48833  
  49175    49373    49440    49466    49527    49586    49890    50000
```

...

```
49      #tcwF1  
nnum  
  0
```

...

```
99      #tcw&1  
nnum  
  278  
  1      176      270      323      417      446      522      556  
  770    829      884      944      973     1023    1052    1169  
 1511   1709    1776    1802    1863    1922    2226    2336
```

...

```
500     #fracture repository nodes  
nnum  
  275  
 31351    31394    31439    31482    31525    31571    31615    31658  
 31703    31748    31793    31839    31883    31927    31970    32014  
 32059    32102    32145    32189    32233    32276    32323    32367
```

...

```
501     #matrix repository nodes  
nnum  
  275  
 79015    79058    79103    79146    79189    79235    79279    79322  
 79367    79412    79457    79503    79547    79591    79634    79678  
 79723    79766    79809    79853    79897    79940    79987    80031
```

...

stop

```
#Total number of nodes = 95328  
#Total number of active boundary materials = 2  
#Total number of active boundary nodes = 2648
```

(4) Verification:

The core of this software routine has been verified as in 't2fehm2\_v3x.f' (CRWMS M&O 2000e). The modifications specific to this AMR have also been verified to be correct.

Specifically, files 'fnpt3d.files' and 'fnpt3d.dat' are generated from the same operations as in 'tefehm2\_v3.f' (CRWMS M&O 2000e) and can be confirmed to be correct by visual inspection. File 'fnpt3d.grid' simply lists the coordinates of grid nodal locations, which can be seen to be consistent with file 'MESH.3d10grid'. File 'fnpt3d.zone' contains the nodal numbers that define the zones of fracture and matrix nodes; as an example, zone 'tcw&1' represents the identifier of the zone that is perturbed from the zone 'tcwF1' in the base case, and as a result, 'tcw&1' is composed of the '278' nodes that are associated with 'tcwF1' in the base case, and consequently 'tcwF1' becomes empty. In file 'fnpt3d.ini', the saturation, pressure, and mass flux for each node is taken from file 'tough2.inp3d10grid.out'; for example, the saturation value for the first node in 'fnpt3d.ini', '0.12041E-01', corresponds the saturation for element 'Faa 1' in 'tough2.inp3d10grid.out'. File 'fnpt3d.dpdp' identifies the fracture zones and their porosity values, and file 'fnpt3d.rock' identifies all the zones and their thermal parameters and porosity values; both can be verified to be correct by comparing with the data in 'tough2.inp3d10grid'. File 'fnpt3d.stor' is generated in the same way as in 't2fehm2\_v3.f' (CRWMS M&O 2000e) and thus considered to be correct. File 'fnpt3d.zone2' differs from file 'fnpt3d.zone' only in that the former file set aside those nodes in the fracture and matrix zones for the repository area as specified in file 'SR-repo-nodes'.

(5) Range of Validation:

The range of validation remains the same as for 'tefehm2\_v3.f' (CRWMS M&O 2000e).

**ATTACHMENT VI**  
**SOFTWARE ROUTINE 'mb\_tough2\_v1.4.f v.1'**

## ATTACHMENT VI

### Software routine 'mb\_tough2\_v1.4.f v.1'

The is a software routine for calculating total water inflow and outflow for the TSPA-SR TOUGH2 UZ flow model, so that water balance can be checked for a TOUGH2 output. This routine and related data can be found in the database under DTN: MO0006SPAUZ20.002.

#### (1) Code Listing:

```

c
c   To process tough2 output to check global mass balance.
c
c   input file: tough2 output file.
c
c   output to screen: total output kg/s at WT from tough2,
c                       total output kg/s fat WT from GENER,
c                       absolute error, and relative error.
c
character dumc*140,elem1*5,elem2*5,cindex*5,cidum*2
character*40 tough2_out

write(*,*) 'tough2 output file:'
read(*,'(a40)') tough2_out

open (12,file=tough2_out,status='old')
tot_tough2=0.
320 read(12,'(a140)') dumc
   if(dumc(7:11).eq.'ELEM1') then
350     read(12,*)
       read(12,*)
360     read(12,'(a140)') dumc
       if(dumc(2:6).eq.'@@@@') goto 700
       if(dumc(7:11).eq.'ELEM1') goto 350
       backspace(12)
       read(12,5070) elem1,elem2,cindex,flo,vel,flof,velf,flom,velm
5070  FORMAT(5X,a5,4x,a5,A13,6e13.5)
       if(ELEM1(1:2).eq.'BT') tot_tough2=tot_tough2+flo
       goto 360
   endif
   goto 320

700  tot_gener=0.
720  read(12,'(a140)') dumc
   if(dumc(10:15).eq.'SOURCE') then
       read(12,*)
       read(12,*)
760  read(12,'(a140)') dumc
       if(dumc(2:6).eq.'@@@@') goto 900
   if(dumc(2:2).ne.'F') goto 760
       backspace(12)
       read(12,5130) elem1,elem2,cidum,flx
5130  FORMAT(2X,A5,3X,A5,3X,A2,10X,E12.5,2X,6(1X,E12.5))

```

```
        tot_gener=tot_gener+flx
        goto 760
    endif
    goto 720

900    aerr=abs(tot_tough2-tot_gener)
        rerr=100*aerr/tot_gener
        write(*,*) 'tot_tough2,tot_gener,aerr,rerr(%):'
        write(*,920) tot_tough2,tot_gener,aerr,rerr
920    format(4e15.5)
        end
```

### (2) Example Input File:

'tough2.inp3d10grid.out'

See Appendix V, (2), (c) for the sample listing.

### (3) Example Output File (taken from screen output):

```
tot_tough2,tot_gener,aerr,rerr(%) :
    0.56404E+01    0.56404E+01    0.81062E-05    0.14372E-03
```

These four numbers are the total water flux (kg/s) at the water table summed from the solution data in file 'tough2.inp3d10grid.out', the total infiltration flux (kg/s) summed from the GENER data in file 'tough2.inp3d10grid.out', the absolute error, and the relative error between the two summation numbers.

### (4) Verification:

By summing up the water flux at the water table from the solution data and the infiltration flux from the GENER data in file 'tough2.inp3d10grid.out' without using 'mb\_tough2\_v1.4.f', it has been confirmed that results obtained from 'mb\_tough2\_v1.4.f' are correct. Incidentally, the small absolute and relative errors indicate that global mass balance has been sufficiently satisfied and thus the solution can be considered as steady state solution.

### (5) Range of Validation:

This software routine can be used for any TOUGH2 EOS9 model solutions.

**ATTACHMENT VII**

**SOFTWARE ROUTINE 'post\_tough2sr.f v.1'**

## ATTACHMENT VII

### Software routine 'post\_tough2sr.f v.1'

This is a software routine for extracting flow variables from a TOUGH2 output file for the TSPA-SR TOUGH2 UZ flow model, so that their distributions can be graphed. This routine and related data can be found in the database under DTN: MO0006SPAUZ20.002.

#### (1) Code Listing:

```

c
c   To process tough2 output.
c
c   input files: tough2 output file; MESH file.
c
c   output files: processed data files for plots.
c
double precision VOLX
character dumc*140,elem1*5,elem2*5,ciden*3,ELNE*5,refn*20
character*40 file_mesh,file_out,file_post1f,file_post2f
character*40 file_post1m,file_post2m,file_postfm

write(*,*) 'MESH file:'
read(*,'(a40)') file_mesh
write(*,*) 'tough2 output file:'
read(*,'(a40)') file_out
write(*,*) 'one column identifier (A3):'
read(*,'(a3)') ciden
write(*,*) 'reference name:'
read(*,'(a20)') refn

kend=index(refn,' ')
file_post1f=refn(1:kend-1)//'.sf'
file_post2f=refn(1:kend-1)//'.vf'
file_post1m=refn(1:kend-1)//'.sm'
file_post2m=refn(1:kend-1)//'.vm'
file_postfm=refn(1:kend-1)//'.fm'

open (11,file=file_mesh,status='old')
open (12,file=file_out,status='old')
open (14,file=file_post1f)
open (15,file=file_post2f)
open (16,file=file_post1m)
open (17,file=file_post2m)
open (18,file=file_postfm)

cc  open (11,file='MESH.ext2a',status='old')
cc  open (12,file='tough2.out2a',status='old')
cc  open (14,file='out2a.sf')
cc  open (15,file='out2a.vf')
cc  open (16,file='out2a.sm')
cc  open (17,file='out2a.vm')
cc  open (18,file='out2a.fm')

```

## Fault Displacement Effects on Transport in the Unsaturated Zone

---

```
cc      ciden='B43'
        write(14,'(a3)') ciden
        write(16,'(a3)') ciden
        write(14,*) 'elem1,Z,sliq,pcap,relk:'
        write(16,*) 'elem1,Z,sliq,pcap,relk:'

40      read(12,'(a140)') dumc
        if(dumc(4:9).eq.'ELEM.') then
50          read(12,*)
            read(12,*)
60          read(12,'(a140)') dumc
            if(dumc(2:6).eq.'@@@@') goto 300
            if(dumc(4:9).eq.'ELEM.') goto 50
            backspace(12)
            read(12,5040) elem1,indx,pres,sliq,pcap,relk,diffu,denw
5040        FORMAT(1X,A5,6X,I6,6E12.5)

            if(elem1(3:5).eq.ciden) then
                rewind(11)
100          read(11,'(a140)') dumc
                if(dumc(1:3).eq.'  ') goto 60
                backspace(11)
                read(11,150) ELNE,NSEQ,NADD,MATR,VOLX,AHTX,X,Y,Z
150          FORMAT(A5,2I5,A5,2E10.4,10X,3f10.3)
                if(ELNE.eq.elem1) then
                    if(elem1(1:1).eq.'F') then
                        write(14,200) elem1,Z,sliq,pcap,relk
                    elseif(elem1(1:1).eq.'M') then
                        write(16,200) elem1,Z,sliq,pcap,relk
                    endif
                if(elem1(1:2).eq.'TP'.or.elem1(1:2).eq.'BT') then
                    write(14,200) elem1,Z,sliq,pcap,relk
                    write(16,200) elem1,Z,sliq,pcap,relk
                endif
200          format(a5,f10.2,3e12.4)
                goto 60
            endif
            goto 100
        endif
        goto 60
    endif
    goto 40

300     continue
        close(14)
        close(16)
        write(15,'(a3)') ciden
        write(17,'(a3)') ciden
        write(18,'(a3)') ciden
        write(15,*) 'elem1,elem2,Z,flo,vel:'
        write(17,*) 'elem1,elem2,Z,flo,vel:'
        write(18,*) 'elem1,elem2,Z,flo,vel:'

        rewind(12)
320     read(12,'(a140)') dumc
        if(dumc(7:11).eq.'ELEM1') then
350         read(12,*)
```

```

        read(12,*)
360      read(12,'(a140)') dumc
        if(dumc(2:6).eq.'@@@@') stop
        if(dumc(7:11).eq.'ELEM1') goto 350
        backspace(12)
        read(12,5070) elem1,elem2,indx,flo,vel,flof,velf,flom,velm
5070     FORMAT(5X,a5,4x,a5,6X,I6,10E13.5)
        if(elem1(3:5).eq.ciden.and.elem2(3:5).eq.ciden) then
            rewind(11)
400      read(11,'(a140)') dumc
            if(dumc(1:3).eq.'  ') goto 360
            backspace(11)
            read(11,150) ELNE,NSEQ,NADD,MATR,VOLX,AHTX,X,Y,Z
            if(ELNE.eq.elem1) then
                if(elem1(1:1).eq.'F'.and.elem2(1:1).eq.'F') then
                    write(15,500) elem1,elem2,Z,flo,vel
                elseif(elem1(1:1).eq.'M'.and.elem2(1:1).eq.'M') then
                    write(17,500) elem1,elem2,Z,flo,vel
                elseif(elem1(1:1).eq.'F'.and.elem2(1:1).eq.'M') then
                    write(18,500) elem1,elem2,Z,flo,vel
                endif
            if(elem1(1:2).eq.'BT') then
                if(elem2(1:1).eq.'F') write(15,500) elem1,elem2,Z,flo,vel
                if(elem2(1:1).eq.'M') write(17,500) elem1,elem2,Z,flo,vel
            endif
            if(elem2(1:2).eq.'TP') then
                if(elem1(1:1).eq.'F') write(15,500) elem1,elem2,Z,flo,vel
                if(elem1(1:1).eq.'M') write(17,500) elem1,elem2,Z,flo,vel
            endif
500      format(2a5,f10.2,2e12.4)
            goto 360
        endif
        goto 400
    endif
    goto 360
endif
goto 320

end

```

(2) Example Input Files:

(a) 'MESH.1d'

1-D MESH file for TOUGH2 V1.4, corresponding to the 1-D model located as shown in Figure 4 in Section 6.2.1.4.

```

ELEME
Fah36   0   0tcwF20.1978E+050.1000E+01   170725.156232017.078  1372.928
Mah36   0   0tcwM20.9694E+060.0000E+00   170724.656232017.078  1372.928
Fbh36   0   0tcwF20.1978E+050.1000E+01   170725.156232017.078  1327.344

...
CONNE
Feh36Fdh36  0   0   0   30.2621E+010.1577E+010.2170E+05-.1000E+01   1
Meh36Mdh36  0   0   0   30.2621E+010.1577E+010.2170E+05-.1000E+01   0
Fdh36Fch36  0   0   0   30.1577E+010.3004E+010.2170E+05-.1000E+01   1

```



(3) Example Output Files:

(a) 'h36\_1d10grid.sf'

List of elevation (m), saturation, capillary pressure (Pa), and relative permeability for the fracture nodes in the prescribed column 'h36' within the TSPA-SR UZ grid.

```
h36
  elem1,z,sliq,pcap,relk:
Fah36  1372.93  .1051E-01  -.1314E+04  .9102E-10
Fbh36  1327.34  .1051E-01  -.1314E+04  .9096E-10
Fch36  1301.55  .1147E-01  -.1503E+04  .1680E-08
Fdh36  1296.97  .1741E-01  -.1495E+04  .5020E-08
Feh36  1292.77  .1764E-01  -.4313E+03  .1861E-07
Ffh36  1289.08  .1564E-01  -.2100E+04  .1161E-07
```

...

(b) 'h36\_1d10grid.sm'

List of elevation (m), saturation, capillary pressure (Pa), and relative permeability for the matrix nodes in the prescribed column 'h36' within the TSPA-SR UZ grid.

```
h36
  elem1,z,sliq,pcap,relk:
Mah36  1372.93  .5140E+00  -.9730E+06  .1863E-04
Mbh36  1327.34  .5810E+00  -.5274E+06  .9932E-04
Mch36  1301.55  .8430E+00  -.2752E+06  .5717E-01
Mdh36  1296.97  .8391E+00  -.2304E+06  .2455E-02
Meh36  1292.77  .4627E+00  -.1893E+06  .5152E-05
Mfh36  1289.08  .4013E+00  -.1540E+06  .1221E-03
```

...

(c) 'h36\_1d10grid.vf'

List of reference elevation (m), water flux (kg/s), and pore water velocity (m/s) for the fracture connections in the prescribed column 'h36' within the TSPA-SR UZ grid.

```
h36
  elem1,elem2,z,flo,vel:
Feh36Fdh36  1292.77  .2161E-02  .5216E-07
Fdh36Fch36  1296.97  .2163E-02  .5807E-07
Fch36Fbh36  1301.55  .2163E-02  .4754E-07
Fbh36Fah36  1327.34  .2163E-02  .4753E-07
Ffh36Feh36  1289.08  .2161E-02  .4717E-07
Fgh36Ffh36  1283.02  .2161E-02  .1030E-06
```

...

(d) 'h36\_1d10grid.vm'

List of reference elevation (m), water flux (kg/s), and pore water velocity (m/s) for the matrix connections in the prescribed column 'h36' within the TSPA-SR UZ grid.

```
h36
  elem1,elem2,z,flo,vel:
Meh36Mdh36  1292.77  .1684E-05  .2903E-12
```

## Fault Displacement Effects on Transport in the Unsaturated Zone

---

Mdh36Mch36	1296.97	.8289E-10	.1524E-15
Mch36Mbh36	1301.55	.3252E-12	.3166E-18
Mbh36Mah36	1327.34	.2110E-12	.2317E-18
Mfh36Meh36	1289.08	.1848E-05	.4492E-12
Mgh36Mfh36	1283.02	.1927E-05	.4447E-12

...

### (e) 'h36\_1d10grid.fm'

List of reference elevation (m), water flux (kg/s), and pore water velocity (m/s) for the fracture-matrix connections in the prescribed column 'h36' within the TSPA-SR UZ grid.

```
h36
  elem1,elem2,Z,flo,vel:
Fah36Mah36  1372.93  -.2110E-12  -.2951E-16
Fbh36Mbh36  1327.34  -.1141E-12  -.1596E-16
Fch36Mch36  1301.55  -.8256E-10  -.6976E-13
Fdh36Mdh36  1296.97  -.1684E-05  -.2949E-09
Feh36Meh36  1292.77  -.1643E-06  -.4855E-10
Ffh36Mfh36  1289.08  -.7827E-07  -.2767E-10
```

...

### (4) Verification:

Comparing the output files with the input file 'tough2.inp1d10grid.out', it has been verified that the program 'post\_toughsr.f' produces the intended extraction of data.

### (5) Range of Validation:

This software routine can be used to extract flow variables from any TOUGH2 EOS9 model solutions.